Subcellular Localisation of Recombinant Densin-180 Clones Expressed in HEK293 TSA Cells

MPhil, Molecular Pharmacology

Jonathan Ranatunga

ABSTRACT: Densin-180 is one of the first discovered, most abundant and, yet, most obscure core components of the postsynaptic density, a specialised structure playing a key role in synaptic transmission of excitatory neurons in the central nervous system, a process fundamental to the learning and memory processes of the brain. A founding member of the LAP (Leucine-rich repeat and PDZ domain containing) protein family, it features 16 leucine-rich repeat domains, 2 LAP specific domains, a phosphorylation rich region and a PDZ domain, and has identified interactions with a number of PSD components which include CaMKII-α, α-actinin, Cav1.3 (L-type Ca2+) channels, MAGUIN-1, δ-catenin and Shank. Densin-180 is thought to function as a key adapter protein, coordinating cytoskeletal, scaffolding and receptor molecules in the adaptation, maintenance and regulation of the highly dynamic cell to cell contacts that are synapses of the CNS. Here, we present 9 eGFP-tagged Densin-180 fusion constructs for the detailed study of Densin-180's function and show that C-terminal PDZ domain and C-terminal terminal amino acid mediated protein-protein interactions play a key role in Densin-180 punctate behaviour in HEK 293 TSA Cells.

I, Jonathan Ranatunga, confirm that the work presented in this thesis is my own. Where information has been derived from other sources, I confirm that this has been indicated in the thesis.

Table of Contents

Acknowledgments

I would like to thank Professor Ralf Schoepfer and Dr Agnes Thalhammer for everything they have done: I am in their debt for the rest of my life. Dr Martin Stocker, for all the recipes, methods and conversations he kindly provided, and everybody in the lab and faculty, for providing a deeply stimulating environment, as well as UCL as an institution, just for being a great institution.

Special thanks go to Moheb Constandi, for inspiring this project.

I would also like to thank my family and friends for their continuous, invaluable support.

Foreword

Since the dawn of mankind, thinkers from all walks of the Earth have philosophised, questioning the nature and meaning of Life.

Throughout history, human civilisations have created, celebrated and immortalised countless schools of thought; innumerable pieces of knowledge have been applied in infinite ways, shaping the culture and survival of past societies.

Is there, or is there not a God, or many Gods? That's a matter of opinion. Is there such a thing as chance, that probability of an event occurring, that entropy applicable to all physical matter in the universe? Definitely. Religion is arbitrary, but entropy is fundamental.

Since its advent, the scientific method has broken many boundaries for the first time, ushering in the advance of new technologies through the investigation of natural phenomena, drawing on, correcting and adding to existing knowledge. As a direct consequence of the spring in scientific and technological advancement that has occurred to date, we live in an age of impressive sociocultural evolution, currently occurring at an unprecedented rate and scale. The world is changing, faster and faster.

The advances incurred by the emerging mechanistic understanding of the brain will allow us to directly interfere with the fabric of the mind.

"We saw that an exact knowledge of the structure of the brain was of supreme interest for the building up of a rational psychology. To know the brain, we said, is equivalent to ascertaining the material course of thought and will, to discovering the intimate history of life in its perpetual duel with external forces; a history summarized, and in a way engraved in the defensive neuronal coordinations of the reflex, of instinct, and of the association of ideas."

p305 Ramon y Cajal: Recollections of My Life. E. Horne Craigie.

Introduction

Neuroscience, the synapse and its underlying machinery

Until the emergence of modern neuroscience, history's most influential thinkers have only been able to study the human mind based solely on non-invasive observations of human behaviour. An understanding comparable to an amateur understanding of how a modern car works based solely on observations of how it moves.

Examples of contemporary developments spurred by modern neuroscience include:

- powerful psychological models of employee motivation, bringing together research from neuroscience, biology, and evolutionary psychology [1];
- potential stem cell therapies for neurological disorders, including Parkinson's disease, Alzheimer's disease and spinal cord injury [2][3], and
- brain-machine interface technology allowing people with spinal cord injury, brainstem stroke, and amyotrophic lateral sclerosis to control a computer cursor simply by thinking about the movement of their own paralyzed hand [4][5].

Molecular Neuroscience

Molecular neuroscience combines modern molecular biology, traditional biochemistry and contemporary proteomics to, essentially, open up the brain, allowing us to take a peek under the hood, and gain mechanistic insight into the brain's complex functioning.

However, unlike the mechanics of a car, the mechanics of the brain are composed of lipid, protein, sugar and nucleic acid components, all arranged in a naturally evolved order. Therefore, the task of interpreting the arrangement of these components is more like interpreting a piece of contemporary art than it is like making sense of an engineering diagram.

Synaptic transmission

The principle unit of the nervous system is the neuron, whose function is to receive information from other cells via dendrites, to integrate this information and to transmit this information via its axon. The information is electric, caused by ion fluxes across the nerve cell membrane relying on gradients (*Table 1-1*), established by a panoply of ion transporters, and on a range of ion channels selectively permeable to these ions. The dendrites, soma and axon have varying membrane constituents and therefore appropriately varied electrical properties to suit their functions within the neuron.

	Concentration (mM)	
Ion	***Intracellular***	***Extracellular***
Potassium (K^+)	140	5
Sodium (Na^+)	5-15	145
Chloride (Cl^-)	4-30	110
Calcium (Ca^{2+})	0.0001	1-2

Table 1-1. Extracellular and Intracellular Ion Concentrations in Mammalian Neuron. The gradients established by membrane spanning ion pumps and transporters mean that there is a potential charge across the plasma membrane of a neuron, like the voltage of a charged battery. Adapted from [6].

An action potential is triggered when the resting membrane potential of an axon (usually -70mV) is depolarised past a certain threshold, causing the activation of voltage gated Na^+ channels. The influx of Na^+ ions into the cell cause a rapid depolarisation lasting 0.5 to 1 ms, short-lasting due to the inactivation property of voltage gated Na^+ channels and voltage gated K^+ channels opening. The action potential therefore propagates unidirectionally along the axon in an all or none fashion (*figure 1-1)*.

Since neurons do not touch, when the action potential reaches the axon terminal, the signal is transmitted via a chemical synapse (*figure 1-2*). When the action potential arrives here, the depolarisation activates voltage gated Ca^{2+} channels and the resulting influx of Ca^{2+} ions initiates the fusion of neurotransmitter containing vesicles to the presynaptic membrane, releasing neurotransmitter into the synaptic cleft. Neurotransmitter diffuses rapidly across the approximately 20 nm wide synaptic cleft and is picked up by either neurotransmitter receptors, uptake or breakdown mechanisms, the latter two of which terminate the transmission. When picked up by neurotransmitter receptors, the neurotransmitter will elicit a response.

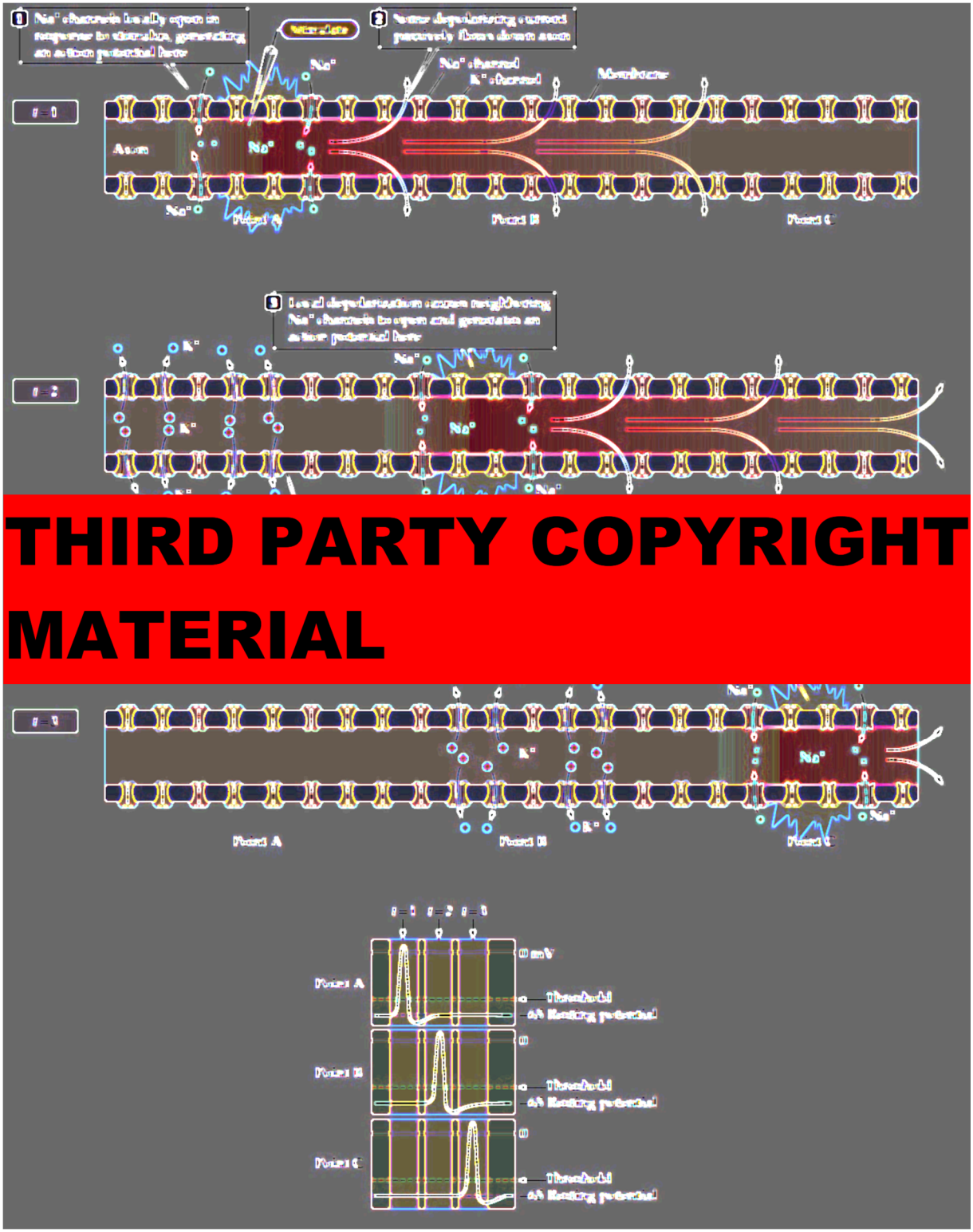

Figure 1-1. The action potential. At t = 1, action potential arrives point A, depolarisation of the membrane causes opening of Na^+ channels. The inward current flows passively onwards resulting from channel opening activates adjacent Na^+ channels: action potential is now at point B. K^+ channel opening and Na^+ channel inactivation repolarise the membrane at point A. At t = 3, inward current spreads onwards from point B, action potential propagates to point C. The time course of the membrane potential at these points is illustrated in the bottom panel. Adapted from [6].

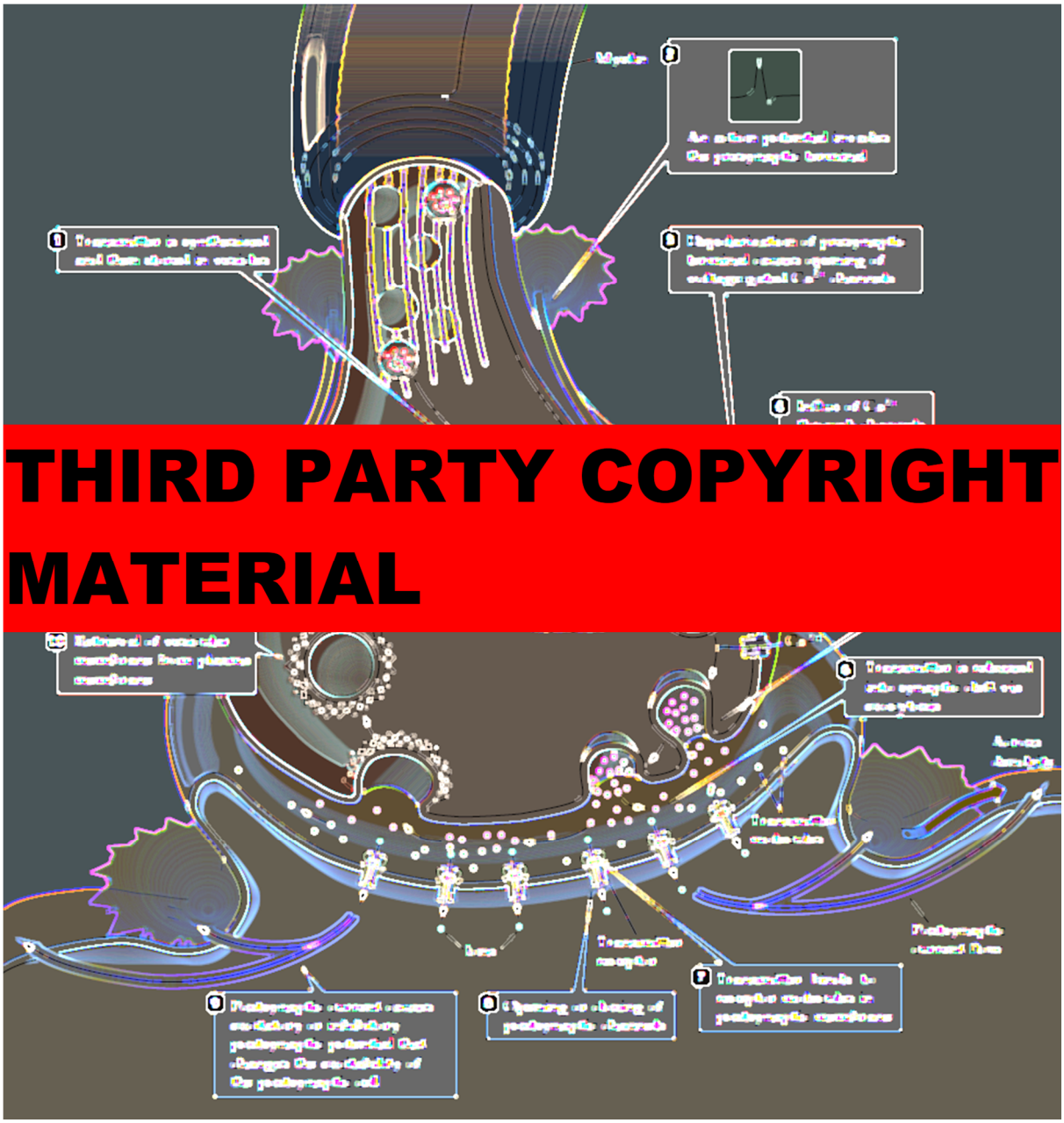

Figure 1-2. Basic sequence of events of a typical synaptic transmission. Adapted from [6].

Types of neurotransmitters and neurotransmitter receptors

There are many neurotransmitters and many more neurotransmitter receptors, many identified using the patch clamp technique, which could measure single channel currents, and using modern molecular biology techniques, which allowed the identification and cloning of ion channels. CNS neurotransmitters include: amino acids, glutamate and γ-Amino-Butyric-Acid (GABA); catecholamines dopamine, noradrenaline, adrenaline; amines, 5-hydroxytryptamine, histamine and melatonin; purines, adenosine and adenosine 5'-triphosphate (ATP); gases, nitric oxide and carbon monoxide; lipids, arachidonic acid and Anandamide; peptides, β-endorphin, and many more established and being established. [7]

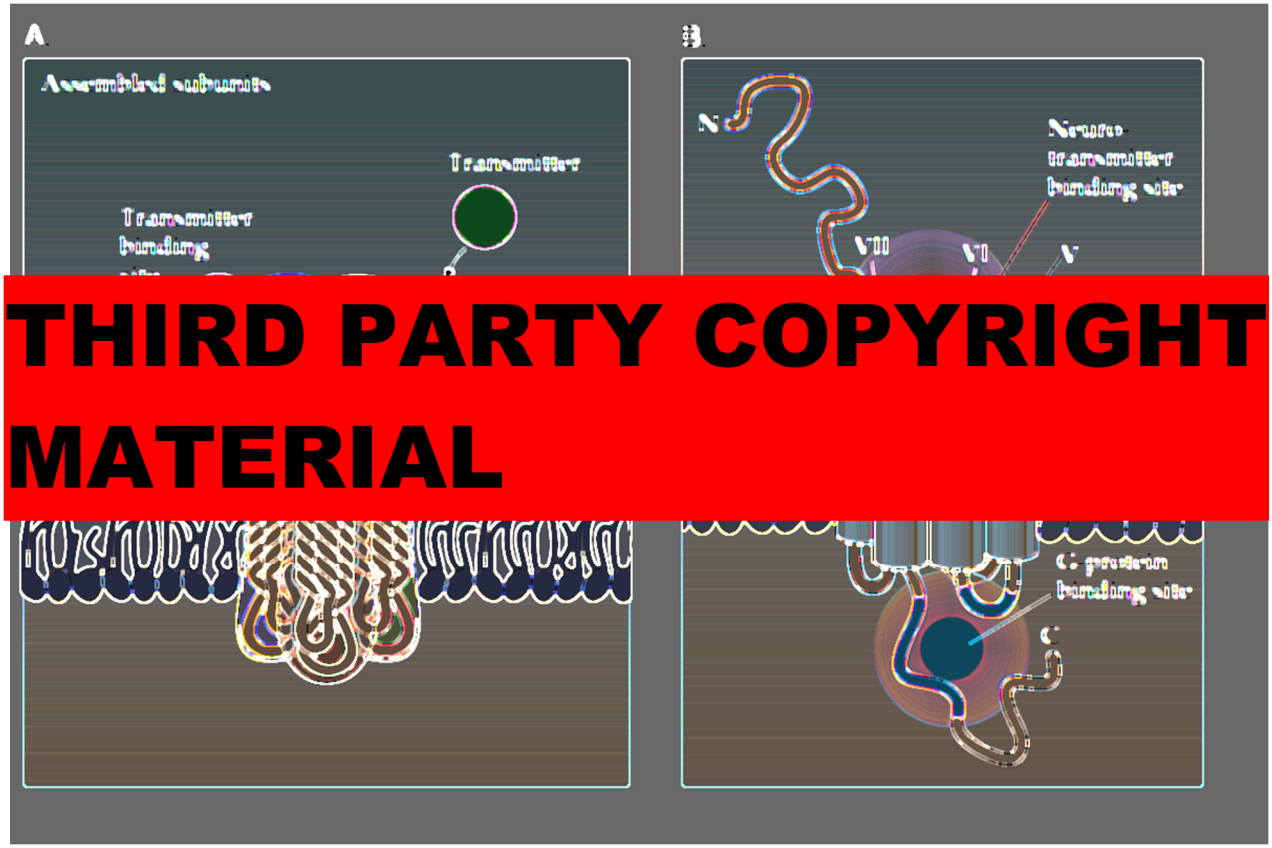

Figure 1-3. Ionotropic and G-Protein Coupled Receptors. A) Diverse subunits assemble to form functioning ionotropic receptors, which have an extracellular transmitter binding sites and a gated, central ion permeable pore. B) G-Protein Coupled Receptors are monomeric and have 7 transmembrane domains: neurotransmitter binding region is linked to domains II, III, VI and VII; G-Protein binding domain is linked parts of C-terminal and to domains V and VI. Adapted from [6].

Due to the varied nature of neurotransmitters, their properties and modes of function are varied. For example, while a classical neurotransmitter such as glutamate functions in the classical manner described above, nitric oxide, an organic gas, diffuses rapidly across plasma membranes following synthesis by neuronal Nitric Oxide Synthase (nNOS) and activates soluble guanylate cyclase, which catalyses the conversion of GTP (guanosine triphosphate) to cGMP (3',5'-cyclic guanosine monophosphate), an intracellular second messenger, like cAMP, which drives adaptive and developmental changes.

It is important to bear in mind that a neurotransmitter does not act on a single receptor. Nature has done away with the restrictions of such an arrangement and has evolved a large number of receptor types, each with a variety of configurations, devoted to each neurotransmitter.

Neurotransmitter receptors are far more varied than the neurotransmitters themselves, and for classical neurotransmitters these fall into 2 main types: ionotropic, or ligand gated ion channels,

which increase membrane permeability to specific ions upon activation, and metabotropic, or G-protein coupled receptors, which initiate intracellular signalling processes upon activation (*figure 1-3*). All have subtypes.

To illustrate neurotransmitter receptor variety, glutamate has 3 types of ionotropic receptors, NMDA (N-Methyl-D-aspartate) receptors, AMPA (α-amino-3-hydroxy-5-methyl-4-isoxazolepropionic) receptors, Kainate receptors, as well as G-protein coupled receptors termed metabotropic glutamate receptors (mGluRs).

NMDA receptors are composed of two NR1 and two NR2 subunits. The NR1 subunits are coded for by a single gene, but have eight functionally different splice variants (3 independent splice sites [8]). Four genes code for NR2A/B/C/D subunits. There are two NR3 subunits (NR3A and NR3B), which may coassemble with NR1/NR2 subunits to form triheteromeric receptors (different NR2 subunits may also dimerise to form triheteromeric receptors). NR2 and NR3 subunits have splice variants. Various subunit compositions make for varied receptor properties: in NMDA receptors single channel conduction properties (*figure 1-4*) and sensitivity to Mg^{2+} block depend on NR2 subunit composition; NR1 isoforms dictate receptor targeting to different membrane regions [9], the pH, polyamine and Zn^{2+} sensitivity, as well as deactivation properties of NMDA receptors [8].

AMPA receptors are each composed of 4 subunits (GluR1, GluR2, GluR3 and GluR4), which assemble as dimers of dimers of GluR2 and either GluR1, GluR3 and GluR4, giving a total of 4 possible arrangements. Kainate receptors have five types of receptor subunits forming tetramers, and there are 5 possible arrangements, while there are 8 types of mGluRs ($mGluR_{1-8}$), with further subtypes (e.g. $mGluR_{7a}$ and $mGluR_{7b}$).

With this degree of neurotransmitter receptor variety, the impact of presynaptic activity on postsynaptic activity can be varied.

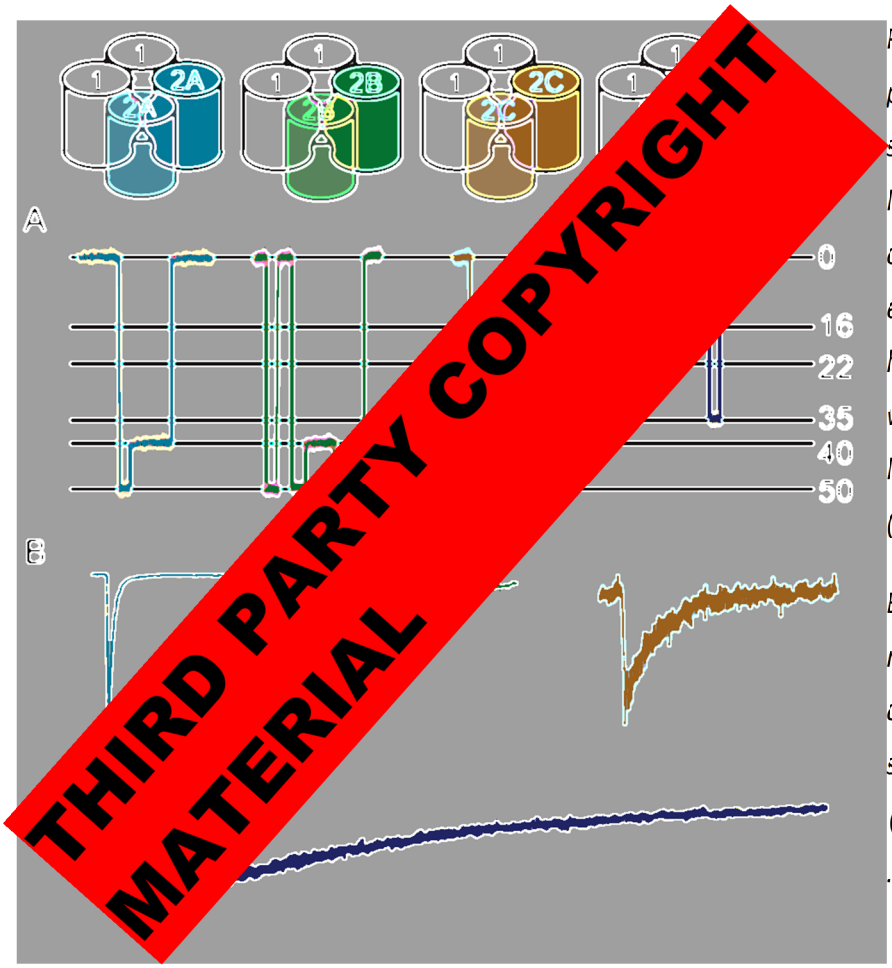

Figure 1-4. NMDAR channel properties depend on NR2 subunit composition. A) NMDAR single channel conductances: NR2A (cyan) and NR2B (green) channels have high conductances, while NR2C (orange) and NR2D (purple) have lower (but differing) conductances. B) NMDAR whole cell responses: receptor time constants vary depending on subunit composition (NR2D>>NR2C=NR2B>NR2A). Figure adapted from [8].

Excitatory and inhibitory synapses

A synapse can either be excitatory or inhibitory. In the CNS, glutamate is the neurotransmitter at the majority of excitatory synapses, while GABA is the neurotransmitter at the majority of inhibitory synapses. The reasons for glutamate's excitatory nature and GABA's inhibitory nature are their ionotropic receptors. These are positioned in the postsynaptic membrane in close proximity to the presynaptic membrane, and it is their permeability to specific ions when activated which may cause either a depolarisation or hyperpolarisation of the postsynaptic membrane, therefore promoting or attenuating postsynaptic excitability. What determines whether the postsynaptic response is excitation or inhibition is therefore the type of receptor that is activated, its ion permeability and the prevailing ionic gradients.

Excitatory glutamatergic synapses are located, in their majority, on dendritic spines [10], are less than 1 μm wide [11], and have active zones visible in electron micrographs, termed PostSynaptic Densities (PSDs), where large amounts of cellular machinery are present, underlying biochemical signal transduction processes of the highly dynamic synapses. Located there, AMPA and NMDA receptors both have 4 ligand binding domains and have cation selective pores, yet the two receptor

types have very distinct roles, the former adapted towards rapid information transfer on a millisecond timescale and the latter towards information storage (*figure 1-5*).

Figure 1-5. Time course of activation of AMPA and NMDA receptors are adapted to their functions. Adapted from [11].

The four ligand binding sites of AMPA receptors require only two glutamate molecules to activate the channel, allowing for quick activation. The cation permeable pore selectivity depends on subunit composition: GluR1, GluR3 and GluR4 all display strong inwardly rectifying current voltage, due to polyamine pore block, and calcium permeability, whereas the GluR2 subunit removes calcium permeability and polyamine pore block [12]; most AMPA receptor channels in the CNS are not calcium permeable [13]. AMPA receptors have low binding affinity for glutamate, which means they stay activated for very short periods of time, allowing signalling on the millisecond timescale [12]. "Flip" and "Flop" GluR subunit splice variants change the receptor's pharmacological and physiological properties, Q/R RNA editing of GluR2 subunits affect Ca^{2+} permeability and a host of TARPs (Transmembrane AMPA receptor Regulatory Proteins) serve as essential auxiliary subunits regulating AMPA receptors (TARPs).

NMDA receptors are ligand and voltage gated cation channels and act as coincidence detectors. These receptors have a number of interesting and unique features illustrated in *figure 1-6*.

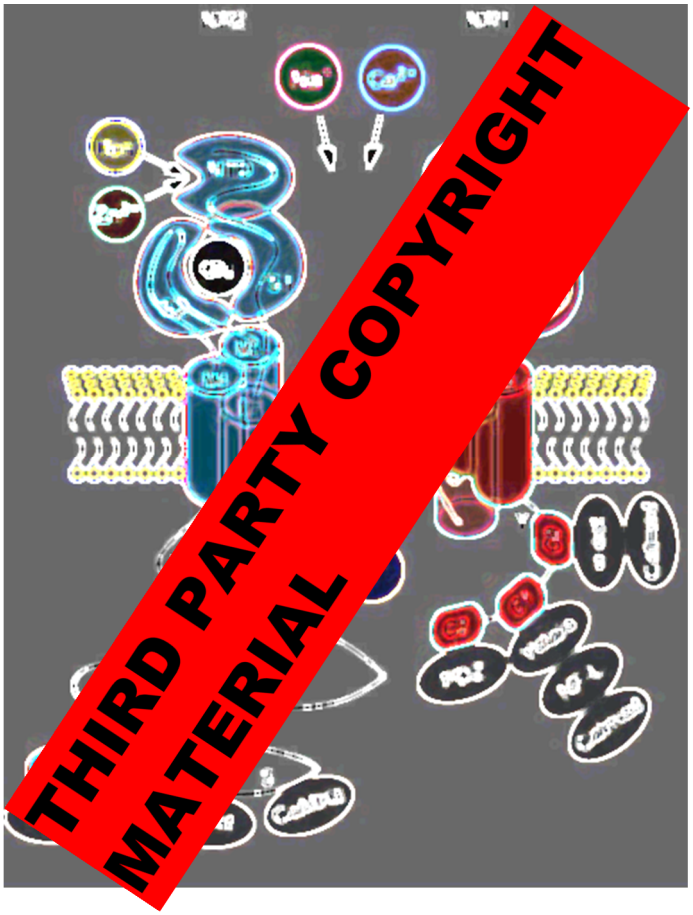

Figure 1-6. Cross section of NMDAR, showing NR1 subunit (right) and NR2 subunit (left) in a dimer of dimer arrangement. Subunits have 3TM topology, both featuring an M2 re-entrant pore loop, which determine pore permeability and voltage dependent Mg^{2+} pore block; large N- and C-termini, which have binding sites for extracellular ligands and intracellular proteins. Large N-termini have Venus-trap style glutamate and glycine binding sites are formed by S1 domain emerging from M1 TM domain, and S2 loop, between M3 and M4 TM domains. Other ligand binding sites are located on the N-termini of NR2 subunits (Zn^{2+} channel block through binding to LIVBP-like domain; Ifenprodil and polyamines). C-termini of NR1 and NR2 subunits have numerous binding sites for intracellular polyamines and to many postsynaptic proteins. Adapted from [8].

The fact that they can only be activated during periods of high activity which lift the Mg^{2+} pore block means that these receptors detect coinciding pre- and post-synaptic activity. Their cation selective, Ca^{2+} permeable pores and currents lasting over 100 ms, mean that the activation of NMDA receptors is inextricably linked to Ca^{2+} homeostasis, and thus to synaptic plasticity, cell development, survival and excitotoxicity.

Glutamate diffuses from the synaptic cleft into surrounding areas where high densities of Excitatory Amino Acid Transporters (EAATs) are positioned on surrounding Glial cells to rapidly transport glutamate, which diffuses from the synaptic cleft into surrounding area, ensuring rapid transmitter clearance and terminating the excitatory neurotransmitter signal in less than 1 ms [11]. EAATs are similar to ion channels, but carry out active transport coupled to the Na^{+} ion gradient.

The GABA ionophores ($GABA_a$ and $GABA_c$ receptors) are analogous, pentameric and their activation is coupled to binding of 2 agonist molecules at distinct binding sites [14], presumably (again in analogy to nAChRs, located subunit interface sites). A key difference, though, is that activation of GABA ionophores opens a Cl^- and HCO_3^- permeable channel, in contrast to the cation selective pore of nAChRs; since the ratio of ion to HCO_3^-/Cl^- is about 0.2-0.4 [15], the ion flux that occurs upon channel opening is dominated by Cl^- ions, causing a membrane hyperpolarisation.

GABA, like glutamate, is accompanied by its own complement of uptake pumps (GAT1-3, BGT-1).

However, the similarities do not stop there, since GABA transmission has been observed to be excitatory in immature neurons [16] (*figure 1-7*), where KCC2, a K^+/Cl^- transporter, is not expressed, and where as a consequence there were more intracellular Cl^- ions than extracellular. [17]

It was demonstrated that GABA excitatory synapses formed prior to Glutamatergic synapses [16], and it is thought that this provides "a solution to the problem of how to excite developing neurons to promote growth and synapse formation while avoiding the potentially toxic effects of mismatch between GABA mediated inhibition and glutamatergic excitation" [18].

Figure 1-7. The NKCC1 co-transporter (first identified in 1998 by Zhang and Jackson) is expressed from immature stages of neuronal development, before the expression of the KCC2 co-transporter. The developmental shift in KCC2 expression changes intracellular Chloride concentrations, consequently regulating the nature of GABAaR currents. Adapted from [17].

It is worth noting that it is technically incorrect to call a neurotransmitter excitatory or inhibitory since some, like acetylcholine, have receptors with inhibitory and excitatory effects. However, since

glutamate and GABA receptors are excitatory and inhibitory, usually and respectively, this usage is frequent and convenient.

Receptor interactions with intracellular PSD proteins

Neurotransmitter receptors are part of a highly organised, dense and regulated protein complex known as the postsynaptic density (PSD). Recent proteomic profiling of mouse PSD preparations revealed 2159 unique proteins [19] with functional groups including: scaffolding molecules; kinases and phosphatases, which regulate protein function; G-proteins and their effectors, which compose intracellular functional cascades, and adhesion proteins.

To illustrate, NMDA receptors interact with a number of PSD components, which include: α-actinin, calmodulin, Ca^{2+}/calmodulin-dependent protein kinase II (CaMKII), PDZ-domain-containing proteins, Yotaio, Neurofilament-Long (NF-L) and AP-2 [8].

The arrangement and composition of the PSD will directly control submembranous receptor-binding sites that in turn determine receptor abundance within synapses [20].

One of the best studied examples, PSD-95, is a Membrane-Associated GUanylate Kinase (MAGUK), a core PSD protein concentrated at glutamatergic synapses and a prototypical PDZ (Psd-95/Drosophila Discs Large/Zona Occludens-1) protein. It acts as a postsynaptic scaffolding molecule, associating with other PSD proteins such as GKAP and Shank, anchoring NMDA receptors and associated signalling complexes, that regulate synaptic plasticity, to synapses.[21][22][23]

PSD proteins can also directly regulate receptor function, as is the case with CaMKII-α, a dodecameric holoenzyme, a core PSD component [24] and one of the most abundant CNS proteins [25]. CaMKII-α phosphorylates AMPA receptor GluR1 subunits on Ser831 residues, potentiating channel currents [26], and NMDA receptor NR2B subunits on Ser1303 residues [27], providing a way in which the function of these receptors can be modified rapidly upon Ca^{2+} influx following NMDA receptor activation. CaMKII-α function itself has been shown to be regulated in an activity dependent manner, via autophosphorylation on residue T286, in the enzyme's regulatory region, occurring in an intraholoenzyme, intersubunit manner [28], which disrupts binding of its inhibitory pseudosubstrate region to its catalytic domain, rendering its activity autonomous of Ca^{2+} concentrations and allowing binding of the T286 site to NR2B subunit residues resulting in anchoring of enzyme complexes to specific synapses [29]. CaMKII-α has been shown to translocate to the PSD following NMDA receptor activation mediated Ca^{2+} influx [30].

Synaptic plasticity

The strength of signal transmission between pre- and postsynaptic neurons relies on the coordinated function of the PSD's molecular constituents, which can be regulated in a number of ways: changes in protein levels through local synthesis and degradation; reversible post-translational modification of the proteins themselves, such as phosphorylation and O-GlcNAc glycosylation, and changes in protein localisation. In synergy, these processes, underlying the long term changes in synaptic efficacy, are fundamental to higher cognitive processes such as learning and memory.

There are many types of synaptic plasticity, which may be short-term or long-term and can be mediated pre-synaptically or post-synaptically, all occurring simultaneously.

Short term plasticity

This type of plasticity occurs in the millisecond to minutes timescale, influences the information processing function of synapses, allowing them to act as high- or low- pass filters.

Paired-pulse facilitation

Paired-pulse facilitation is when 2 stimuli are delivered within a short interval of each other and where the second stimulus is either enhanced relative to the first [31], or depressed. If the interval is less than 20 ms, depression occurs because of the inactivation of presynaptic voltage gated N-type calcium channels, but also transient depression of release-ready pool of vesicles docked at presynaptic terminal. With a longer interval of 20 to 500 ms, facilitation occurs because of residual intracellular Ca^{2+} from the stimulation contributing to neurotransmitter release during the second stimulation. However, whether facilitation or depression occurs also depends on the synapse's activation history such that synapses that start with a high transmitter release probability are likely to depress their response to the second pulse and vice versa. [32]

Facilitation and depression following trains of stimuli

Facilitation and depression with longer timescales occurs in response to trains of stimuli. Augmentation is enhancement in neurotransmitter release lasting seconds, and Post-Tetanic Potentiation (PTP) is the same but lasting several minutes. Enhancement in neurotransmitter release in both is due to Ca^{2+} presynaptic influx in response to new stimuli coupled with residual presynaptic Ca^{2+} from previous stimuli.

In synapses that start with a high neurotransmitter release probability, however, depression occurs due to: the depletion of the release-ready pool of neurotransmitter vesicles; the release of neuromodulatory substances from cells in the vicinity including the presynaptic terminal and postsynaptic cells, initiating signalling cascades that lead to the inhibition of presynaptic release machinery; and due to the desensitisation of postsynaptic ligand gated receptors, making target

neurons less sensitive to neurotransmitter. Since glia play an important part in neurotransmitter clearance, mechanisms modulating the speed and extent of neurotransmitter reuptake can also modulate synaptic transmission.

Long Term Plasticity: Long Term Potentiation and Long Term Depression

Long Term Potentiation (LTP) is a type of synaptic plasticity lasting hours to days, studied in hippocampal CA1 slices, which displays the following properties: cooperativity, since LTP can be induced by coincident activation of a critical number of synapses, allowing the activation of postsynaptic NMDA receptors; associativity: since a weak input can be potentiated when coupled to a strong input, a property of Hebbian synapses, which could underly classical conditioning, and input specificity, since LTP occurs only at activated synapses. This means each synapse can encode individual bits of information.

Figure 1-8. LTP triggered by NMDAR at hippocampal CA1 synapses. Left panel: High-frequency tetanic stimulation triggers LTP. Initial slope of the field excitatory postsynaptic potential (fEPSP; normalised to baseline) defines synaptic strength. Right panel: schema illustrating typical electrode placement for studying LTP using rodent hippocampal slice preparation, showing the CA1, CA3 regions, Dentate Gyrus (DG), Schaffer Collaterals (SC), Mossy Fibers (MF), Stimulating electrode (Stim) and Recording electrode (Rec). Adapted from [34].

Following activation of NMDA receptors, which requires strong postsynaptic depolarisation coupled with presynaptic neurotransmitter release, usually achieved experimentally by applying high frequency tetanic stimulation, the influx of Ca^{2+} into the postsynaptic terminal activates a number of kinases which induces signalling cascades resulting in the increase of AMPA receptors at the active PSD, and, thus, in an increased postsynaptic response to presynaptic activity (*figure 1-8*).

A very complex biochemical machinery is involved in the process, which involves recycling endosomes containing reserve pools of AMPA receptors being mobilised and exocytosed at perisynaptic sites from which the receptors laterally diffuse to the PSD where they are anchored by MAGUKs, such as PSD-95, TARPs and others. Although a number of kinases are involved, CaMKII-α, and its special autophosphorylation property, play a key role in mediating LTP, since it has been shown to be impossible to induce LTP in knock-in mice in which the endogenous enzyme was replaced with a form lacking the autophosphorylation sites [33].

Long Term Depression (LTD) is a decrease in postsynaptic response lasting hours to days. A smaller stimulation than used to induce LTP, causing smaller activation of NMDA receptors, causes an increase in postsynaptic Ca^{2+} small enough to activate protein phosphatases in preference to kinases. The function of protein phosphatases is to remove phosphorylation groups from proteins, and therefore to undo the work of kinases, and this leads to dissociation of AMPA receptors from PSD scaffolds and their subsequent internalisation. As with LTP, the mechanisms involved are both numerous and complex.

Activation of mGluR1 receptors, located extrasynaptically, may also trigger LTD. These activated receptors induce phosphoinositide hydrolysis and diacylglycerol and inositol triphosphate production: second messengers that activate signalling cascades leading to changes associated with LTD. [34]

LTD may also be initiated by a very different mechanism via endocannabinoids (termed Endocannabinoid Mediated LTD, or EM-LTD), whereby the retrograde messenger is released in response to strong postsynaptic depolarisation or activation of postsynaptic G-protein coupled receptors (such as mGluRs), and act via presynaptic CB1 receptors to inhibit neurotransmitter release. [33]

In both LTP and LTD, rapid morphological changes to dendritic spines in response to activity are involved, and can include the growth of new spines, the enlargement of existing spines, the splitting of a single spine into two, and the opposite of these, highlighting how form and function go hand in hand in the CNS. [35]

The occurrence of LTP and LTD mean that synaptic activity can bi-directionally control synaptic strength, and since there are 10^{11} neurons in the CNS, each with approximately 7000 synapses, these processes underly a huge memory storage capacity.

Other forms of plasticity

Other, longer term forms of plasticity exist such as metaplasticity and synaptic scaling. Metaplasticity is the changes in the capacity of synapses to express long term plasticity, and synaptic scaling, a form of homeostatic plasticity, is when the strength of all synapses on a given neuron adjust in response to a prolonged change in activity. These forms of plasticity may exist to regulate shorter term plasticity in neurons, and to maintain the integrity of inter-neuronal circuitry within the CNS. [34]

Densin-180

Densin-180 is one of the first discovered, most abundant and, yet, most obscure constituents of the PSD: today a PubMed search for Densin-180 only reveals 23 publications.

It was identified in the mid-90s as a core PSD protein in rat by the Kennedy lab in Caltech, along with PSD-95, CaMKII-α and the NR2B NMDA receptor subunit. These core PSD proteins are all highly enriched (~10 to ~30 fold) in PSD fractions prepared by successive extraction with detergents, and remain associated with the PSD fraction even after extraction with N-lauroyl sarcosinate, a relatively harsh detergent. [37]

Structure and domains

The first mammalian member of the LAP (Leucine-rich-repeats and PDZ-domain containing) protein family, Densin-180, has 16 LRRs (Leucine rich repeats) located within its 400 N-terminal amino acid residues, and a PDZ (PSD95/Dlg1/ZO-1) domain located within its 100 C-terminal amino acid residues. In addition, there are two LAPSDs (LAP Specific Domain) situated between the LRRs and PDZ domains, which, although their function is currently unknown, have been used for the phylogenic analysis of LAP proteins: LAPSDa, a 38 amino acid LRR-like domain signature for the LAP protein family closely flanking the LRR region from the C-terminus; LAPSDb, a 24 amino acid motif, also conserved in LAP proteins, yet unrelated to LRR motifs, and a 42 amino acid spacer region between the two, which is folded in a putative α-helix. This is illustrated in *figure 1-9* below. [38][39][40]

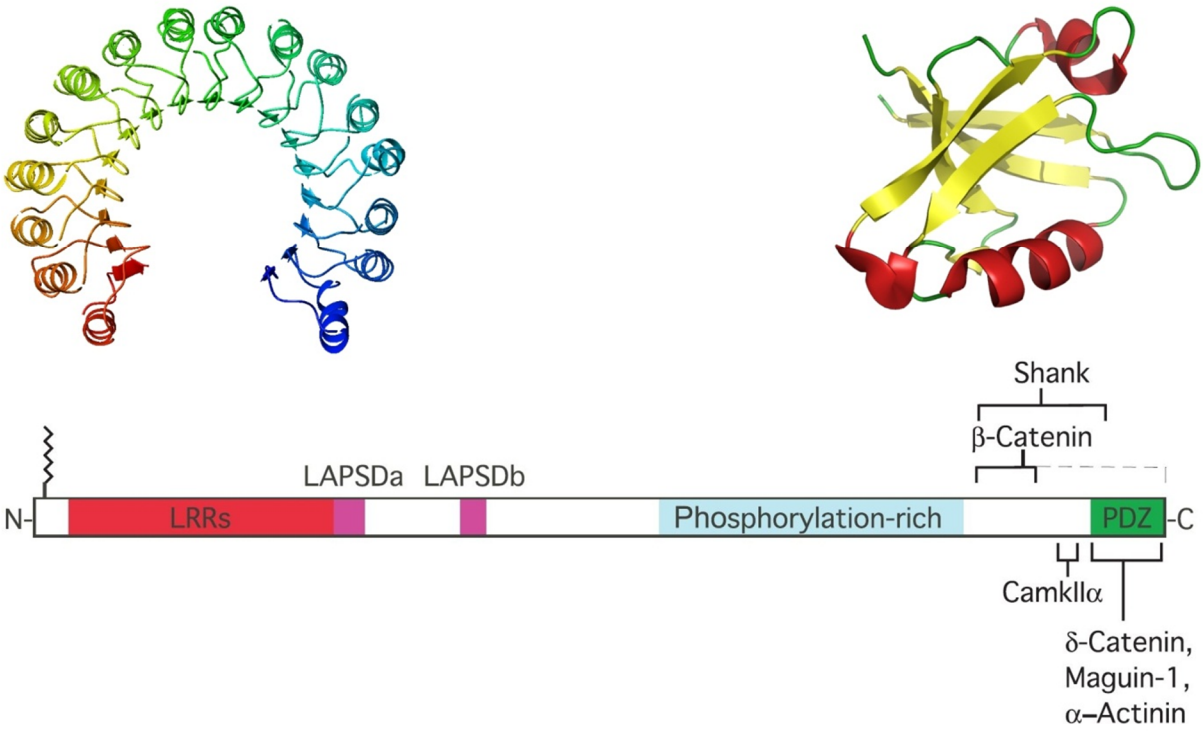

Figure 1-9. Densin-180 and its domains. Domains from the N-terminus to the C-terminus: Cys14/16 palmitoylation site (zigzag), LRRs (red) with putative structure shown (top left), LAPSDa and LAPSDb (purple), phosphorylation rich region (blue) and PDZ domain (green) with typical structure shown (top right). Adapted from [38].

The Densin-180 amino acid sequence is highly conserved across species, with mouse and rat sequences sharing 99% identity, and mouse and human sequences sharing 92% identity. The secondary, tertiary and quaternary structures of Densin-180, as well as its function, are therefore likely to be highly conserved across these species.

Phosphorylation sites and the phosphorylation-rich region

Recent phosphoproteomic analysis of the *in vivo* phosphorylation state of Densin-180 from tryptic digests of murine PSD preparations by tandem mass spectrometry using stringent statistical interpretation criteria, combined with manual inspection of the individual spectra, across multiple experiments and several independent sites, has identified a number of phosphorylation sites on the Densin-180 amino acid sequence (*figure 1-10*), and presents strong evidence for a phosphorylation-rich region between amino acid residues 826 and 1213. This phosphorylation-rich area is highly conserved between species, with 99% amino acid sequence identity shared between rat and mouse, and 90% between rat and human. [38]

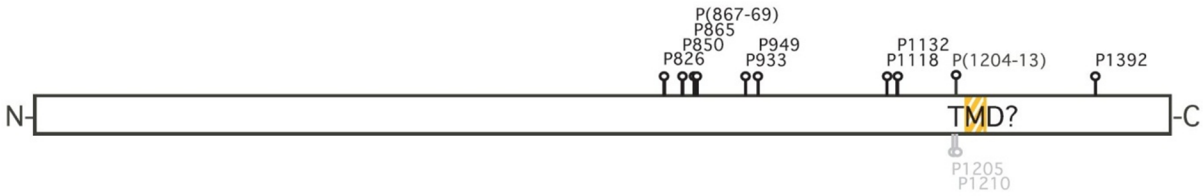

Site/region	Peptide (refs a, c)
S826	T.IVGVPLELEQ**S**THR.H
S850	R.TP**S**PFEDR.T
T865	K.LET**T**PTTSPLPERK.D
T867-869	K.LETTP(**TTS**)PLPER.K
S933	K.STERL**S**PLmK.D
S949	K.SQ**S**DEIDVGTYK.V
S1118	R.RAD**S**LASSTEmAmFR.R
S1132	R.RV**S**EPHELPPGDR.Y
Y1205	not stated
Y1210	not stated
S1204-S1213	R.(**S**Y**ST**E**S**YGA**S**)QTRPVSARPTmAALLEK.I
S1392	R.**S**mDGYPEQFCVR.I

Figure 1-10. Sequence (top) and table (bottom) displaying in vivo phosphorylation sites of murine Densin-180 (Q80TE7-1). Top: Putative Transmembrane Domain (TMD) is shown relative to phosphorylation sites. Bottom: phosphorylation sites and regions are shown in bold, ambiguity is shown with brackets, and lower case "m" refers to oxidation of methionine. Adapted from [38].

Post translational glycosylation modification

Glycosylation is another form of post translational modification in which glycans are added to proteins. Glycans be can mono-, oligo- or polysaccharides; since glycans can vary in size, the glycan contribution to the resulting glycoconjugate can vary greatly, and may constitute a large part of the glycoconjugate. Because the types of glycan that can be added are various, and because each monosaccharide can theoretically generate either an α- or β- linkage to any of several positions on the group to which they are added to, there are different types of glycosylations which include:

- N-linked glycans attached to a nitrogen of asparagine or arginine side chains
- O-linked glycans attached to the hydroxyl oxygen of serine, threonine, tyrosine, hydroxylysine, or hydroxyproline side chains
- Glypiation, the addition of GlycoPhosphatidyl Inositol (GPI) anchor that links the protein to lipids through glycan linkages, similar to isoprenylation and palmitoylation. [70]

O-linked β-N-acetylglucosamine (O-GlcNAc) is a type of glycosylation, which is, unlike complex N- and O-linked glycosylation modifications, poised to take part in dynamic signalling responses. It

occurs when the monosaccharide N-acetylglucosamine is attached in a β-linkage to Serine or Threonine hydroxyl groups of proteins. Unlike enzymes responsible for complex glycosylation, which are located in the Golgi and endoplasmic reticulum, O-GlcNAc Transferase and O-GlcNAcase, which catalyse the addition and removal of the O-GlcNAc modification are found in the cytosol and nucleus of cells, and the proximity of these enzymes to substrate proteins allows for the rapid regulation of these through the post translational modification, as observed in T-cell responses, glucose metabolism and insulin signalling. O-GlcNAc appears as widespread as phosphorylation and is found in all eukaryotes studies, and just like phosphorylation, O-GlcNAc is likely to have protein and site-specific influences on multiple molecular processes. [41]

Pharmacological manipulation, using activators or inhibitors of kinases and phosphatases, of the phosphorylation state of a cell has been shown to affect the levels of O-GlcNAc modifications in different subcellular fractions in an analogous, yet reciprocal manner [71]. Although there is not yet a consensus motif for the modification, many O-GlcNAC sites are identical to phosphosites in a number of proteins, such as c-Myc, the oestrogen receptor and SV-40 large T-antigen. It is therefore possible that O-GlcNAc and Phosphorylation may have a Yin-Yang relationship, in which they act reciprocally, and that proteins exist in a variety of forms through these post translational modifications. [41]

Intracellular or transmembrane?

Upon its discovery, Densin-180 was found to be anchored in the membrane fraction of PSD preparations by a combination of lipid and protein interactions. A transmembrane domain, spanning amino acid residues 1223 and 1246, was speculated in analogy to GPIbα, an LRR protein functioning as a platelet adhesion molecule, backed up, apparently, with evidence from a Kyle and Doolittle hydropathy plot. In the discussion, Apperson *et al* [37] further speculate that Densin-180 may also have an adhesive function, in this case linking pre- and post-synaptic membranes. However, in the same paper, it is observed that no hydrophobic signal sequence, expected in a transmembrane protein, was found, and that the immunocytochemical localisation of Densin-180 in dissociated hippocampal neurons appears to be solely postsynaptic.

In the 2009 review, Thalhammer *et al* [38] show, using numerous bioinformatics methods, that the existence and evidence for this transmembrane domain is pure machination [38]. Interestingly, a hydrophobicity plot of the rat Densin-180 sequence using the Kyte-Doolittle method (the same method used by Apperson *et al* [37]) shows no evidence of a transmembrane domain: as illustrated in *figure 1-11*, a transmembrane domain stands out rather clearly as a peak, as for the example Glycoprotein G, but no such peak can be seen in the plot for Densin-180.

Furthermore, biotinylation of surface proteins in dissociated hippocampal neurons followed by their precipitation, via streptavidin beads, and immunoblotting failed to detect Densin-180 when free of association with N-Cadherin [42], supporting the case for Densin-180's cytosolic localisation.

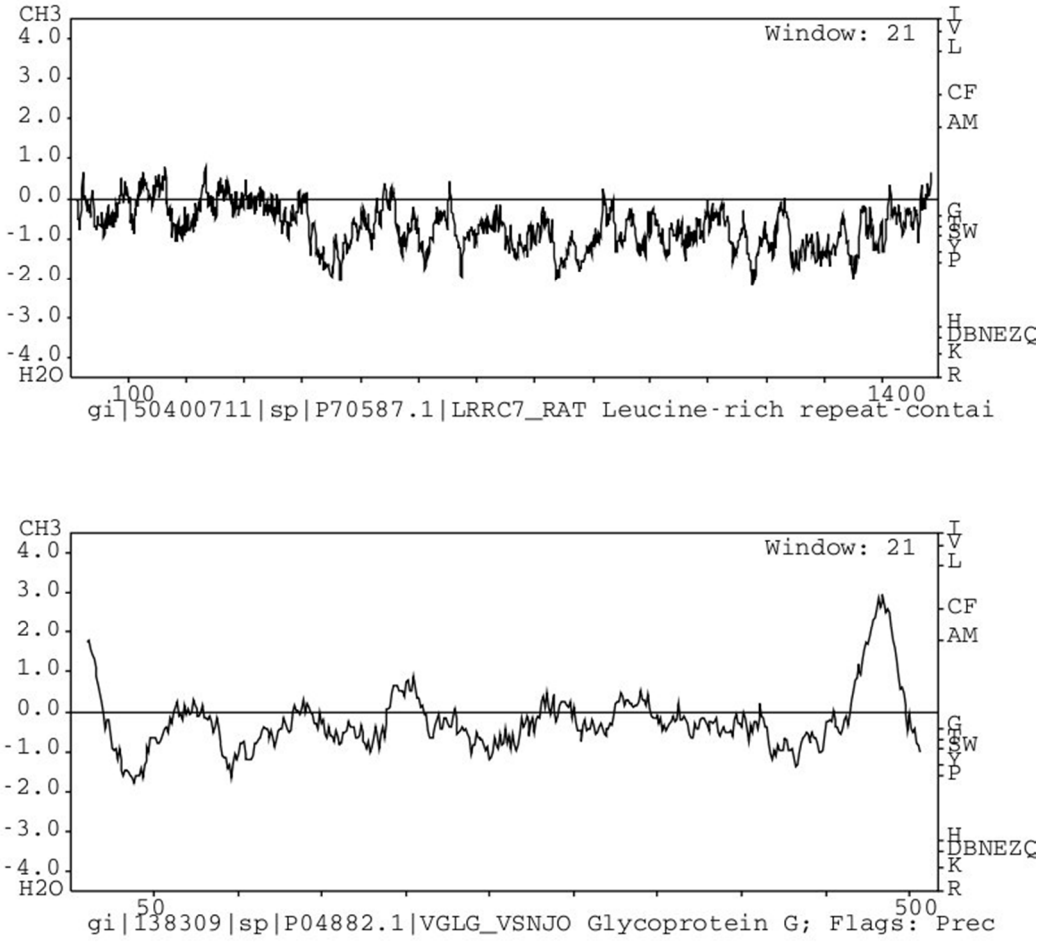

Figure 1-11. Kyte and Doolittle hydropathy plots of rat Lrrc7 (top; Uniprot identifier P70587) and of Glycoprotein G (bottom; Uniprot identifier P04882). While Glycoprotein G shows a large peak in hydrophobicity indicative of a transmembrane region near the carboxy-terminus of the protein, there is no indication of such a feature in Densin-180. Window size: 21. Plot generated using http://fasta.bioch.virginia.edu/fasta_www2/fasta_www.cgi?rm=misc1.

In their 2008 paper, Izawa *et al* [43] also showed that Densin-180 is palmitoylated. They demonstrated that *in vivo* palmitoylation, of Cysteine residues 14 and 16, and the presence of the full LRRs were requirements for the plasma membrane localisation of Erbin, suggesting that this localisation was therefore dependant on interactions with both the plasma membrane, via palmitoylated residues, and with cytosolic components, via LRR region. Densin-180 is a close

homologue of Erbin, also featuring Cysteines at residues 14 and 16, and, it is fair to assume that Densin-180's intracellular localisation is also determined through similar mechanisms [43]. It is important here to note that palmitoylation is exclusively an intracellular phenomenon, furthering the case against the existence of Densin-180's putative transmembrane domain.

Considering the evidence presented above, the existence of a transmembrane domain on Densin-180, as described in the original Apperson *et al* paper [37], is unlikely and Densin-180 is more probably an intracellular protein, natively localised to the plasma membrane through interactions with membrane and cytosolic components.

Protein-protein interactions

As illustrated in *figure 1-9 and figure 1-12*, the currently exposed interactions of Densin-180 portray the protein as a promiscuous player amongst key synaptic players, fitting with the original observation of the protein's dense presence among core PSD proteins [37]. One must note, however, that published literature only exposes protein-protein interactions involving Densin-180's C-terminus; no interactions involving Densin-180's LRR region have been observed in the current literature. LRR regions are thought to act as a ligand-binding domain [44]; Densin-180's LRR region has been found to be indispensable for the protein's correct native targeting [43] and so the function of Densin-180's LRR domain should not be overlooked in future research.

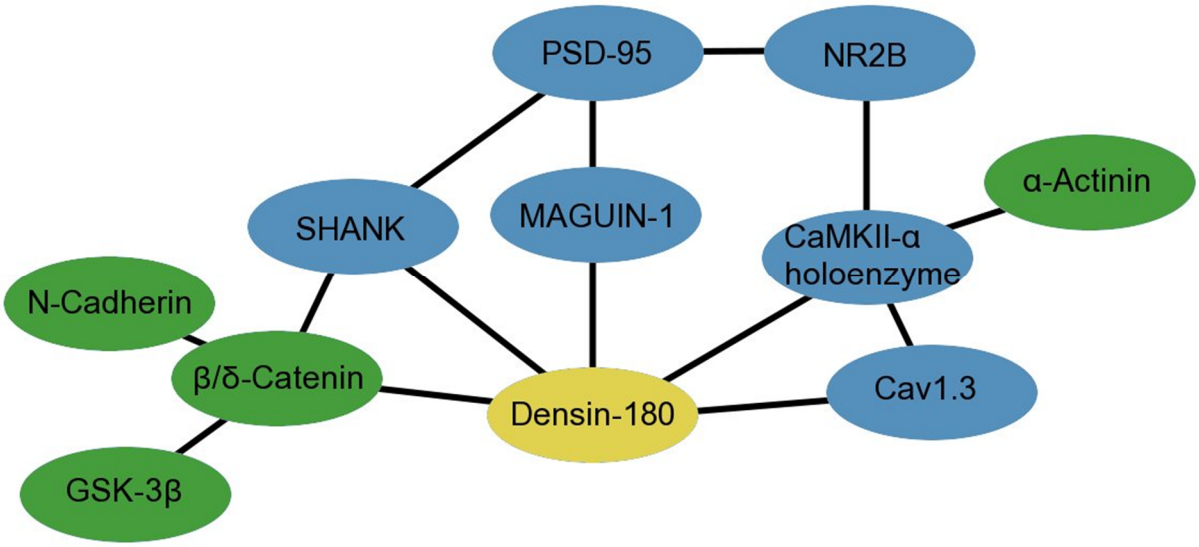

Figure 1-12. Densin-180 interacts with 2 functional groups of PSD protein complexes: signal transduction proteins (blue) and proteins involved in the regulation of structure and morphology (green).

Identified interaction partners	Interaction with Densin-180	Reference
CaMKII-α	Targeted to PSD by Densin-180; developmentally regulated expression of splice variants that can't do this may regulate this function.	[45]
CaMKII-α and α-actinin	Interaction via CaMKII-α association domain. Activity dependant: binding affinity increases with CaMKII T286 autophosphorylation. Densin-180 localises CaMKII-α holoenzymes (newly synthesised in dendrite in response to excitation in glutamatergic synapses)	[46]
	Ternary complex: CaMKII interacts with NR2B, Densin-180 and α-actinin-2	[47]
$Ca_v1.3$ (L-type Ca^{2+}) channels	Calcium dependant facilitation of Cav1.3 channel current requiring association of active CaMKII with Densin-180 and direct association of Densin-180 with Cav1.3-alpha subunit C-terminal domain.	[48]
MAGUIN-1	Ternary complex: Densin-180 --- MAGUIN-1 --- PSD-95	[49]
δ-catenin	Ternary complex: Densin-180 --- δ-catenin --- N-Cadherin. Densin-180 is cytosolic.	[42]
Shank	Densin-180 overexpression causes increased dendritic branching and loss of PSD-95 synaptic clusters; Shank inhibits this effect and targets Densin to PSD membrane; δ-catenin is involved in this pathway.	[51]
β-catenin	Densin-180 associates with Catenin-Cadherin complex (and with Nephrin complex)	[53]

Table 1-2 (above). Densin-180 interaction partners. Table 2-3 (below).

Identified interaction partners	Function	Reference
CaMKII-α	Core PSD component, one of the most abundant proteins in the CNS. Important in the mediation of LTP.	[24][25][29]
α -actinin	Present in multiple cellular regions. Plays multiple key roles, including: linking cytoskeleton to many transmembrane proteins in a variety of junstions; regulating the activity of a variety of receptors; serving as a scaffold to connect the cytoskeleton to diverse signalling pathways.	[64]
Cav1.3 (L-type Ca2+) channels	Expressed together with $Ca_v1.2$ in many tissues, serves a pacemaker function. In neurons, couples activity with transcription events; mediates LTP in amygdala and participates in the consolidation of fear memory.	[61]
MAGUIN-1	A member of the MAGUK protein family, expressed in neurons and localised in cell body and neurites. Interacts with S-SCAM and PSD-95; may play an important role in assembling components of synaptic junctions.	[65]
Shank	Interacts with many signalling and scaffolding PSD molecules via SH3, PDZ, long proline rich region and Sterile Alpha Motif domains. One of the most abundant binding partners of Homer in the PSD; together these are major determinants of size of synaptic spines and of the PSD.	[66]
δ-catenin	Neuron specific Catenin, implicated in adhesion and dendritic branching. Important for normal cognitive development	[67]
β-catenin	Part of adherens junction protein complex. Necessary for creation and maintenance of epithelial cell layers by regulating cell growth and adhesion between cells. Achors actin cytoskeleton and involved in Wnt signalling.	[68]
Other proteins		
NR2B	Core PSD component, an NMDA receptor subunit which acts as binding site for glutamate. Receptors containing this subunit are deeply implicated in the induction of LTP.	[8][9]
PSD-95	A member of the MAGUK protein family, a core PSD protein that acts as a postsynaptic scaffolding molecule, anchoring receptors and cytoskeletal elements at synapses. Associates with other PSD proteins, like GKAP and Shank, where it anchors NMDA receptor associated signalling complexes that regulate synaptic plasticity.	[21][22][23]
N-Cadherin	Neuronal, Calcium-dependent adhesion protein. Transmembrane protein important in cell adhesion, that mediates presynaptic to postsynaptic adhesion and is necessary for the establishment of left-right asymmetry during gastrulation.	[69]

Table 1-3 (above). Function of interacting proteins

Identified interaction partners include: CaMKII-α, α-Actinin and NR2B (via CaMKII-α), $Ca_v1.3$ (L-type Ca^{2+}) channels, MAGUIN-1, Shank, PSD-95 (via Shank and MAGUIN-1), β-Catenin, δ-Catenins and N-Cadherin (via the Catenins). The nature and function of these interactions, detailed in *tables 1-1 and 1-2*, portray Densin-180 as a key interactor in the midst of receptor proteins, scaffolding proteins and structural proteins.

CaMKII-α, α-Actinin, NR2B and $Ca_v1.3$

The direct interaction with CaMKII-α, another core PSD protein, is most interesting, due to its established role in synaptic plasticity. Strack *et al* [45] were first to report this interaction: they found that Densin-180 binds CaMKII-α stoichiometrically and with high affinity, non-competitively to the CaMKII-α--NR2B interaction. Testing developmentally regulated Densin-180 splice variants, they found that one, missing amino acid residues 1331 to 1404, does not bind CaMKII-α, showing that these residues must be of importance to CaMKII-α binding. [^{32}P-Thr^{286}]CaMKII-α bound Densin-180 with a *Kd* of 150 to 250 nM, a *Kd* similar to that for the CaMKII-α – NR2B interaction; Scatchard plot analysis showed that the interaction between CaMKII-α and Densin-180 is a simple bimolecular event. Although NR2B only binds Thr^{286}-CaMKII, it was also shown that Densin-180 also binds inactive CaMKII-α, suggesting that the interactions occur via different mechanisms and that there may be the formation of a ternary complex, consistent with a role for Densin-180 as a CaMKII-α targeting molecule. Furthermore, they showed that coexpression of a membrane targeted fusion protein containing these residues shifted CaMKII-α subcellular localisation, resulting in strong colocalisation, and suggest that Densin-180 constitutively targets CaMKII-α to PSD membranes. [45]

A year later, Walikonis *et al* [46] found this interaction to specifically involve CaMKII-α's association domain and to be activity dependant (CaMKII-α T286 autophosphorylation increased binding affinity), also finding that this interaction does not include CaMKII-holoenzymes including CaMKII-β and other isoforms. They found that this interaction involves Densin-180's C-terminal half, supporting the hypothesis that amino acid residues 1331 to 1404 are important for the interaction. Both Strack *et al* [45] and Walikonis *et al* [46] found that Densin-180 is phosphorylated by CaMKII-α at Serine residue 1397, but suggest that more phosphorylation sites are present. Walikonis *et al* [46] add to the hypothesis presented by Strack *et al* [45], suggesting that CaMKII-α holoenzyme, which is newly synthesised in the dendrites of active glutamatergic synapses, is targeted by Densin-180 to the PSD, and that this function is enhanced when CaMKII-α is in its auto-phosphorylated form and when Densin-180 is phosphorylated. This conforms with the roles played by other LAP proteins, which play essential roles in sorting membrane proteins, and in organising signalling and structural proteins at cellular junctions. They also found that Densin-180 and CaMKII-α form a ternary complex with α-

actinin, a cytoskeletal bundling protein, involving Densin-180 PDZ domain interaction to α-actinin; a complex which was expanded in 2005 by Robison *et al* [47] to include the NR2B NMDA receptor subunit. [46][47]

Earlier this year, Jenkins *et al* [48] reported a facilitation of $Ca_v1.3$ Ca^{2+} channel currents, requiring active CaMKII-α, CaMKII-α association with Densin-180, Densin-180 association with the C-terminal domain of the $Ca_v1.3$ α1 subunit and Ca^{2+}, presenting a novel mechanism for the intensification of postsynaptic Ca^{2+} signals during high frequency signalling involving Densin-180. [48]

MAGUIN-1 and PSD-95

In 2002, an interaction between Densin-180 and MAGUIN-1 (Membrane-Associated GUanylate kinase INteracting protein-1) was discovered [49]. MAGUIN-1 was found to link Densin-180 to PSD-95 [49], another core PSD protein discovered in the 1990s by the Kennedy group. PSD-95, a Membrane Associated GUanylate Kinase (MAGUK), heteromultimerises with another MAGUK, Dlg2, and the complex, with many interaction partners, forms an integral part of the PSD scaffold.

δ-Catenin, N-Cadherin and Shank

The interaction between δ-Catenin (aka NPRAP) and Densin-180 was reported in 2002, and the cell-cell adhesion molecule, N-Cadherin, was also found to be associated with this complex [42].

This supports the idea that Densin-180 has an indirect role in the organisation of synaptic cell-to-cell junction: N-Cadherin has a transmembrane domain, is a known cell-cell adhesion protein that is regulated via the interaction with δ-Catenin; Cadherin-Catenin complexes are known in both pre- and postsynaptic locations.

Furthermore, δ-Catenin has been linked to GSK-3β, linking the protein to the Wnt signalling pathway. The proper expression of δ-Catenin is critical for normal brain function and its turnover is regulated via GSK-3β signalling: an important event influencing synaptic structures and dendritic morphogenesis. [50]

Densin-180 was also found to interact with Shank proteins, prominent constituents of the PSD localised at the interface between membrane receptors and the actin cytoskeleton, believed to play a role in the functional and morphological maturation of spines, via a 2-point interaction, one of these involving Densin-180 amino acid residues 1125-1542 and Shank SH3 domain, and the other involving Densin-180 region immediately preceding the PDZ domain and the N-terminal part of Shank proline rich region (between Shank amino acid residues 318 and 451). Intriguingly, deletions from both the N-terminal and the C-terminal end of Densin-180 were found to gradually affect binding to Shank, highlighting a possible role for Densin-180's LRR region in the interaction. [51]

In HEK cells, coexpression of Shank led to redirection of Densin-180 from plasma membrane to intracellular clusters. In cultured hippocampal neurons, overexpression of Densin-180 caused excessive dendritic branching and the loss of PSD-95 clusters at the PSD, which may be due either to a reduction of the amount of dendritic PSD-95 or to a diffusion of the localisation of PSD-95; coexpression of Shank3 reversed this effect, abrogating branch formation, and retargeted Densin-180 away from the PSD and plasma membrane, and blocked the interaction between δ-Catenin and Densin-180, leading to the suggestion that Shank changes the overall conformation of Densin-180 such that the N-terminal part may no longer target the protein to the membrane. This supports Densin-180's postsynaptic, intracellular localisation and the protein's role in the regulation of synaptic and dendritic spine morphology. [51]

Densin-180 in other tissues

In the kidney, a systematic search by Ahola *et al* [52] for Nephrin-associated molecules, involving the precipitation of glomerular lysates with anti-Nephrin antibody and MALDI-TOF-MS analysis, identified Densin-180 outside the CNS for the first time. Interestingly, 2 molecular weights were observed: 185 kDa, as with previously identified Densin-180, in human podocyte lysates, and, more predominantly, 210 kDa in human glomerular lysates, highlighting the importance of post-translational modifications in fine tuning the protein's function. Electron microscopy found that Densin-180 localised at the slit diaphragms of glomerular podocytes, an important structure thought to be involved in glomerular filtration: a vital function. [52]

Heikkilä *et al* [53] confirmed this in their 2007 paper, in which they report an interaction between Densin, P-cadherin and β-Catenin in kidney glomerular lysates, and find colocalisation of Densin, β-Catenin, and F-Actin in the cell-to-cell contacts of cultured mouse podocytes; they propose that Densin may be involved in the formation of cell-to-cell contacts, including slit diaphragms. [53]

Interestingly, Densin was also found at another vital junction, in the Sertoli cells of the testes. Sertoli cells are responsible for establishing and maintaining the spermatogonial stem cell niche, binding spermatogonial cells via N-Cadherins and carbohydrate residues. Densin was found colocalised with β-Catenin and N-Cadherin at the junction between Sertoli cells and spermatogonial cells, a junction that undergoes extensive restructuring during the process of spermatogenesis. [54]

Much like dendritic spines and glomerular podocytes, Sertoli cells form foot-shaped structures; in line with Densin-180's likely role in dendritic spines, it is thought that Densin-180 plays a similar role in these locations, maintaining cytoarchitecture and connections to the cytoskeleton at these vital junctions, via similar interactions and mechanisms.

Other LAP proteins

Since the discovery of Densin-180, other LAP proteins have been identified, which led to the definition of the LAP protein family, which are classified according to the number of PDZ domains they carry. Examples include Scribble, Erbin and Lano.

Of these, Erbin is Densin-180's closest relative, sharing 69% of its amino acid sequence identity (see *appendix* section for protein alignments); the two proteins, carrying 1 PDZ domain, define the LAP1 subfamilly of proteins and with 59 hits on Pubmed, Erbin is also Densin-180's better characterised relative.

First reported in the 2000 paper by Borg *et al* [55], Erbin was identified interacting with Receptor Tyrosine Kinase (RTK): ErbB2/HER2, an orphan receptor, activated by heterodimerisation with other RTKs such as EGFR and involved in morphogenesis and oncogenesis. Erbin was found to act as an adapter protein binding directly and specifically via its PDZ domain to ERBB2/HER2; mutations to Erbin binding site led to mislocalisation of the ERBB2/HER2 receptor [55].

An interesting example of Erbin's involvement in ErbB receptor mediated signalling is outlined in a 2009 paper, in which Tao *et al* [56] demonstrate the necessity of Erbin in NRG1 signalling (via the Akt intracellular pathway) and how this effects myelination in the peripheral nervous system. In Erbin-null mice, they observed hypomyelination of myelinated axons and abnormal ensheathing of unmyelinated axons in Remak bundles, as well as an increased number of axons per Remak bundle, causing decreased nerve conduction velocity and increased sensory threshold to mechanical stimulation (Remak bundles occur when Schwann cells group together unmyelinated axons from multiple neurons, ensheathing them in a way that prevents any of the axons from touching). They were able to reproduce these effects in mice expressing mutant Erbin, lacking the PDZ domain, which is important in mediating the interaction between Erbin and ErbB2. They observed a reduction of ErbB2 protein in the sciatic nerves of mice expressing this mutant Erbin and demonstrated that the ErbB2 receptor becomes unstable, compromising NRG1 signalling, when Erbin expression was suppressed. They suggest that Erbin binds to, via its PDZ domain, and stabilises ErbB2 receptors in mouse sciatic nerves, a process that is necessary for NRG1 signalling. [56]

Erbin was also implicated in the MAP Kinase pathway by Huang *et al* [57], who show that the protein hinders Raf activation through an interaction between Erbin and active Ras, which inhibits the interaction between active Ras and Raf. They showed that Erbin overexpression leads to inhibition of NGF-induced neuronal differentiation of PC12 cells, while downregulation of Erbin caused the opposite effect, potentiating NGF-induced neuronal differentiation of these cells. [57]

The parallels between Densin-180 and Erbin are many, as can be seen in *table 1-4*, a comparison of their domain sequence identities.

Domain	% Identity
LRR rich	70
LAPSDa	71
LAPSDb	79
Spacer region between LAPSD motifs	54
Phosphorich region	27
PDZ domain	72
Total	*69*

Table 1-4. Densin-180 vs Erbin: domain homology

Densin-180 and Erbin are close homologues, sharing 69% amino acid sequence identity. Since Densin-180 and Erbin have the same complement of identified domains, with a high degree of amino acid sequence identity across these, it is likely that Densin-180, like Erbin, is adapted to function as an anchor protein for receptor complexes and may even have a role in cell signalling events.

As reviewed above, the N-terminal end, with its LRR region, is thought to act as a ligand binding domain, conferring localisation to specialised lipid microdomains in the plasma membrane, while the C-terminal end, with its PDZ domain, mediates protein-protein interactions with a number of proteins.

The major differences between the two proteins are Densin-180's phosphorylation rich region and, to a lesser extent, the spacer region between LAPSD motifs. The phosphorylation rich region may underlie differences in how Densin-180 interacts with kinases and other proteins and how these interactions are regulated, while the spacer region, being longer in Densin-180 than in Erbin, may affect the tertiary structure of Densin-180, adding flexibility to its N-terminal end, and may underly differences in how Densin-180's LRR region may interact with proteins

In this thesis

In order to study the subcellular localisation and behaviour of Densin-180, eGFP-tagged fusion constructs were designed and generated, allowing live imaging and convenient antibody tagging when expressed in cells. Phospho-null, phosphorylation rich region truncation and PDZ domain / C-terminal amino acid deletion variants of the eGFP-tagged Densin-180 fusion constructs were also generated. The eGFP-tagged Densin-180 fusion constructs come in two flavours (*figure 1-13*):

- N-terminally eGFP-tagged Densin-180, pRK7a-N-eGFP-hLrrc7-WT, in which an eGFP tag is introduced between the Cys 14/16 and LRR sequences, so as to minimise any effect that the introduction of the tag may have on the function of either of these features.
- C-terminally eGFP-tagged Densin-180, pRK7a-hLrrc7-eGFP-C-WT, in which an eGFP tag is introduced at the end of the Densin-180 sequence.

Since the eGFP tag, comprised of 238 amino acid residues, is a rather large tag, it can be expected that its introduction into Densin-180 may alter the normal functioning of the protein. By introducing the tag in either the N-terminus or the C-terminus, any alterations to the protein's behaviour or function will allow extrapolations to be made with regards to the characterisation of the protein's features and domains.

For the detailed study of Densin-180's C-terminus, which is known to be involved in a number of protein-protein interactions, 3 deletion constructs were also designed and generated (*figure 1-13*):

- pRK7a-N-eGFP-hLrrc7-PDZ-A, N-terminally eGFP-tagged Densin-180 missing the entire PDZ domain except for its last 3 terminal amino acids residues,
- pRK7a-N-eGFP-hLrrc7-PDZ-B, N-terminally eGFP-tagged Densin-180 missing the entire PDZ domain and the very C-terminal amino acids,
- pRK7a-N-eGFP-hLrrc7-PDZ-C, N-terminally eGFP-tagged Densin-180 missing the very C-terminal 3 amino acids.

Any effect caused by the introduction of the C-terminal eGFP-tag is likely to be caused by a disruption of function linked to the amino acids most closely neighbouring the tag; PDZ domains are known to bind selected peptides with hydrophobic residues at their C-termini and have unique optimal binding motifs specific to their types. These deletion constructs are designed to study the importance of Densin-180's C-terminal amino acid residues, should they be acting as PDZ-domain ligands, and of its PDZ domain.

Further, to elucidate the function of Densin-180's phosphorylation rich region, amino acid residues 826 to 1213, which may be fundamental in Densin-180's unique role in the PSD, since it represents, as mentioned above, the major structural difference between Densin-180 and Erbin, its closest homologue, as well as an area in which regulation of Densin-180 may occur. Of the phosphorylation sites discovered to date, the sites at residues T865, T868 and T869 were chosen because these together constitute the highest density of phosphorylation sites within the phosphorylation region. What's more, inserting phosphorylation-null mutations knocking out all three sites could be done using a single pair of primers. The following 4 constructs were designed and generated (*figure 1-14 and 1-15*):

- N-terminally eGFP-tagged TTT865/868/869AAA triple phospho-null Densin-180, pRK7a-N-eGFP-hLrrc7-TTT865/868/869AAA,
- C-terminally eGFP-tagged TTT865/868/869AAA triple phospho-null Densin-180, pRK7a-hLrrc7-eGFP-C-TTT865/868/869AAA,
- N-terminally eGFP-tagged phosphorylation rich region truncated Densin-180, pRK7a-N-eGFP-hLrrc7-nophosphorich, in which amino acids 702 to 1422 are removed,
- C-terminally eGFP-tagged phosphorylation rich region truncated Densin-180, pRK7a-hLrrc7-eGFP-C-nophosphorich, in which amino acids 702 to 1422 are removed.

Densin-180 appears to function as a key adapter protein, coordinating cytoskeletal, scaffolding and receptor molecules in the adaptation, maintenance and regulation of highly dynamic cell to cell contacts in the synapses of the CNS, and in the kidney and testis of the periphery, yet its function remains obscure.

Here we present constructs allowing for the functional characterisation of Densin-180 and of its specific domains. We also present observations and data from HEK cell expression studies of these constructs showing that Densin-180's N-terminal Cys 14/16 residues and LRR region may be of importance for its membrane localisation and that its PDZ domain and very C-terminal amino acid residues play key roles in protein-protein interactions. We also show that CaMKII-α has a targeting effect, altering Densin-180's subcellular localisation, an effect dependant on Densin-180's C-terminal region.

Figure 1-13 (following page). Top: N-terminally eGFP-tagged Densin-180, pRK7a-N-eGFP-hLrrc7-WT, in which an eGFP tag is introduced between the Cys 14/16 and LRR sequences. Middle: C-terminally eGFP-tagged Densin-180, pRK7a-hLrrc7-eGFP-C-WT. Bottom: N-terminally eGFP tagged C-terminal and PDZ Domain deletion construction: pRK7a-N-eGFP-hLrrc7-PDZ-A, pRK7a-N-eGFP-hLrrc7-PDZ-B, pRK7a-N-eGFP-hLrrc7-PDZ-C, with deletions detailed in the box.

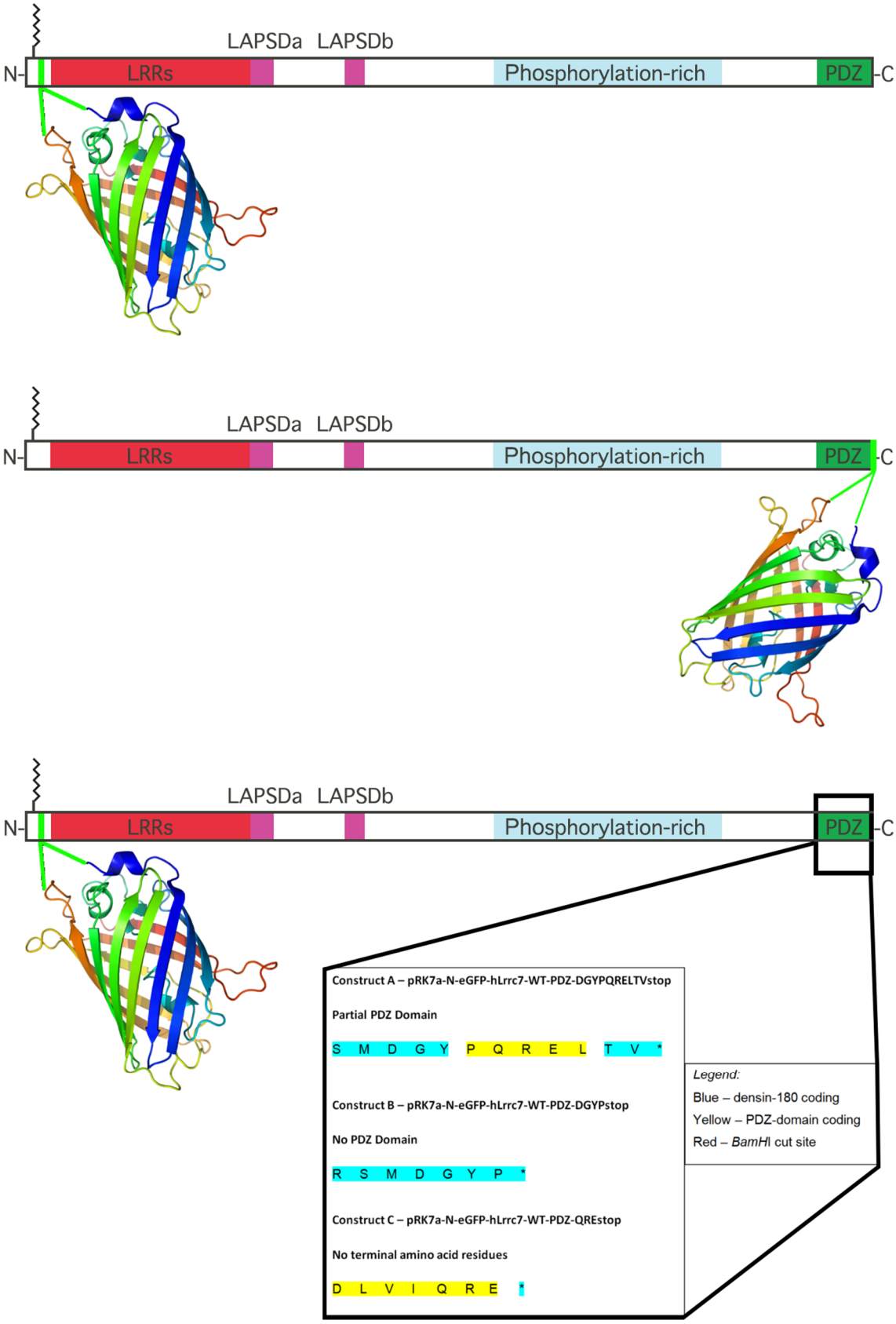
LAPSDa LAPSDb
N-
LRRs
Phosphorylation-rich
PDZ
-C
LAPSDa LAPSDb
N-
LRRs
Phosphorylation-rich
PDZ
-C
LAPSDa LAPSDb
N-
LRRs
Phosphorylation-rich
PDZ
-C
Construct A – pRK7a-N-eGFP-hLrrc7-WT-PDZ-DGYPQRELTVstop
Partial PDZ Domain
S M D G Y P Q R E L T V *
Construct B – pRK7a-N-eGFP-hLrrc7-WT-PDZ-DGYPstop
No PDZ Domain
R S M D G Y P *
Construct C – pRK7a-N-eGFP-hLrrc7-WT-PDZ-QREstop
No terminal amino acid residues
D L V I Q R E *
Legend:
Blue – densin-180 coding
Yellow – PDZ-domain coding
Red – BamHI cut site

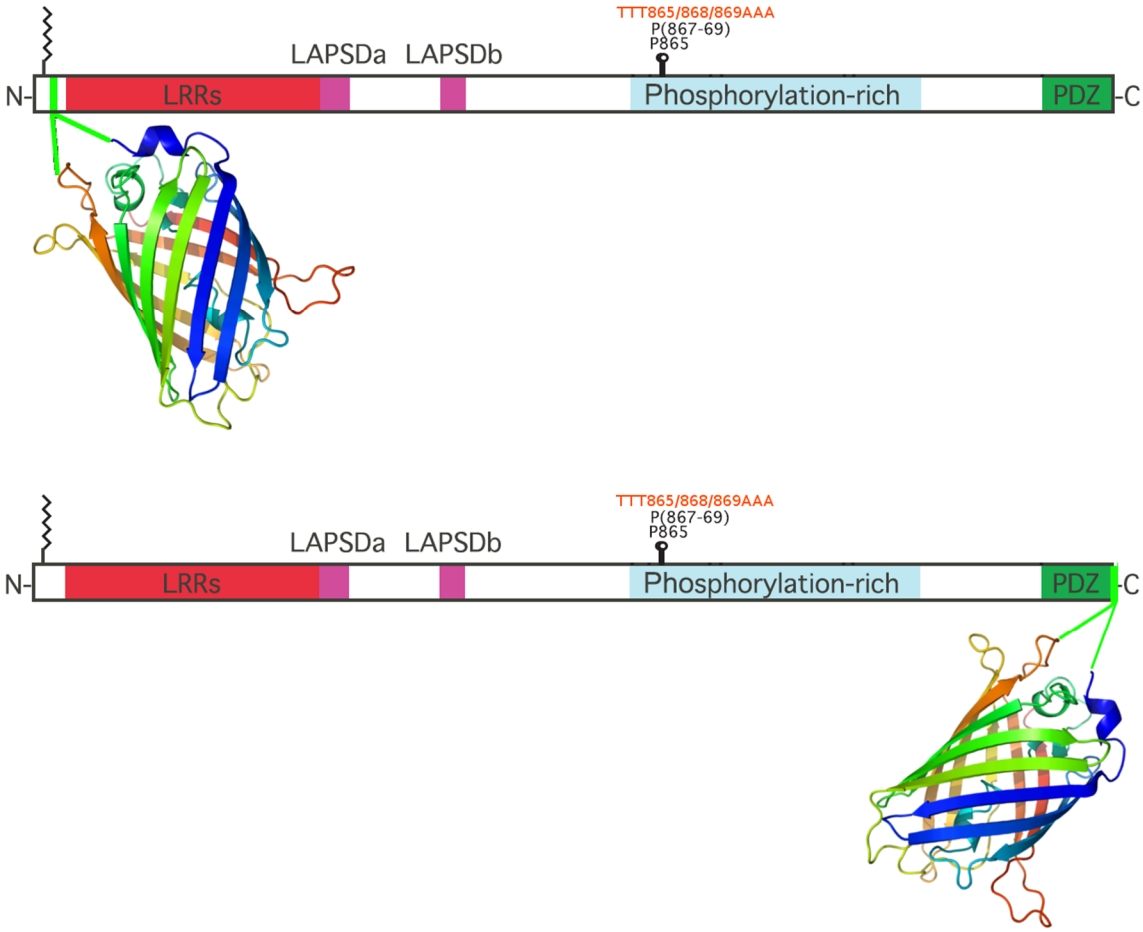

Figure 1-14. Top: N-terminally eGFP-tagged TTT865/868/869AAA triple phospho-null Densin-180, pRK7a-N-eGFP-hLrrc7-TTT865/868/869AAA. Bottom: C-terminally eGFP-tagged TTT865/868/869AAA triple phospho-null Densin-180, pRK7a-hLrrc7-eGFP-C-TTT865/868/869AAA.

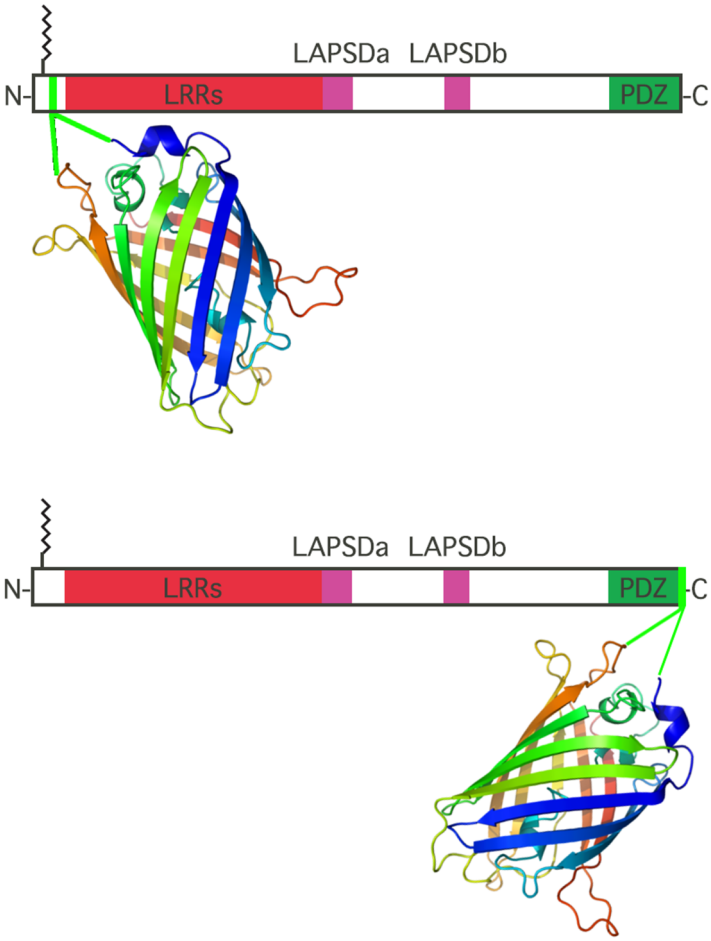

Figure 1-15. N-terminally eGFP-tagged phosphorylation rich region truncated Densin-180, pRK7a-N-eGFP-hLrrc7-nophosphorich (top), C-terminally eGFP-tagged phosphorylation rich region truncated Densin-180, pRK7a-hLrrc7-eGFP-C-nophosphorich (bottom). In both, amino acid residues 702 to 1422 are truncated, effectively truncating the phosphorylation rich region between amino acid residues 826 to 1213.

Materials and methods

Materials

Chemicals

All chemicals were purchased from Sigma-Aldrich [St Louis, Missouri, USA], Invitrogen [Carlsbad, CA, USA], Merck [Whitehouse Station, New Jersey, USA] or VWR [West Chester, PA, USA]. Cell culture media, sera and buffers were purchased from Invitrogen, culture dishes and tubes from Nunc [Roskilde, Denmark] and BD labware [Franklin Lakes, NJ USA]. Milli-Q [Millipore, Billerica, Massachusetts, USA] purified water was used throughout. Oligonucleotides were purchased from Sigma-Aldrich and diluted in TE or H_2O to 100 µM stocks.

Standards and buffers

Buffer	Components
PBS	16 mM Na_2HPO_4, 4 mM NaH_2PO_4, 150 mM NaCl
TAE	40 mM Tris-acetate, 1 mM EDTA, pH 8.0
TE	10 mM Tris, 1 mM EDTA, pH 8.0
HEK Medium	90% DMEM + Glutamax (1x) + 4.5 g/L Glutamate - pyruvate; 10% FBS; 1x Na^+Pyruvate; 1x Penicillin-Streptomycin
Inoue Transformation Buffer	10.88 g $MnCl_2$, 2.2 g $CaCl_2$, 18.65 g KCl, 2.13 g BES and H_2O to a total volume of 1l

Methods

Standard Molecular Biology techniques

Bacterial cultures

DH5-α cells were streaked onto LB-agar plates and incubated overnight at 37°C to obtain single colonies. Single colonies were picked and used to inoculate 2 ml Terrific Broth (TB) medium cultures, which were incubated overnight at 37°C with vigorous shaking (250 rpm). For selection, 100 µg.ml^{-1} Ampicillin was added to culture media.

Minipreparation of plasmid DNA

1.5 ml of TB medium overnight culture was centrifuged for 30 seconds at 10,000 rpm on a Centrifuge 5415C [Eppendorf, Hamburg, Germany], supernatant removed by careful suction and cell pellet resuspended on ice in 150 µl of miniprep solution I (50 mM glucose, 20 mM Tris-HCl (pH 8.0), 2.5 mM EDTA (pH 8.0)). 300 µl of freshly prepared miniprep solution II (100 mM NaOH, 1% SDS in H_2O) was then added and samples were mixed vigorously and incubated on ice for 5 mins to allow cell

lysis. Still on ice, 200 µl of miniprep solution III (3.375 M potassium acetate and 2 M acetic acid) in water was added, the mixture vortexed, incubated for 5 mins on ice to allow its neutralisation and centrifuged (5 mins at 14,000 rpm). 30 mg RNAase A was then added and mixture was incubated at 37°C on a heat block for digestion. 300 µl Phenol:Chloroform:Isoamylalcohol (25:24:1) was then added, mixture vortexed for 15 seconds, centrifuged (5 mins at 14,000 rpm) and aqueous layer transferred to new tube in order to clean up sample. 1 ml of 100% EtOH was then added to precipitate DNA and mixture was then centrifuged at 4°C (5 mins at 14,000 rpm) and dried. This was repeated with 500 µl 70% EtOH. Plasmid DNA was then resuspended in 50 µl H_2O or TE buffer and analysed by Nanodrop spectrometry (see below for details), restriction digest and gel electrophoresis. Typical yields of 0.1 µg per µl.

Maxipreparation of plasmid DNA

Method based on Qiagen [Hilden, Germany] Plasmid Maxi protocol, using QIAGEN-tip 500.

A single colony from a freshly streaked plate was picked to inoculate a 2 ml LB containing 200 $\mu g.ml^{-1}$ Ampicillin pre-culture, which is then incubated for 6 hrs at 37°C with vigorous shaking (250 rpm). 100 µl of this pre-culture was then used to inoculate 100 ml LB containing 200 $\mu g.ml^{-1}$ Ampicillin culture in a 1 L Erlenmeyer flask, which was incubated for 19 hrs at 37°C with vigorous shaking (250 rpm). Culture was then centrifuged at 4°C (6500 rpm in a Beckman JA-14 rotor) and cleared of medium. Pellet was then processed as specified in Qiagen Plasmid Maxi protocol and plasmid DNA was resuspended in 300 µl TE buffer (pH 8.0). Yield was determined by Nanodrop spectrometry (see below) and volume adjusted to achieve a DNA concentration of 1 $\mu g.\mu l^{-1}$; typical yields of 300 to 600 µg of plasmid DNA were obtained.

Polymerase Chain Reaction

cDNA fragments containing coding sequence of the mutations S949A and TTT865/868/869AAA were designed and generated by Professor Ralf Schoepfer and by Moheb Costandi.

Strategy for the construction of N- and C-terminally eGFP-tagged Wild Type hLrrc7 fusion constructs was designed by Dr Agnes Thalhammer.

cDNA fragments containing the coding sequence of eGFP were generated by Polymerase Chain Reaction (PCR). This was performed in 50 µl 1x KOD Polymerase buffer [Toyobo, Osaka, Japan], containing 1:100 dilution of pBS.EGFP-MT-CK2a [30] miniprep DNA with 0.4 µM of each primer, 0.2 mM of each nucleotide and 1.25 Units of KOD Polymerase enzyme [Toyobo, Osaka, Japan]. The PCR cycle was started with a 95°C, 5 min hot start step, in order to heat activate polymerase and to ensure melting of all DNA components, and was followed by 30 rounds of: a) melting, 95°C; b)

annealing, at lowest predicted primer Tm, c) polymerisation, 72°C. The cycle ended with a pause at 10°C. Products were separated by gel extraction, which was followed by analytical restriction digests prior to usage in subcloning steps.

Estimation of DNA concentration

Throughout, DNA concentrations and 260/280 readings were estimated using a Nanodrop 1000 spectrophotometer [Thermo Scientific, Waltham, Massachusetts, USA].

Restriction enzyme digestion of DNA

0.5 µg (analytical) to 4 µg (preparative) plasmid DNA was digested with 5 Units of restriction enzyme(s) in a total volume of 20 to 50 µl with appropriate buffers and conditions, as specified by enzyme suppliers [New England Biolabs, Ipswich, Massachusetts, USA]. Products were separated and purified by gel extraction prior to usage in ligation step(s).

Agarose gel electrophoresis of DNA

DNA was run in TAE buffer on 0.6% to 1.2% Agarose gels containing 0.5 $\mu g.ml^{-1}$ Ethidium Bromide. SeaKem LE Agarose [Lonza, Basel, Switzerland] was used for analytical gels and SeaKem GTG, low-melting Agarose [Lonza, Basel, Switzerland] was used for purification of DNA fragments. Orange G buffer (1 $mg.ml^{-1}$, 10 mM Tris-HCl pH 7.5 and 30% Glycerol) was used as DNA loading buffer.

λ-phage DNA digested with *Sty*I or pBluescript II KS+ (Stratagene) plasmid DNA digested with MspI were used as DNA standard ladders.

Gel extraction of DNA fragments

Following separation of DNA fragments by electrophoresis on GTG Agarose gels, desired DNA fragments were excised and purified using the JETSORB DNA extraction kit [GENOMED GmbH, Löhne, Germany] following instructions available on manufacturer website http://www.genomed-dna.com/.

Ligation of DNA fragments

Reaction was carried out in a total volume of 10 µl 1x Ligase buffer (supplied by manufacturer), containing vector and insert fragments in a 1:1 volume ratio and 1-2 Units of T4 DNA Ligase [Roche, Penzberg, Upper Bavaria, Germany]. Reaction mixture was then incubated overnight at 16°C.

Preparation of frozen stocks of chemically competent E. Coli cells

Based on protocol from Hannah Morgan, Stocker lab. Modified from Inoue *et al* [58]

DH5-α were streaked on an LB plate and incubated for 16 to 20 hrs at 37°C. A single colony was picked to inoculate a 25 ml SOB medium [Difco, BD – Diagnostic Systems, New Jersey, USA] starter

culture (prepared per label directions), which was incubated at 37°C for 6 to 8 hrs with vigorous shaking (250 rpm). From this, 3 x 130 SOB medium cultures in 1 L Erlenmeyer flasks were inoculated with: 1) 5 ml starter culture; 2) 2 ml starter culture; 3) 1 ml starter culture and were incubated for 16 to 20 hrs at 18°C. Absorption readings were measured and cultures with OD600 of 0.55 to 0.6 were processed on ice, following sterile handling procedure.

First, cultures were centrifuged at 4°C (4,000 rpm in a Beckman JA-10 rotor), supernatant was removed, cells were resuspended in 40 ml Inoue transformation buffer and incubated on ice for 10 mins. These were then centrifuged again at 4°C (4,000 rpm in a Beckman JA-10 rotor), cleared of supernatant and resuspended in 5 ml Inoue transformation buffer. 750 µl DMSO (pure grade) was added to suspension while gently shaking mixture; 100 µl aliquots were made in 1.5 ml Eppendorf tubes, shock frozen with liquid nitrogen and stored at -70°C.

Competence was tested by transforming with pBluescriptII KS+ plasmid (Stratagene) yielding efficiencies on LB containing 100 $\mu g.ml^{-1}$ Ampicillin agar plates of 2 to $3x10^7$ colonies per µg DNA.

Transformation of chemically competent E. Coli cells

For each transformation, 1 (100 µl) aliquot of frozen chemically competent cells was thawed on ice. 10 µl of DNA solution was added and mixture incubated on ice for 10 mins before 5 min incubation at 37°C in a waterbath, after which 110 µl LB medium was added and mixed in gently. The mixture was then incubated for 15 mins at 37°C for 15 mins and plated onto LB + 100 $\mu g.ml^{-1}$ Ampicillin agar plates, which were then incubated overnight at 37°C.

PEG (polyethylene glycol) precipitation of DNA

Used to clean up Miniprep DNA for sequencing.

In a 1.5 ml Eppendorf tube, 8 µl of miniprep DNA (~4 µg DNA) was precipated on ice in 2 µl of 4 M NaCl and 10 µl of 13% PEG solution for 15 mins. This was centrifuged for 15 mins at 14,000 rpm at 4°C. Supernatant was removed by careful pipetting, making sure not to disturb invisible pellet, which was then washed once with 50 µl 70% EtOH, air-dried and resuspended in 10 µl H_2O. DNA concentration was estimated using a Nanodrop spectrophotometer.

DNA sequencing

Clean DNA was sequenced via the dideoxy method using the BigDye v3.1 terminator cycle sequencing kit [Applied Biosystems Inc]. A 10 µl total volume containing 1x BigDye Sequencing buffer, 1x Ready Reaction Premix, 3.2 pmol of primer and 400 ng of template DNA was cycled as follows: a) 96°C, 5 mins, hot start, followed by 30 cycles of b) DNA melting, 96°C, 30 seconds; c) annealing, 50°C, 15 seconds; d) polymerisation, 60°C, 4 mins, and ending with e) pause at 10°C.

Reactions were precipitated in 24 µl 100% EtOH and 1 µl 3 M NaAc pH 4.5 on ice for 15 mins and centrifuged at 4°C at 14,000 rpm (Biofuge 1.3, Heraeus) for 15 mins. Supernatant was carefully removed, pellet washed with 50 µl 70% EtOH and air dried. This was processed in-house by Stuart Martin in the Andrew Huxley building at UCL. Sequencing files were analysed with Sequencher v3.1 (Gene Codes Corporation Inc.). Accurate sequences of 500 to 700 base pairs were generally obtained.

HEK-TSA cell expression system

All solutions used below are autoclaved or sterile filtered to ensure sterility. Sterile handling procedure is used throughout and most parts described are conducted in microbiological hazard containment unit.

Thawing HEK-TSA cells

Aliquots stored in -140°C Nitrogen storage device were thawed in 37°C waterbath over a couple of mins. Using sterile handling procedure, 1 ml HEK medium, pre-warmed to 37°C, was added to vial and contents transferred to a 14 ml tube, to which a further 8 ml warm HEK medium was added. This was then centrifuged at 800 rpm for 3 mins in a Megafuge 1.0 [Hereaus], cleared of supernatant, resuspended in 5 ml warm HEK medium, transferred to a 28 cm^2 flask and, then, left overnight in a humidified incubator at 37°C, 5% CO_2. Medium was changed the next day, cells checked and flask replaced in humidified incubator. 3 days later, cells were confluent enough for splitting into 80 cm^2 culture flasks.

Splitting HEK cells

Medium is removed from confluent cells in 80 cm^2 culture flask and replaced with 1x PBS which is left to stand on the monolayer for a few seconds. 1x PBS is then replaced with 5 ml 1x Trypsin and trypsinisation is allowed for 1 min. 5 ml of warm HEK medium is added to stop trypsinisation and monolayer is rinsed with this solution a few times to resuspend cells. Suspension is transferred to a new 14 ml tube and centrifuged (3 mins at 2000 rpm in Megafuge 1.0, Heraeus). Supernatant is removed and pellet resuspended in 10 ml warm HEK medium. Cell count is estimated using haemocytometer and cells plated in warm HEK medium in the following amounts:

-5 to $7x10^5$ cells for 80 cm^2 culture flasks or 9 cm diameter culture dish with total volume of 10 ml, -$7.5x10^4$ cells for Laminin and poly-D-ornithine coated 13 mm diameter coverslips in 24-well plates with total volume of 500 µl.

These are left in a humidified incubator (37°C, 5% CO_2). Cells are confluent for next splitting 3 days later.

Transfection of HEK-TSA cells using Lipofectamine 2000 reagent

50 µl of Lipofectamine 2000 solution (2 µl of Lipofectamine 2000 reagent in 48 µl OptiMEM) was added to 50 µl of 1 µg DNA in OptiMEM and left to form complexes for 30 mins. Medium was removed from 60% confluent cells on coverslips, the 100 µl of Lipofectamine 2000 + DNA solution was added and incubated in humidified incubator (37°C, 5% CO_2) for 20 mins. This was then replaced with warm HEK medium; cells were then replaced in incubator overnight and checked for expression the following day.

Confocal microscopy

The localisation of recombinant fusion protein in HEK-TSA cells was examined by confocal microscopy. Following transfection and appropriate expression time (1 to 2 days), cells were fixed in 4% PFA, 4% sucrose and 1x PBS solution and coverslips mounted onto SuperFrost microscope slides using Gel Mount Aqueous Mounting Medium.

A Radiance 2100 system [BioRad, Hercules, California, USA] was used to take stack images with an oil-immersion 100x oil objective + 2.8x optical zoom with 0.2 µm step size, corresponding to a lateral resolution of 212.63 nm and an axial resolution of 520 nm (computed using resolution calculator on the MRC Cell Biology Unit's Light Microscopy Facility website). A 488 nm Argon laser was used for excitation of eGFP-tag and a Green HeNe laser at 543nm excitation wavelength for excitation of co-expressed mRFP. The pinhole size was set to 1.4 Airy disc units.

Analysis

Analysis was carried out using ImageJ, MS Excel and IgorPro. Raw stack images were Z-projected (Images => Stacks => Z-Project: maximum intensity) and colour channels were merged (Image => Colour => Merge Channels) prior to analysis to improve file handling.

Fluorescence profile analysis

This was done on eGFP signal of cells by applying the plot profile function (Analyze => Plot profile) on straight line selections drawn across each cell being analysed. The data was then exported into MS Excel and analysed to determine the occurrence of type I, type II or other subcellular behaviour.

Particle distribution analysis

Files were blind labelled, kindly done by Yogesh Malam, in order to reduce bias in this analysis. eGFP-channel of images was manually thresholded to produce binary representations of Densin-180 subcellular distribution (Images => Adjust => Threshold) on which particle analysis was carried out (Analyze => Analyze Particles: particle size = 0 to infinity; circularity = 0 to 1). This is shown in the figure below.

Raw particle area data was exported to MS Excel, blind labels were decoded and the data were concatenated according to Densin-180 variant imaged. This data was then imported into IgorPro and histograms were computed (Analysis => Histogram); a minimum area cut-off was worked out to be 0.04521 μm^2 (= microscope lateral resolution^2) and bin sizes were set to twice this value in order to prevent subsampling, in accordance to Nyquist's Theorem. Cumulative frequency distribution and Kolmogorov-Smirnoff tests were computed In MS Excel; all graphs were generated using IgorPro.

Following page. Workflow: 2D particle distribution analysis. Image channels are split, the eGFP channel is thresholded and particle analysis is run on this 8-bit data yielding particle data.

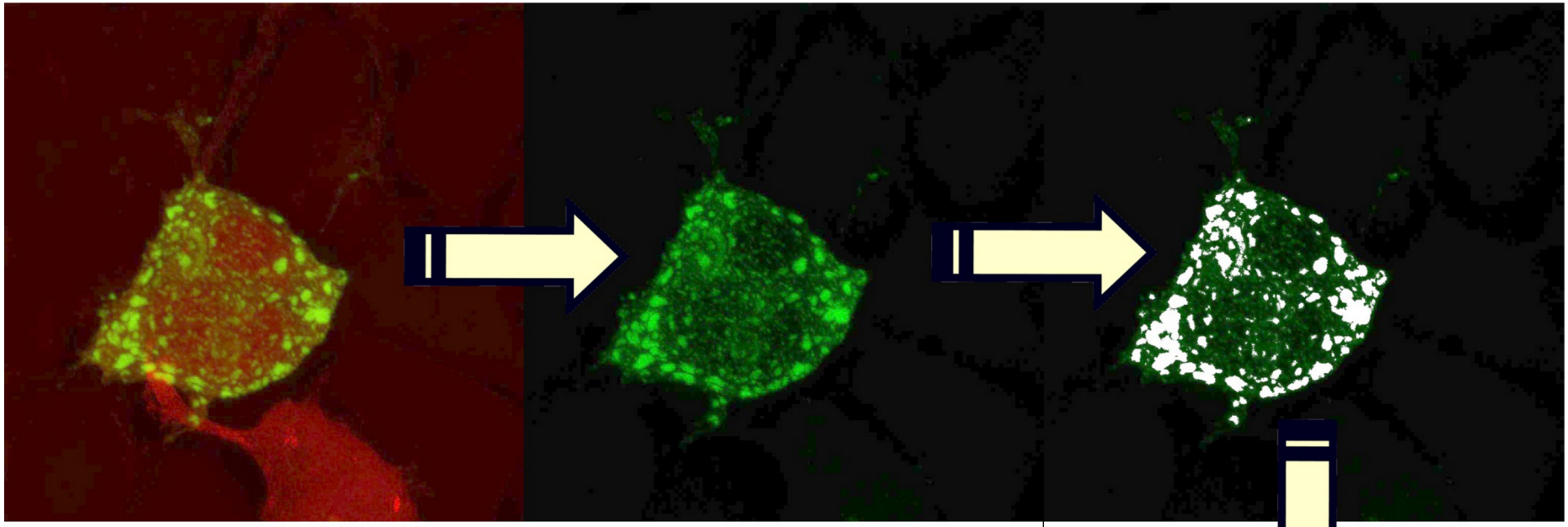

Results

File Edit Font Results

	Area	Mean	Min	Max
390	759	27.941	14	67
391	29	16.103	14	22
392	1	16	16	16
393	1	16	16	16
394	270	23.459	14	41
395	198	21.919	14	33
396	1	15	15	15

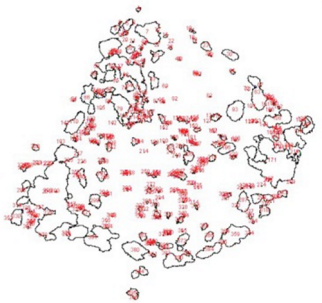

Results

Cloning overview

For cloning purposes, hLrrc7 construct was shuffled into pBluescriptII KS+ vector (Stratagene).

Tagging the N-terminus
This was done using an Overlap Extension Joining PCR approach, joining 2 PCR products.

PCR1 (*schema 1-1*), designed to amplify the first coding sequence of Densin-180's first 33 amino acids from the vector backbone, also adds a 17 base pair overhang complimentary to the first 24 base pairs of the eGFP coding sequence.

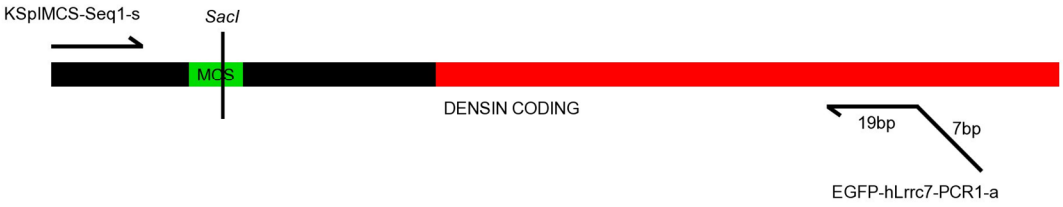

Schema 1-1. PCR1 amplifies the Densin-180 N-terminus coding sequence and the KS+ Multiple Cloning Site (MCS). Template: KS+-hLrrc7-unrepaired. Sense primer: KSpIMCS-Seq1-s. Antisense primer: EGFP-hLrrc7-PCR1-a. Red: Densin code. Black: vector code. Green: MCS.

PCR2 (*schema 1-2*) was designed to amplify the eGFP coding sequence (excluding stop codon) from pBS.EGFP.MT.CK2a [30], adding a 19 base pair overhang complimentary to the end 19 base pairs of PCR1 product fragment, preceding the eGFP coding sequence, and introducing a *BglII* site following the eGFP coding sequence.

Schema 1-2. PCR2 amplifies the eGFP coding region. Template: pBS.EGFP.MT.CK2a. Sense primer: EGFP-hLrrc7-PCR2-s. Antisense primer: EGFP-PCR2-a (designed by Cezar E. Tigaret). Green: eGFP coding. Black: vector coding.

Essentially, the primers EGFP-hLrrc7-PCR1-s and EGFP-hLrrc7-PCR2-s are almost fully complimentary: the product fragments obtained from PCR1 and PCR2 have 36 bp complementary overhangs (*schema 1-3*), on which the Overlap Extension Joining PCR relied on.

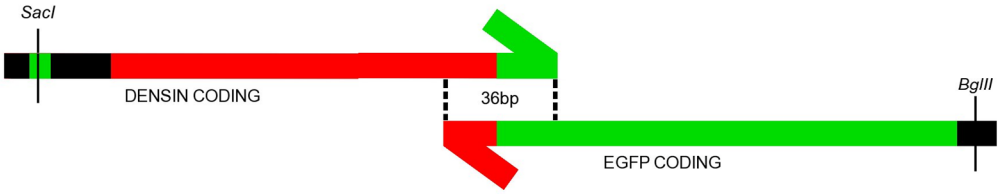

Schema 1-3. PCR3: 1st desired reaction in Overlap Extension Joining PCR in which the products of PCR1 (top) and PCR2 (bottom) act both as primers and templates for the reaction. Red: Densin code. Green: eGFP code.

The Overlap Extension Joining PCR (PCR3) used: the products of PCR1 and PCR2 as both templates and primers; the outer primers used in PCR1 and PCR2, also as primers, this time priming amplification of the first product in the reaction (*schema 1-4*).

Schema 1-4. PCR3: the product of reaction shown in schema 1-3, the desired end product, is amplified by outer primers from PCR1 and PCR2. Red: Densin code. Green: eGFP coding.

The product derived from PCR3 was shuffled into pRSET6a-Ca-His vector using *Sac*I and *Bgl*II restriction sites (*schema 1-5*).

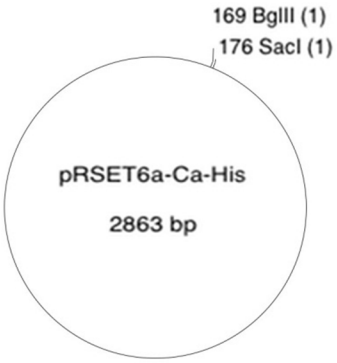

Schema 1-5. pRSET6a-Ca-His used here as an intermediate cloning vector.

The final PCR, PCR4, amplified Densin-180 sequence containing *Xho*I restriction site, necessary for the ultimate replacement of untagged N-terminus with eGFP-tagged N-terminus, downstream of Densin-180 sequence coded in PCR3 derived fragment, while adding a *BamH*I site for shuffling into intermediate construct (pRSET6a-Ca-His-PCR3) immediately adjacent to PCR3 derived sequence (*BamH*I and *Bgl*II have compatible ends).

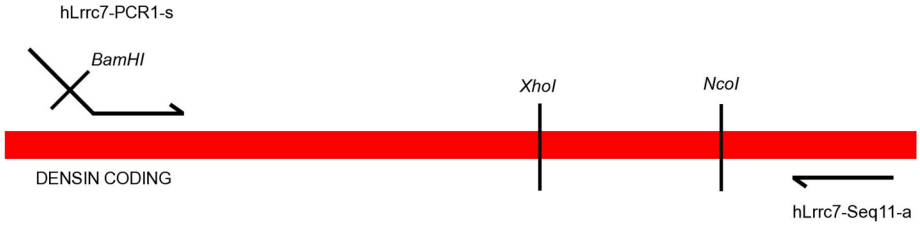

Schema 1-6 – PCR4: Amplification of Densin-180 code downstream from where it was left off in PCR1. Template KS+-hLrrc7-unrepaired. Sense primer: hLrrc7-PCR1-s. Antisense primer: hLrrc7-Seq11-a. Red: Densin coding.

The PCR4 derived product was shuffled into intermediate construct using *BamH*I/*Bgl*II and *Nco*I restriction sites (*schema 1-7*).

Schema 1-7. Insertion of PCR4 product via BglII and NcoI into intermediate vector where PCR3 product has been inserted.

The thereby joined PCR3xPCR4 derived stretch containing the eGFP-tagged Densin-180 N-terminus was shuffled into Densin-180 construct, replacing untagged N-terminus, using *Not*I and *Xho*I restriction sites (*schema 1-8*).

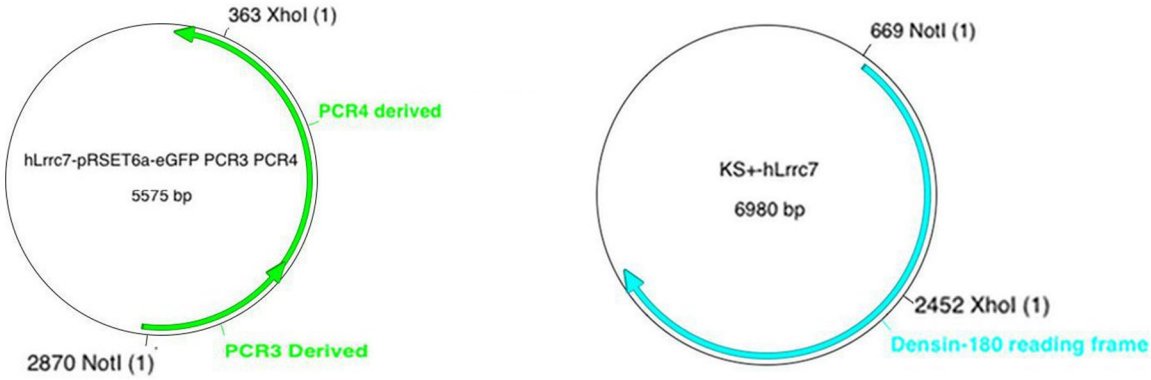

Schema 1-8. Shuffling eGFP tagged Densin-180 N-terminus coding sequence from intermediate cloning vector and into untagged Densin-180 construct via NotI and XhoI restriction sites, replacing untagged N-terminus code.

Tagging the C-terminus

This was done using Overlap Extension Joining PCR, the same principle used to tag the N-terminus (*schema 2-1*): PCR1' was used to amplify the Densin-180 C-terminus coding region, replacing the stop codon with a 24 base pair stretch equating to the N-terminal eGFP code sequence; PCR2' was used to amplify the eGFP coding sequence, adding a 23 base pair stretch equating to the C-terminal Densin-180 code and introducing the *Kpn*I restriction ultimately necessary for the shuffling of the eGFP-tagged Densin-180 C-terminus code into full construct.

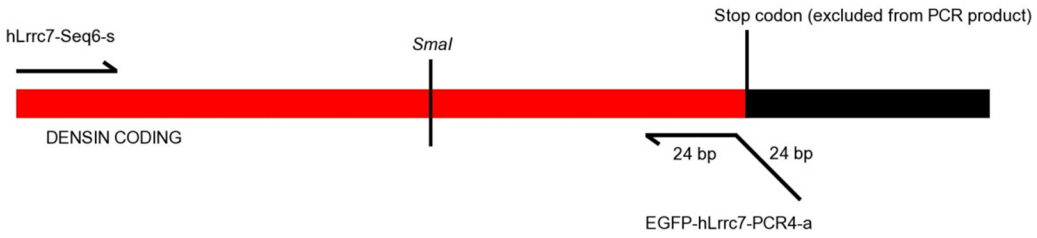

Schema 2-1 – PCR1': amplification of Densin-180 C-terminus, excluding stop codon. Template: KS+-hLrrc7-unrepaired. Sense primer: hLrrc7-Seq6-s. Antisense primer: EGFP-hLrrc7-PCR4-a. Red: Densin coding.

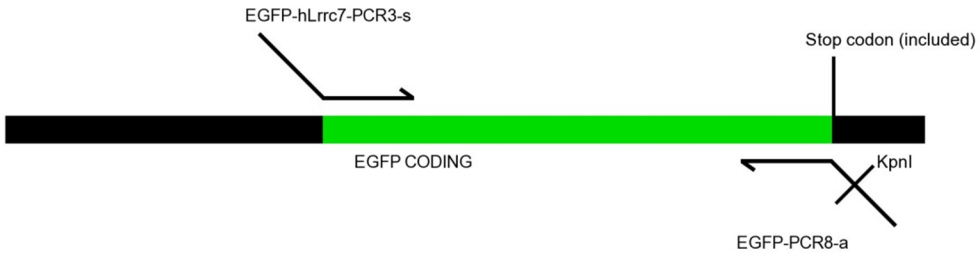

Schema 2-2 – PCR2': amplification of eGFP coding sequence, including stop codon and addition of KpnI cloning site using primer overhang on EGFP-PCR8-a. Template: pBS.EGFP.MT.CK2a. Sense primer: EGFP-hLrrc7-PCR3-s. Antisense primer: EGFP-PCR8-a.

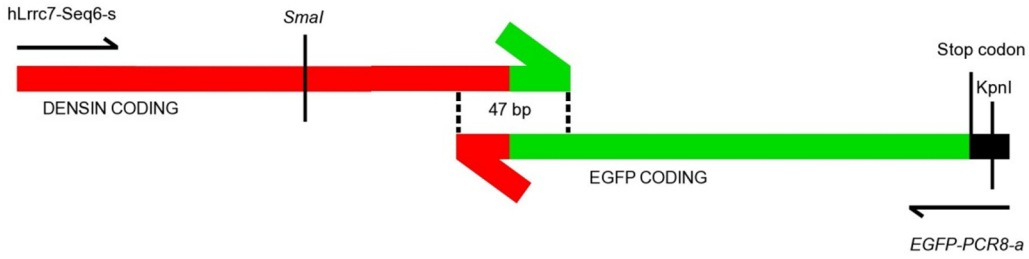

Schema 2-3 – PCR3': Overlap Extension Joining PCR. In the 1st reaction products from PCR1' and PCR2' act as both primers and templates. The product of this reaction, the desired end product, is amplified by outer primers. Templates: PCR1' and PCR2' products. Sense primer: hLrrc7-Seq6-s. Antisense primer: EGFP-PCR8-a. Red: Densin coding. Green: eGFP coding.

Schema 2-4 – PCR3': Overlap Extension Joining PCR end product. Red: Densin coding. Green: eGFP coding.

The product of PCR3' was shuffled into KS+-hLrrc7 using *Kpn*I and *Sma*I sites, replacing the untagged C-terminus coding stretch.

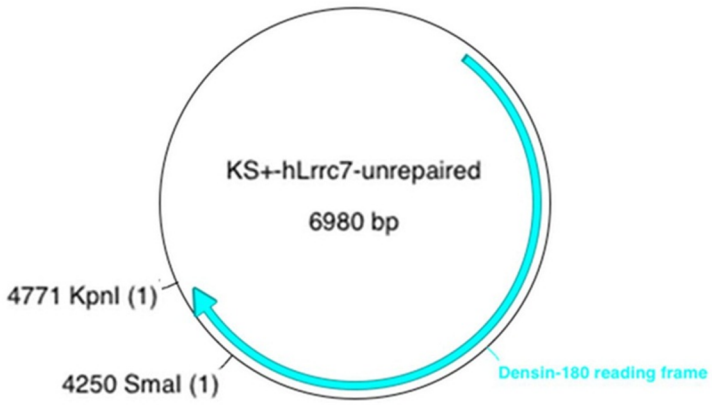

Schema 2-5. KS+-hLrrc7-unrepaired. KpnI and SmaI restriction sites used to replace untagged C-terminus with eGFP tagged C-terminus coding sequence.

Repairing the clone (re-introduction of missing 4 exons) and insertion of mutations

As mentioned at the beginning of this section, the clone, acquired from Open Biosystems, was found to be missing 4 exons. A nested PCR (the resulting fragment is labelled "PCR 2 in *schema 3-1*) was carried out on rat cDNA (kindly provided by Dr Martin Stocker) by Dr Agnes Thalhammer to generate a DNA fragment of sequence corresponding to the missing segment. To consider the inter-species difference between human and rat a sequence alignment done using Readseq (http://www.ebi.ac.uk/cgi-bin/readseq.cgi) found that 97.7% of sequence identity is shared between the two sequences: the differences can be deemed negligible.

This repair fragment and the mutation fragments generated by Moheb Costandi, by PCR site-directed mutagenesis and gene splicing by Overlap Extension Joining PCR, were introduced into eGFP-hLrrc7 fusion constructs, as illustrated in *schema 3-1* and the following four constructs were obtained as confirmed by sequencing: KS+-N-eGFP-hLrrc7-WT, KS+-N-eGFP-hLrrc7-TTT865/868/869AAA, KS+-hLrrc7-eGFP-C-WT and KS+-hLrrc7-eGFP-C-TTT865/868/869AAA.

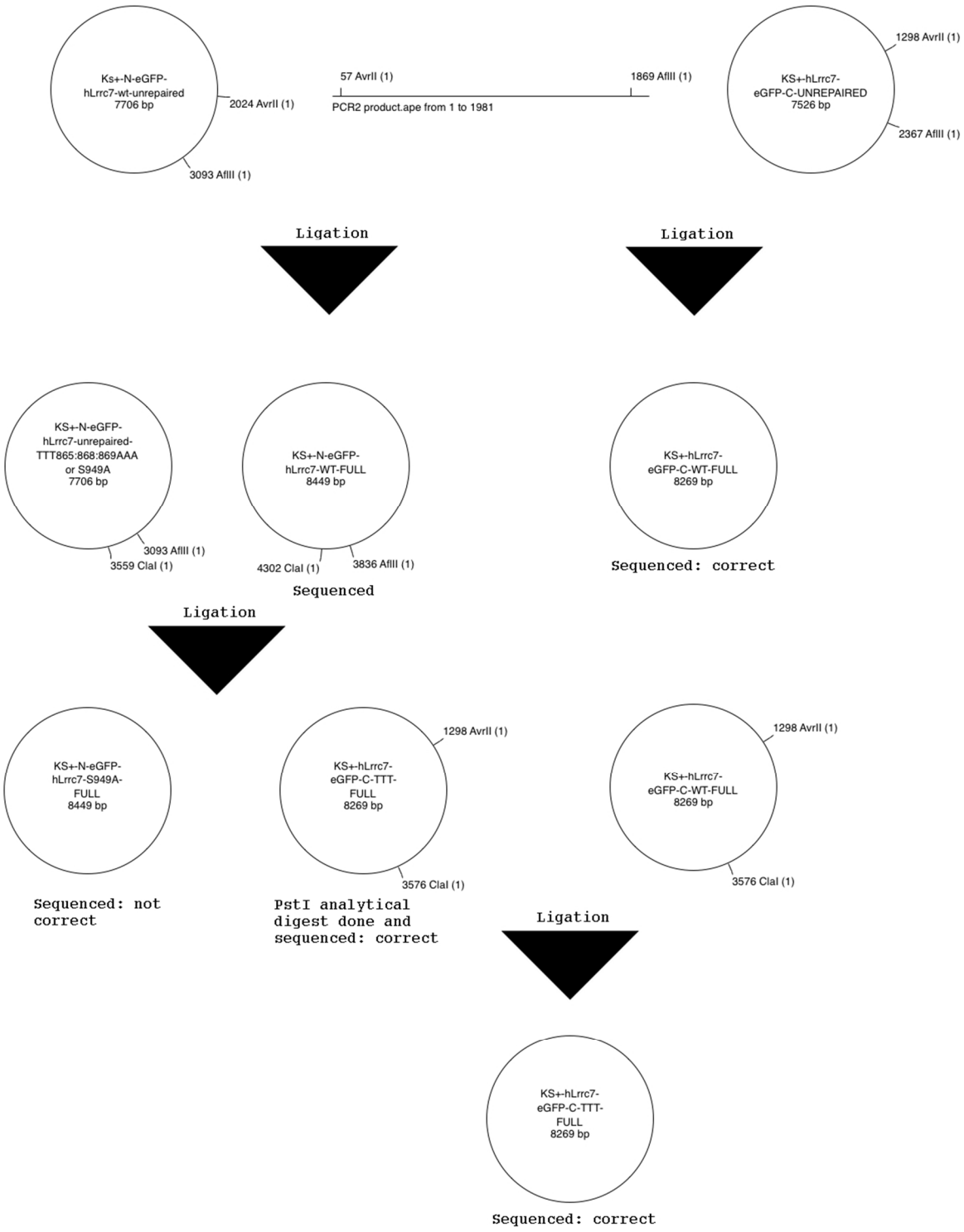

Schema 3-1 Cloning of repair fragment and mutation fragments into N-eGFP-hLrrc7 and hLrrc7-eGFP-C fusion constructs.

Shuffling constructs into pRK7, an expression vector, for expression in mammalian cell expression systems

First, the vector had to be modified, to include the required cloning sites in the correct order, for the shuffling and correct expression of the expression constructs in mammalian cells. A *Not*I restriction site, contained within specifically ordered oligonucleotides, was inserted via *Hind*III and *Sal*I restriction sites (*schema 4-1*).

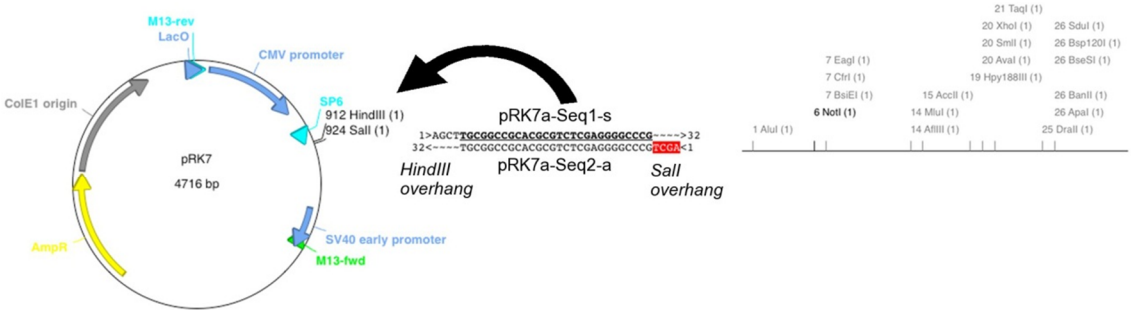

Schema 4-1. pRK7a, with HindIII and SalI restriction sites (in bold), and oligonucleotides, with HindIII and SalI overhangs, containing NotI restriction site (shown in bold).

All Densin-180 constructs were shuffled into the modified vector, named pRK7a, via *Not*I and *Kpn*I restriction sites (*schema 4-2*).

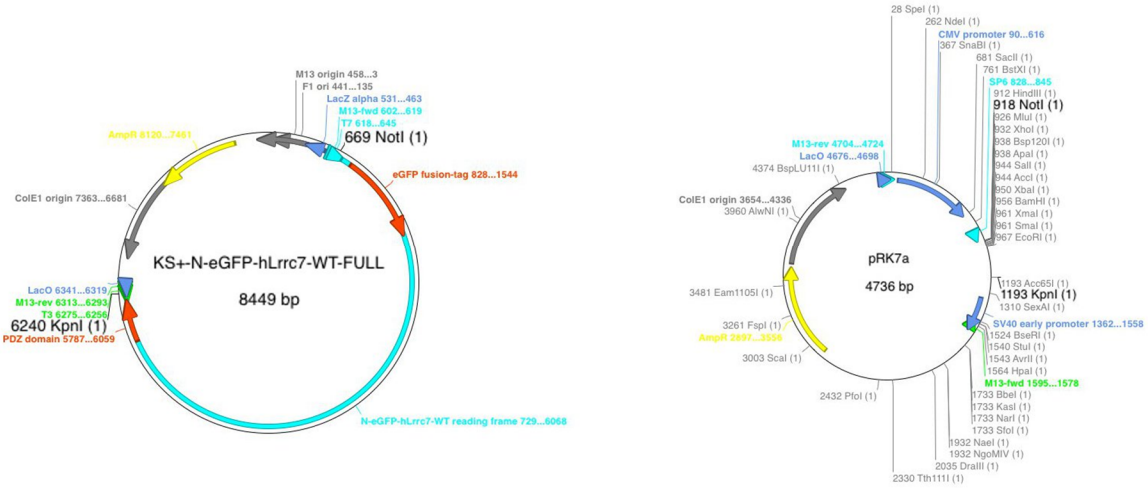

Schema 4-2. N-eGFP-hLrrc7-WT-FULL in KS+ cloning vector and pRK7a. NotI and KpnI sites shown in bold.

This resulted in the following expression constructs: pRK7a-N-eGFP-hLrrc7-WT, pRK7a-N-eGFP-hLrrc7-TTT865/868/869AAA, pRK7a-hLrrc7-C-WT and pRK7a-hLrrc7-eGFP-C-TTT865/868/869AAA.

Generating PDZ truncation constructs

3 N-terminally tagged PDZ truncation constructs were generated with different C-terminal amino acid sequences (shown below). The strategy for their construction involved generating the coding sequences for these endings by PCR and then inserting these via *BamH*I and *Acc*III restriction sites (*schema 5-1*), thereby replacing the original PDZ-domain containing C-terminus coding sequence in the starting construct, pRK7a-N-eGFP-hLrrc7-WT.

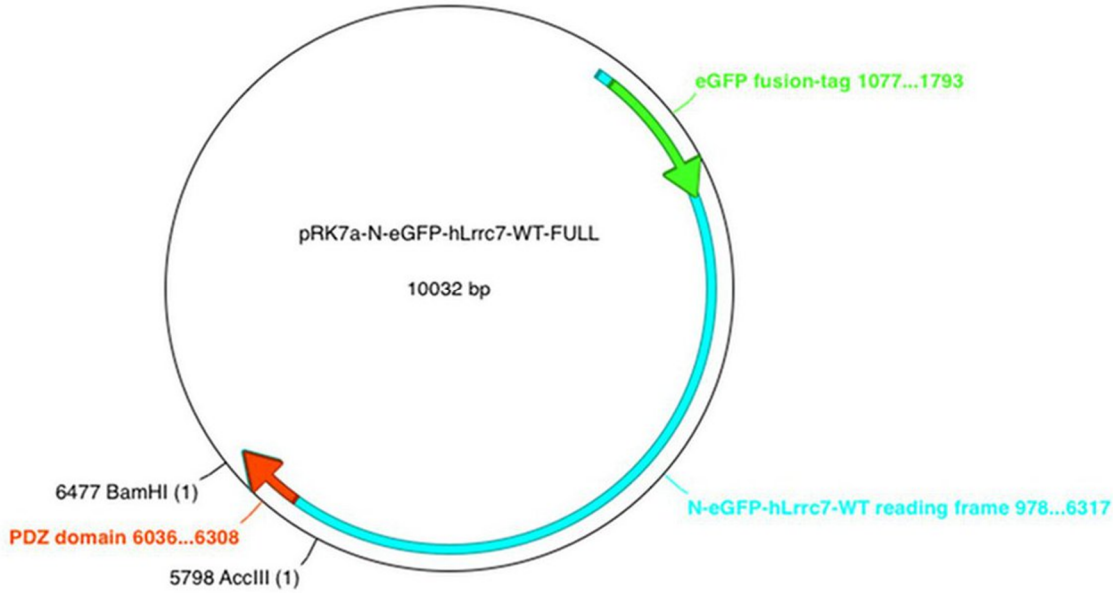

Schema 5-1. pRK7a-N-eGFP-hLrrc7-WT-FULL with BamHI and AccIII restriction sites shown in bold.

Although the same template (pRK7a-N-eGFP-hLrrc7-WT) and sense primer (hLrrc7-Seq6-s) were used for all 3 PCRs, each reaction relied on their own, specific, antisense primers to generate the desired, individual endings, by virtue of the primer overhangs (as shown below).

Legend:

Blue – densin-180 coding

Yellow – PDZ-domain coding

Red – *BamH*I cut site

Construct A – pRK7a-N-eGFP-hLrrc7-WT-PDZ-DGYPQRELTVstop

hLrrc7-PCR11-a

1-ATGggatccTTAGACAGTAAGCTCACGTTGTGGATATCCATCCATACTCC-50

In reverse complementary:

GGAGTATGGATGGATATCCACAACGTGAGCTTACTGTCTAAggatccCAT

S M D G Y P Q R E L T V *

Construct B – pRK7a-N-eGFP-hLrrc7-WT-PDZ-DGYPstop

hLrrc7-PCR12-a

1-ATGATGggatccTTATGGATATCCATCCATACTCCT-36

In reverse complementary:

AGGAGTATGGATGGATATCCATAAggatccCATCAT

R S M D G Y P *

Construct C – pRK7a-N-eGFP-hLrrc7-WT-PDZ-QREstop

hLrrc7-PCR13-a

1-ATGATGggatccTTACTCACGTTGAATAACTAGGTC-36

In reverse complementary:

GACCTAGTTATTCAACGTGAGTAAggatccCATCAT

D L V I Q R E *

hLrrc7 phospho-rich region deletion constructs

The sequence coding for Densin-180's phosphorylation rich region, removing the region coding for amino acids 702 to 1422 without the introduction of frameshift, from pRK7a-N-eGFP-hLrrc7-WT-FULL and pRK7a-hLrrc7-eGFP-C-WT-FULL expression constructs, using *Xma*I restriction sites (*schema 6.1*).

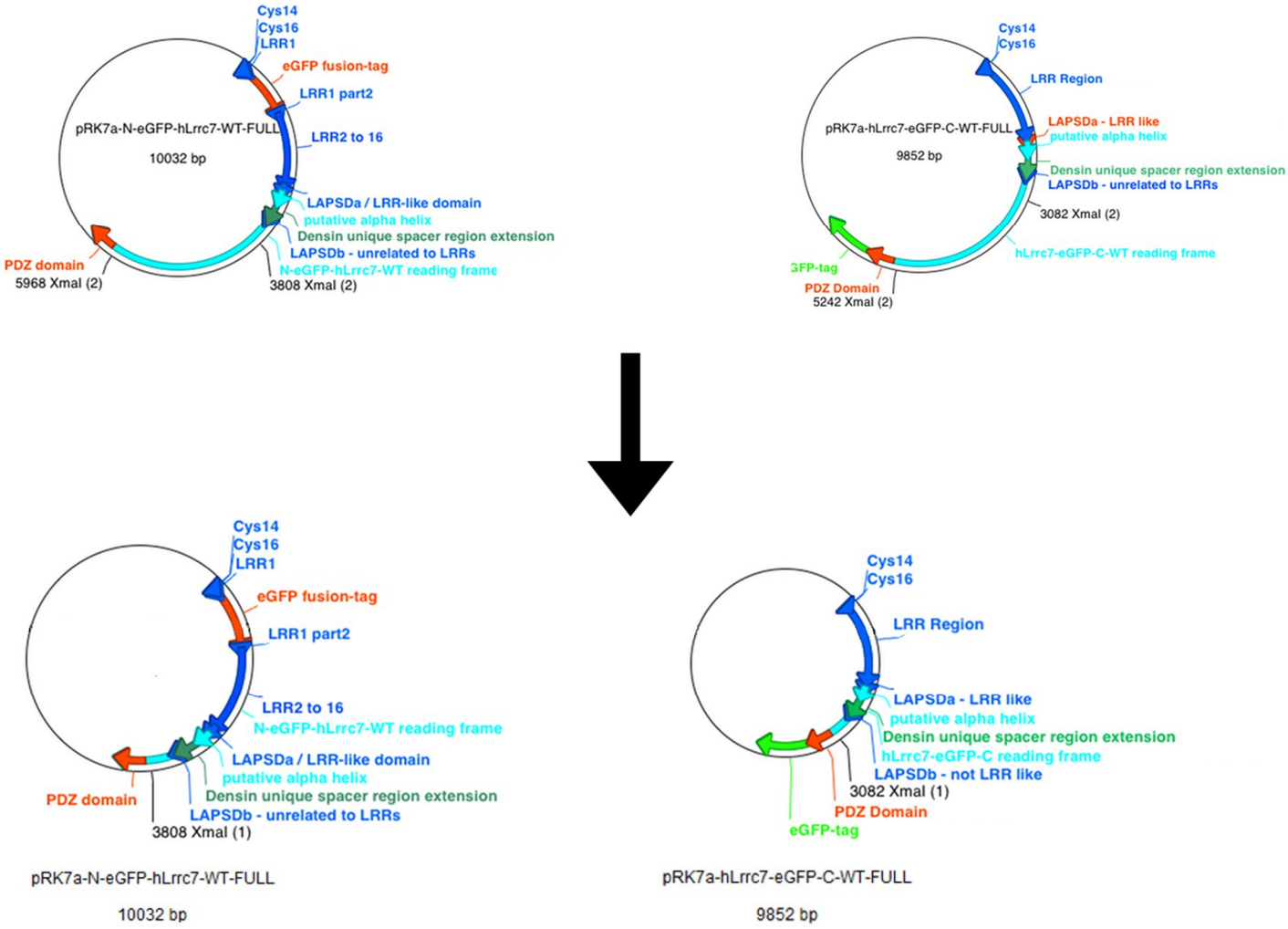

Schema 6-1. pRK7a-N-eGFP-hLrrc7-WT-FULL and pRK7a-hLrrc7-eGFP-C-WT-FULL expression constructs, with XmaI restriction sites labelled, before and after removal of phosphorylation rich region coding sequence.

Expression of recombinant Densin-180 constructs in HEK cells

N-WT vs C-WT

Expressed protein displayed characteristic subcellular localisation depending on whether the eGFP tag was introduced N-terminally or C-terminally in the protein (*figure 2-1*). N-terminally eGFP-tagged wild type Densin-180, pRK7a-N-eGFP-hLrrc7-WT, displayed punctate distribution while the C-terminally eGFP-tagged wild type Densin-180, pRK7a- hLrrc7-WT-eGFP-C-WT lacked puncta and displayed a more diffuse distribution. When observed by eye, the TTT865/868/869 variants of these constructs did not display any differences in subcellular localisation when compared to their wild type counterparts, seemingly following the same patterns.

Fluorescence profile analyses of single cell cross sections (figure 2-2) provide semi-quantitative support to these observations, showing two clear behaviours:

- Type 1: shared by N-terminally eGFP-tagged constructs pRK7a-N-eGFP-hLrrc7-WT and pRK7a-N-eGFP-hLrrc7-TTT865/868/869AAA. Distinctive peaks representing punctate formations in cell cytoplasm and large dip in signal in large central area, representing the nucleus.
- Type 2: shared by C-terminally eGFP-tagged constructs pRK7a-hLrrc7-eGFP-C-WT and pRK7a-hLrrc7-eGFP-TTT865/868/869AAA. Signal is level across the cell and neither distinctive peaks nor dip in signal where nucleus is are observed.

The breakdown of the distribution of cells fitting into these two types of behaviour, shown in *table 2-1*, provides further semi-quantitative evidence for this trend. Notice the shift from type 1 to type 2 behaviour upon the introduction of the triple phosphonull mutation in the N-terminally eGFP-tagged Densin-180 variants.

	Type 1	**Type 2**	**Other**
N-WT	78% (14)	0% (0)	22% (4)
N-TTT	50% (11)	23% (5)	27% (6)
C-WT	0% (0)	63% (12)	37% (7)
C-TTT	6% (1)	69% (11)	25% (4)

Table 2-1. Distribution of cells into type 1, type 2 and other subcellular behaviours as assessed by fluorescence profile analysis. Data shown in percentages and number of cells (in brackets).

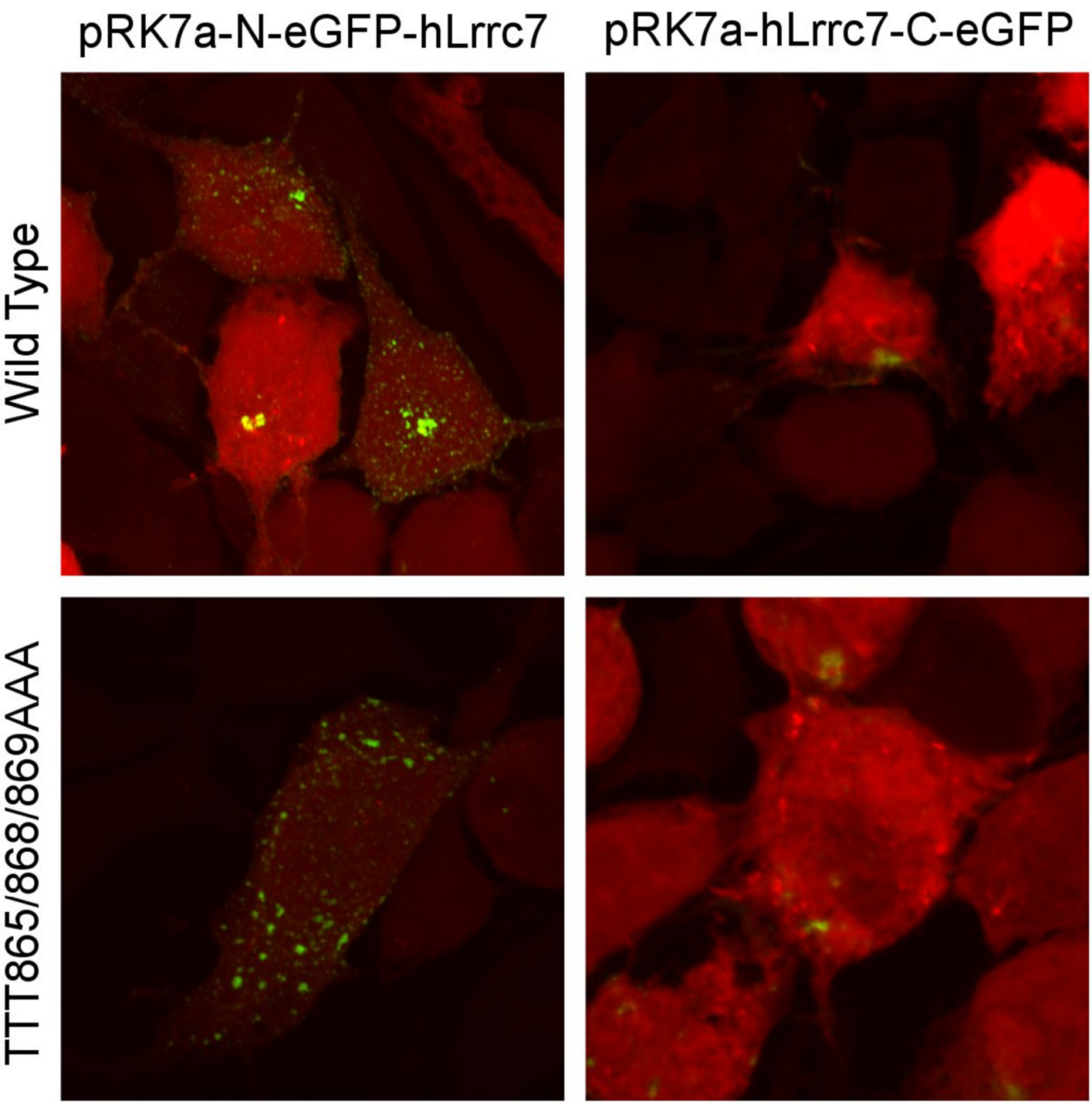

Figure 2-1. Subcellular localisation of eGFP-tagged Densin-180 fusion constructs coexpressed with mRFP in HEK cells (flattened stack images). Top left: pRK7a-N-eGFP-hLrrc7-WT. Top right: pRK7a-hLrrc7-eGFP-C-WT. Bottom left: pRK7a-N-eGFP-hLrrc7-TTT865/868/869AAA. Bottom right: pRK7a-hLrrc7-eGFP-C-TTT865/868/869AAA. Flattened stack images. Scale: 44 μm x 44 μm.

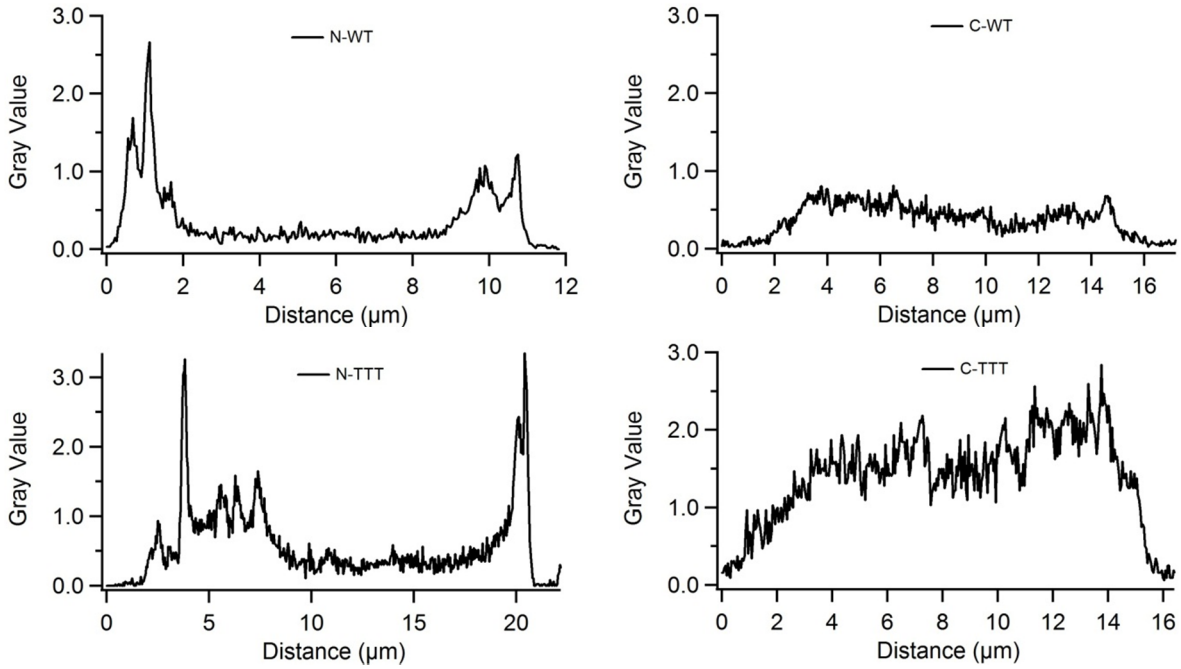

Figure 2-2a. Fluorescence profile analysis of eGFP signal in cross sections of HEK cells expressing pRK7a-N-eGFP-hLrrc7-WT, N-WT (top left), pRK7a-N-eGFP-hLrrc7-TTT865/868/869AAA, N-TTT (bottom left), pRK7a-hLrrc7-eGFP-C-WT, C-WT (top right), and pRK7a-hLrr7-eGFP-C-TTT865/868/869AAA (bottom right).

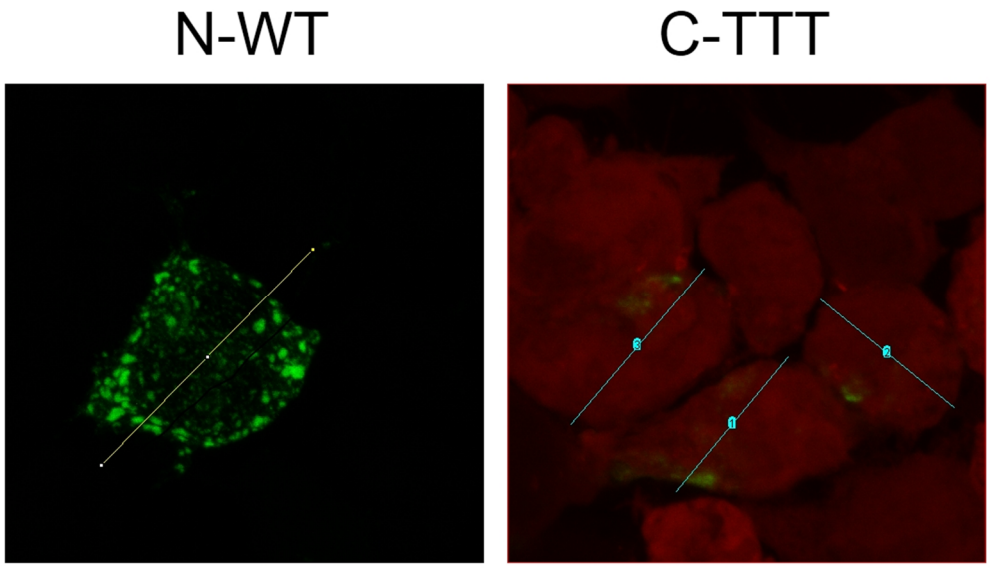

Figure 2-2b. Example cells used for fluorescence profile analysis, with cross section drawn across cells. Left: cell expressing N-terminally eGFP-tagged wild type Densin-180, showing green channel only. Right: cells expressing C-terminally eGFP-tagged TTT865/868/869AAA Densin-180, showing red (cell filler) and green channels. Scale = 44 µm x 44 µm.

2D particle analysis provide further support to these observations (*figure 2-3*), with the histogram (top) showing the N-terminally eGFP-tagged Densin-180 wild type variant expressing approximately 10 times more particles than its C-terminally eGFP-tagged counterpart. Interestingly, HEK cells expressing N-terminally eGFP-tagged WT Densin-180 showed approximately 40% more particles than cells expressing the N-terminally eGFP-tagged TTT865/868/869AAA variant, however, there was no major difference between the amount of particles seen in HEK cells expressing C-terminally eGFP-tagged Densin-180 wild type and C-terminally eGFP-tagged Densin-180 TTT865/868/869AAA.

The distribution of particles below optical resolution, omitted from the top histogram, is shown in the histogram on the bottom left of figure 2-3. This is interesting, in that it shows that the C-terminally eGFP-tagged variant containing the triple phosphonull mutation forms fewer particles than its wild type counterpart.

Cumulative frequency distributions reflect the two types of behaviour outlined above, with N-terminally eGFP-tagged constructs showing prominent formation of smaller particles when compared to the C-terminally tagged constructs. Interestingly, both N-terminally and C-terminally eGFP-tagged TTT865/868/869AAA variants show a common sub-behaviour: both closely followed their Wild Type counterparts' behaviours, but both exhibited a small inhibition in the formation of small particles, visible by a small rightward shift in the distribution curve.

Constructs	D value	Critical value
N-WT vs C-WT	0.21255	0.044862
N-WT vs N-TTT	0.017243	0.044862
N-WT vs C-TTT	0.160767	0.044862
C-WT vs N-TTT	0.20717	0.044862
C-WT vs C-TTT	0.05469	0.044862

Table 2-2. Kolmogorov-Smirnoff test results.

Kolmogorov-Smirnoff tests (*table 2-2*) support these two behaviours distinct between N-terminally and C-terminally eGFP-tagged Densin-180 variants, with D values larger than critical values by a sizeable margin. However, the test shows weaker support for the effect of the triple-phosphonull mutation, supporting difference between C-terminally eGFP-tagged wild type and TTT865/868/869AAA with a D value close to the critical value and identical distributions of N-terminally eGFP-tagged wild type and TTT865/868/869AAA variants.

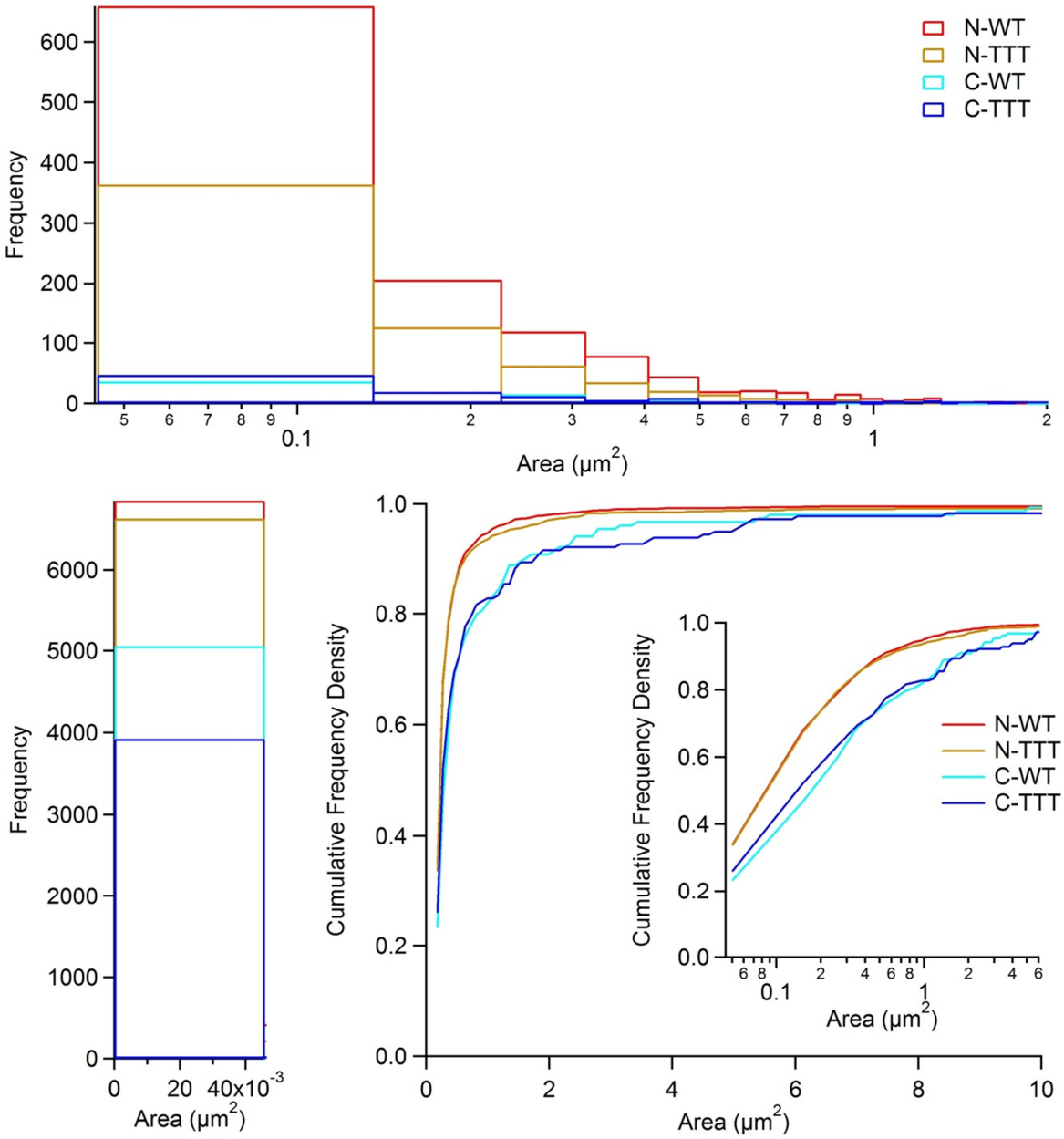

Figure 2-3. Particle distribution of N- and C-terminally eGFP-tagged Densin-180 fusion constructs. N-WT, pRK7a-N-eGFP-hLrrc7-WT, (red), n cells = 18. C-WT, pRK7a-hLrrc7-eGFP-C-WT (cyan), n cells = 19. N-TTT, pRK7a-N-eGFP-hLrrc7-TTT865/868/869AAA (brown), n cells = 22. C-TTT, pRK7a-hLrrc7-eGFP-C-TTT865/868/869AAA (blue), n cells = 16. Histogram (top): bin start = 0.04521 µm²; bin size = 0.09 µm². Histogram (bottom left): bin start = 0 µm²; bin size = 0.04521 µm². Cumulative frequency plot (bottom right) and with logarithmic x axis (inset). N-terminally and C-terminally eGFP-tagged variants show distinct distributions.

The results presented below are from experiments kindly carried out by Dr Agnes Thalhammer and Shi Yi Wang.

PDZ deletion constructs

Visually, each of the PDZ truncation constructs presented distinct subcellular localisation in HEK cells (*figure 2-4*):

- Expressed pRK7a-N-eGFP-hLrrc7-PDZ-A, in which the PDZ domain is truncated with the exception of the last 5 amino acids, forms cytosolic puncta in smaller quantities than in N-terminally tagged wild type construct, some in proximity to cell membrane.
- Expressed pRK7a-N-eGFP-hLrrc7-PDZ-B, in which the PDZ domain remains intact and only the protein's terminal three amino acids are truncated, appears diffusely distributed across the cell with some aggregate formations.
- Expressed pRK7a-N-eGFP-hLrrc7-PDZ-C, in which the entire PDZ domain and C-terminal amino acids are truncated, forms puncta again in smaller amounts than expressing N-WT, and diffusely, showing some preference for membrane proximal localisation.

Based on visual observations, all three constructs presents phenotypes individual from the N-terminally eGFP-tagged wild type construct.

Particle analysis (*figure 2-5*) supports this, showing that PDZ-A, -B, and –C produce approximately 10 times fewer particles than the N-terminally eGFP-tagged wild type construct. The relationship between the PDZ deletion constructs and the wild type is similar to that between C-WT and N-WT constructs. This data should only be considered in a semi-quantitative respect since *n* number for each PDZ deletion construct = 4 cells from 2 transfection experiments, and, therefore, cannot be statistically substantiated. The weakness of the data can be seen in the jagged appearance of the cumulative frequency distribution curves for PDZ-A to –C.

eGFP fluorescence profile analysis (*figure 2-6* and *table 2-3*) suggest that the PDZ / C-terminal variants have a preference for type 2 behaviour, resembling behaviour exhibited by C-terminally eGFP-tagged Densin-180 variants, but that these can still express type 1 behaviours, resembling N-terminally eGFP-tagged Densin-180 variants (e.g. PDZ-C). It should be noted that this data only provides semi-quantitative indications.

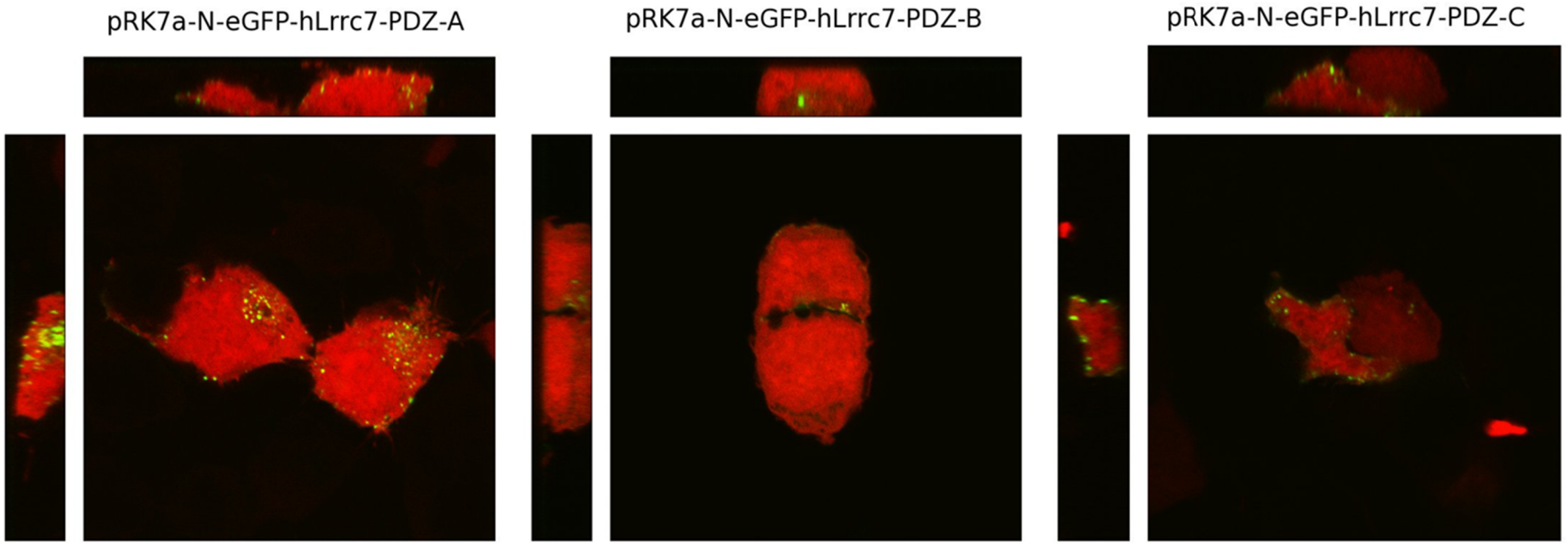

Figure 4. HEK cell subcellular localisation of N-terminally eGFP-tagged Densin-180 PDZ deletion constructs coexpressed with cell filler, mRFP: pRK7a-N-eGFP-hLrrc7-PDZ-A (left), pRK7a-N-eGFP-hLrrc7-PDZ-B (middle) and pRK7a-N-eGFP-hLrrc7-PDZ-C (right). Scale: 60 µm x 60 µm (x and y planes); 6 µm (z planes PDZ A and PDZ B) and 8 µm (z plane, PDZ C).

	Type 1	Type 2	Other
PDZ A	25% (1)	50% (2)	25% (1)
PDZ B	0% (0)	100% (4)	0% (0)
PDZ C	25% (0)	75% (0)	0% (0)

Table 2-3. Distribution of cells into type 1, type 2 and other subcellular behaviours as assessed by fluorescence profile analysis. Data shown in percentages and number of cells (in brackets).

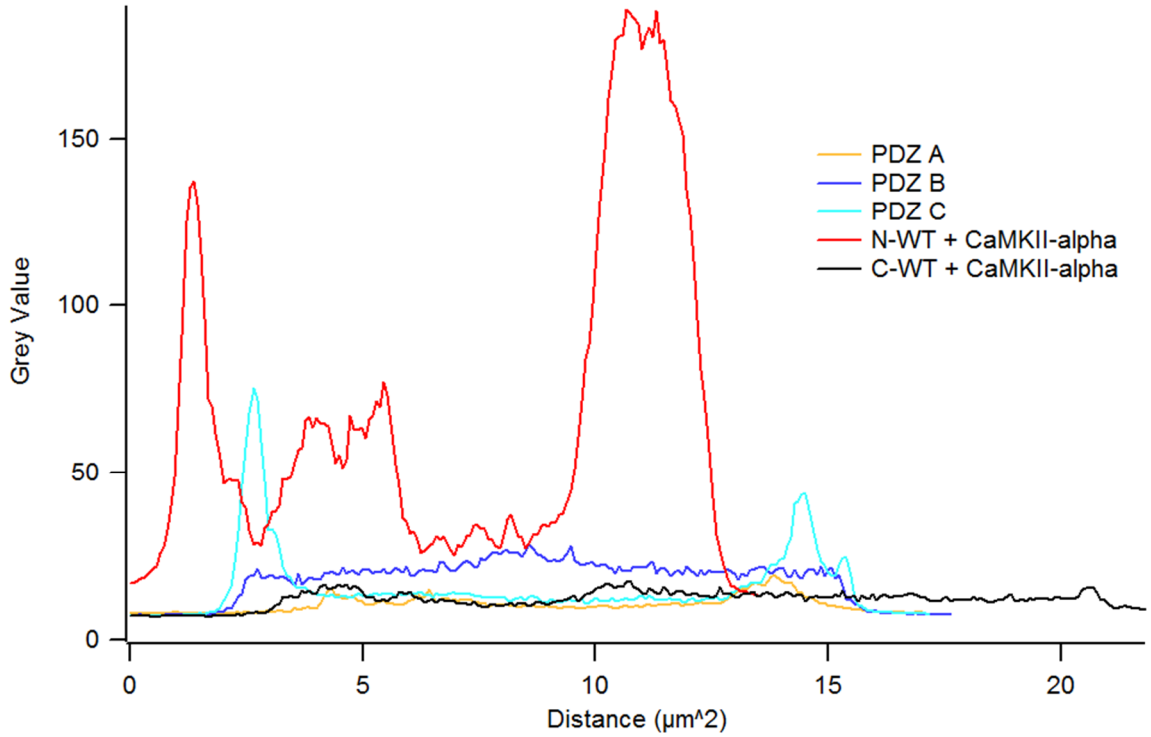

Figure 2-6. Fluorescence profile analysis of eGFP signals in cross sections of HEK cells expressing: pRK7a-N-eGFP-hLrrc7-PDZ-A, PDZ-A (orange); pRK7a-N-eGFP-hLrrc7-PDZ-B, PDZ-B (blue); pRK7a-N-eGFP-hLrrc7-PDZ-C, PDZ-C (cyan); pRK7a-N-eGFP-hLrrc7-WT coexpressed with mRFP-CaMKII-α, N-WT + CaMKII-alpha (red); and pRK7a-hLrrc7-eGFP-C-WT coexpressed with mRFP-CaMKII-α, C-WT + CaMKII-alpha (black).

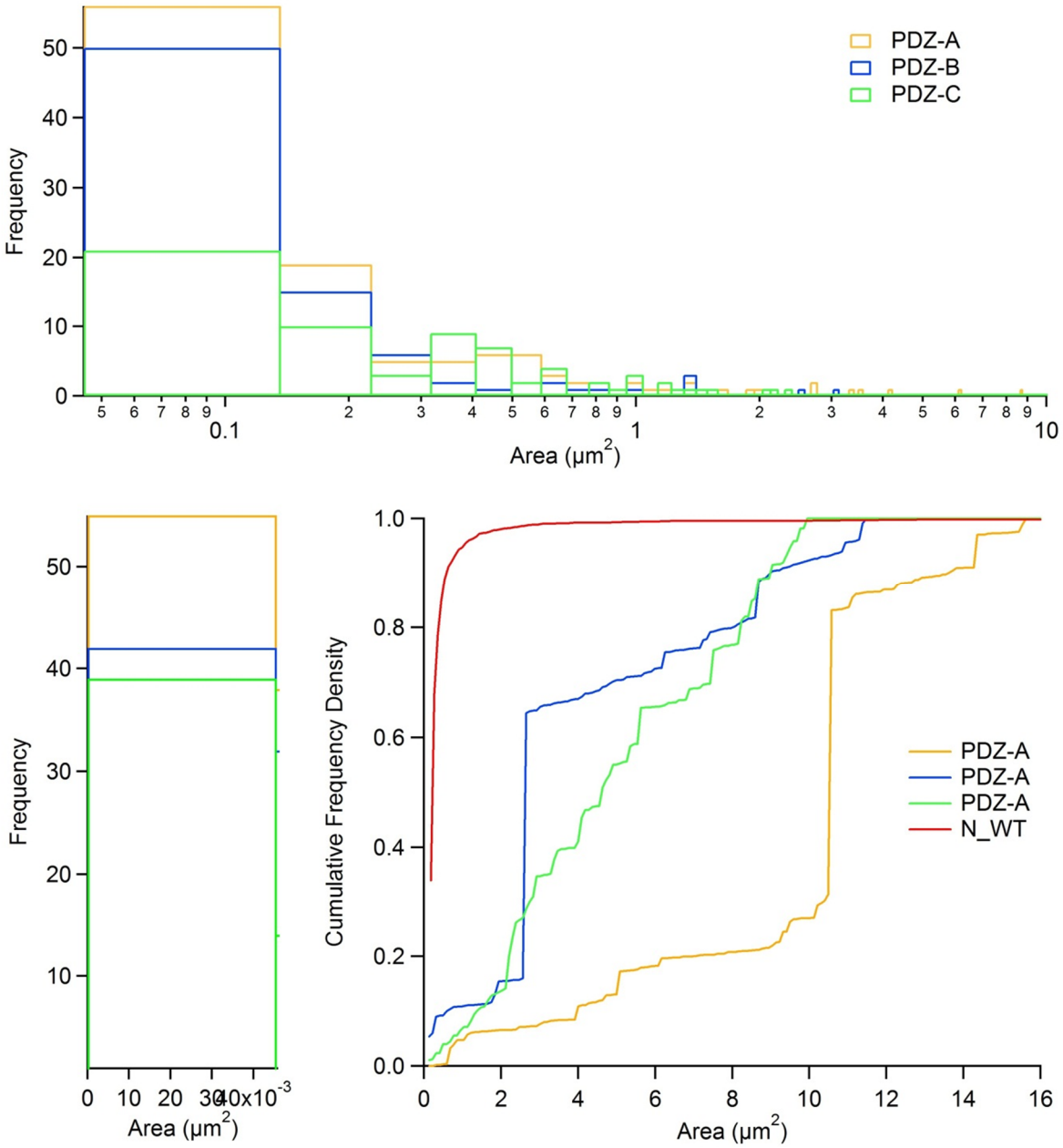

Figure 2-5. Particle distribution of N-terminally eGFP-tagged PDZ deletion constructs: pRK7a-N-eGFP-hLrrc7-PDZ-A, PDZ-A (orange); pRK7a-N-eGFP-hLrrc7-PDZ-B, PDZ-B (blue); pRK7a-N-eGFP-hLrrc7-PDZ-C, PDZ-C (cyan), and pRK7a-N-eGFP-hLrrc7-WT, N-WT (red). For all except N-WT, n = 4 cells from 2 transfection experiments; for N-WT, n = 18 cells from 2 transfection experiments. Histogram (top): bin start = 0.04521 μm²; bin size = 0.09 μm². Histogram (bottom left): bin start = 0 μm²; bin size = 0.04521 μm². Cumulative frequency plot (bottom right).

Coexpression of CaMKII-α leads to retargeting of Densin-180

mRFP-tagged CaMKII-α (pBS.RFP-MT-CK2a [30]) was coexpressed with N- and C-terminally tagged wild type Densin-180 in HEK cells (*figure 2-7*). The orange colour seen in cells when CaMKII-α is coexpressed with both N- and C-terminally tagged variants of Densin-180 is most probably due to some degree of colocalisation of CaMKII-α with Densin-180, leading to a mixing of the green representing the eGFP signal with the red representing the mRFP signal.

The apparent decrease in the size of N-terminally tagged wild type Densin-180 puncta and the apparent shift in localisation of C-terminally tagged Densin-180 towards the plasma membrane, when these constructs are coexpressed with CaMKII-α may be artifactual, and more experiments would have to be carried out, followed by quantitative analysis in order to substantiate these observations.

Figure 2-7 (following page). Subcellular localisation of N- and C-terminally eGFP-tagged Densin-180 constructs in HEK 293 cells. Top left: N-eGFP-hLrrc7-WT, coexpressed with mRFP cell filler; scale – 60 µm x 60 µm x 2.62 µm. Top right: N-eGFP-hLrrc7-WT, coexpressed with mRFP-CaMKII-α; scale – 60 µm x 60 µm x 2.46 µm. Bottom left: hLrrc7-eGFP-C-WT coexpressed with mRFP cell filler; scale – 82.12 µm x 82.12 µm x 4.25 µm. Bottom right: hLrrc7-eGFP-C-WT coexpressed with mRFP-CaMKII-α; scale – 82.12 µm x 82.12 µm x 3.668 µm.

pRK7a-N-eGFP-hLrrc7-WT

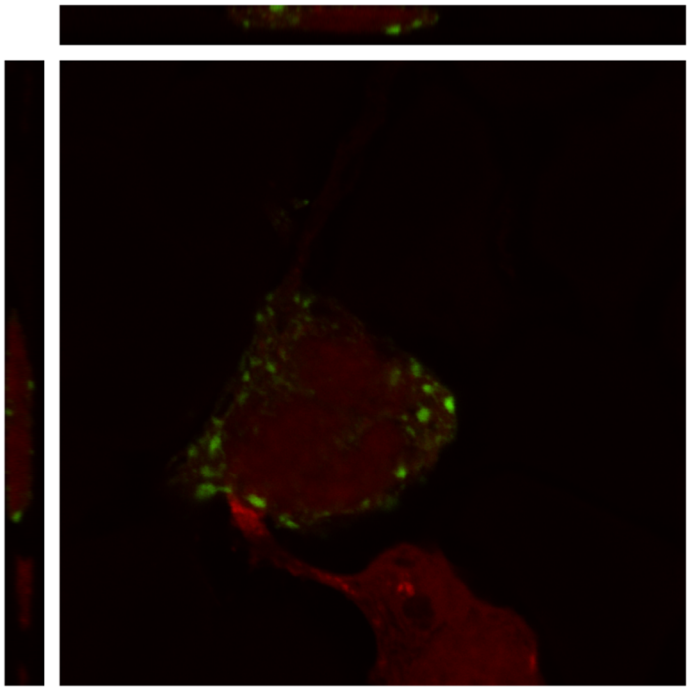

pRK7a-N-eGFP-hLrrc7 + CaMKII-RFP

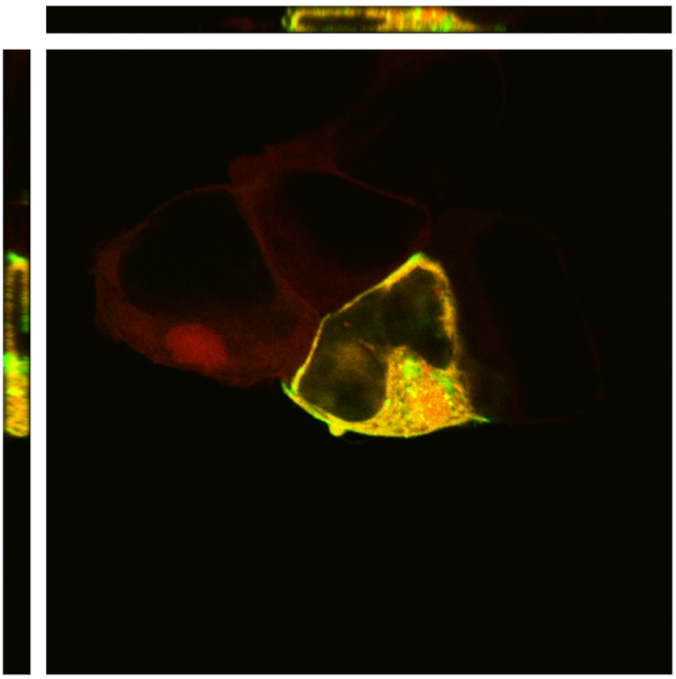

pRK7a-hLrrc7-eGFP-C-WT

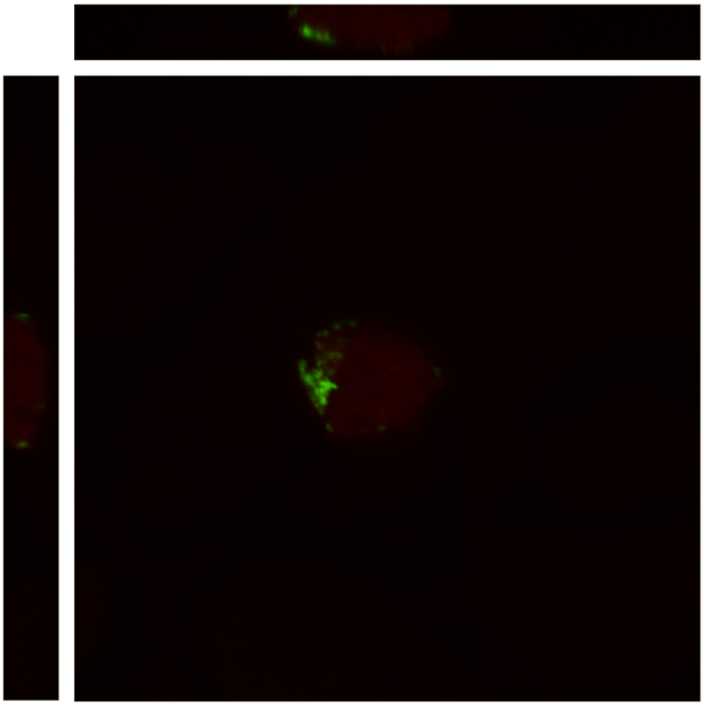

pRK7a-hLrrc7-eGFP-C + CaMKII-RFP

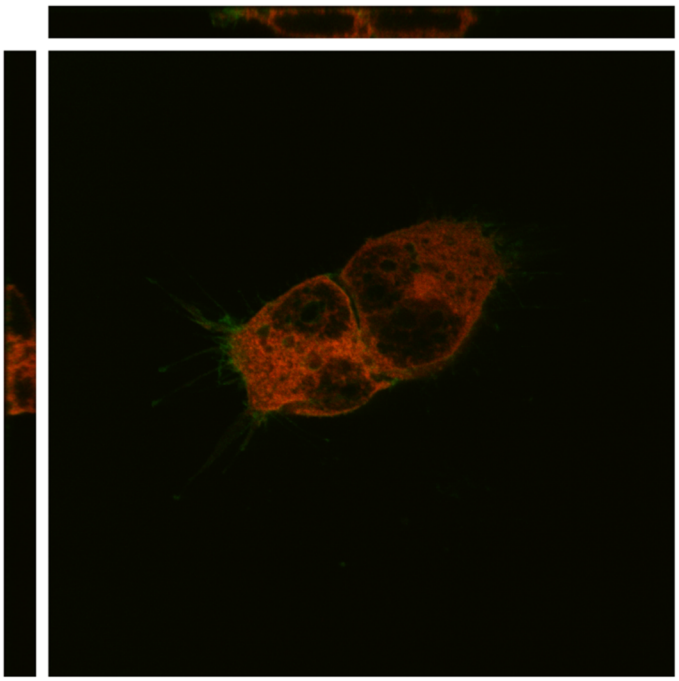

Discussion

The HEK 293 cell expression system

All results presented in this thesis are derived from HEK 293 cell expression studies and, as such, do not reflect Densin-180's *in vivo* behaviour as well as data from hippocampal primary neuron cultures would.

An immortalised cell line, HEK 293 cells are a robust, easy to maintain and very reliable expression system. Setting up a culture is as easy as thawing a vial of cells and plating them. These cells are easy to handle and convenient for transfection studies. What's more, no animals are required when using the HEK 293 cell expression system. Hippocampal primary neuron cultures, on other hand, are extremely fragile and high maintenance, requiring delicate handling. Setting up a culture requires tricky dissection of embryonic mice from a pregnant specimen: a tricky procedure requiring a practised hand. Even in experienced hands, the likelihood of failure of primary hippocampal neuron cultures far exceeds that of HEK 293 cell cultures.

However, the results derived from HEK 293 cell expression studies are of a very different character to those from hippocampal primary neuron cultures, since HEK 293 cells do not express the complement of synaptic proteins specific to neurons. Out of the protein interaction partners of Densin-180 mentioned in the introduction section, only mRNAs from those associated with the cytoskeleton are found: α-actinin, δ-catenin and N-cadherin [59] [60]. This leaves a large set of absent Densin-180 interactors: NR2B, $Ca_v1.3$, MAGUIN-1, PSD-95, and shank are proteins, which have been found to have a role in determining the targeting and subcellular localisation of Densin-180, that are simply not present in HEK cells. Densin-180's subcellular behaviour in HEK cells should therefore be expected to substantially differ from its behaviour *in vivo* or in hippocampal primary neuronal cultures.

However, the surprising presence of neuronal cytoskeletal proteins, as well as other neuronal proteins, considering that HEK 293 cells are derived from kidney epithelial cells, means that the environment presented by HEK cells to Densin-180 is not so far removed from its neuronal environment as would have been expected [59] [60], presenting the HEK 293 cell line as the ideal starting point for expression studies of neuronal proteins like Densin-180. In fact, by removing many of Densin-180's interaction partners, HEK cells provide an excellent platform in which to study specific protein interactions and structure-function relationships in isolation from the many interactions Densin-180 takes part in when in neurons.

Image analysis methods

A special note should be made highlighting the difficulty in analysing image data. In contrast to data which may be obtained from electrophysiological measurements, which are direct and quantitative, data obtained from measurement using a confocal microscope, with more dimensions, is qualitative. This, together with the biological nature of cells, presents the task of extracting some statistical meaningfulness from this type of data as a challenge.

One of them main drawbacks of the analysis presented here is its two dimensional nature. Rather than carrying out fluorescence profile and particle distribution analyses on slices taken from stack images, which may misrepresent cells, or, on 3-dimensional models produced from these (possible using Volocity), which uses up a lot of computer power, these were carried out using Z-projections, presenting the trouble that particles neighbouring each other on the X and Y planes yet distanced from one another on the Z plane may appear to be part of the same particle, adding an element of error to our analyses.

Another element of vagueness can be seen in the fluorescence profile analysis, which was based on analysis of a single, arbitrarily drawn cross section of each cell: the weakness is clear, in that this cross section may misrepresent cells, but this method provides good means of evaluating populations of cells in the manner described above.

The thresholding method used in the particle analysis present another area of error: due to variation in the amount and intensity of eGFP signal between cells, and between particles, no automated thresholding algorithm available was able to threshold signal in a manner representative of visible signal. Because of this, thresholding was carried out manually, with the criteria that the thresholded image must be representative of number, shape and size of particles visible in the unthresholded image. This presented a number of weaknesses in the data because: each cell has a different threshold; particles may disappear, diminish in size, or disintegrate when threshold is increased; particles may appear, increase in size and fuse when threshold is decreased.

Developing a method of printing specified areas with specified amounts of eGFP, a method of calibrating measured signal against amount of protein would offer a large leap in image analysis of expressed proteins.

Subcellular behaviours observed via fluorescence profile analysis

The subcellular behaviours of Densin-180 variants observed via fluorescence profile analysis reflected visual observations and particle distribution analysis, all suggesting the occurrence of two types of subcellular behaviour, with different variants showing preferences for one or the other.

Fluorescence profile analysis gives a good, semi-quantitative breakdown of the behaviours. As shown in *table 2-1*, N-terminally eGFP-tagged variants show a clear preference for type I behaviour, while C-terminally eGFP-tagged variants favour type II behaviour, reflecting what is shown in the particle analysis.

Interestingly, a sizeable proportion of cells expressing the N-terminally eGFP-tagged TTT865/868/869AAA variant show a small shift from type I behaviour to type II behaviour; a shift, also reflected, somewhat, in the particle distribution.

All variants displayed a sizeable proportion of cells (20% to 40%) expressing "other" behaviour. This is mainly due to aggregate formations and particles which appear fused together through Z-projection of raw stack images. High eGFP signal intensities were also notable within the centre of dividing cells expressing N-terminally eGFP-tagged variants: this is likely due to Densin-180's association with cytoskeletal elements of HEK293 cells. Generally, however, most cells falling into the "others" category shared many similarities with the type of behaviour associated with the Densin-180 variant expressed within those cells.

Densin-180 aggregation

Protein aggregation at specialised pre- and post-synaptic structures occurs during synaptic development, and like Densin-180, many of its interactors also form puncta: CaMKII-α (previous observations), MAGUIN-1 [49], PSD-95 [21], Shank [51] and $Ca_v1.4$ [61] are a few examples. Densin-180, has also, itself, previously been observed to form puncta [45][48].

Interestingly, the observations presented here match previous observations: the subcellular localisation of the N-terminally eGFP-tagged Densin-180 construct, pRK7a-N-eGFP-hLrrc7-WT, matches that presented by Strack *et al*, who expressed the C-terminal part of Densin-180 to which they had added a 10 amino acid membrane targeting sequence from Lck tyrosine kinase, containing myristoylation and dual palmitoylation sites [14]. The Lck tyrosine kinase is found in caveolae, the size, shape and subcellular distribution of which is similar to that of the punctate formations observed here.

Caveolae, Latin for 'little caves', are a type of specialised lipid rafts forming small invaginations of the plasma membrane of 50 to 100 nm diameter, with functions in vesicular transport, cholesterol homeostasis, signal transduction and tumour suppression. Their main constituent proteins, caveolin 1-3, are known to interact with G-protein subunits and receptors, tyrosine kinases, small GTPases, MAP Kinases, β-adrenergic receptors, protein kinase C isoforms, Src family kinases, and have regulatory effects on a number of these proteins and thus on their associated signal transduction

pathways [63]. It is possible that in HEK cells, protein-protein interactions with proteins of caveolar complexes underlie the punctate localisation of Densin-180 observed.

However, it is worthwhile considering the behaviour of other PSD proteins in HEK cells. CaMKII-α was found to form puncta similar to those seen when they are expressing N-terminally eGFP-tagged wild type Densin-180 (previous observations). CaMKII-α subunits are known to self-associate, forming dodecameric holoenzymes which themselves associate, which gives a rational mechanism underlying these aggregations. Drawing parallels with CaMKII-α, it may be possible that Densin-180 forms puncta, also, through some mechanism of self-association. MAGUIN-1 is another example of a PSD protein that forms puncta through self-association: in this case dimerization or multimerisation occurs through the proteins C-terminal Leucine-rich region [49].

PSD-95 clustering, however, has a number of elements which may be of similarity to Densin-180 clustering: clustering of this protein at the PSD requires N-terminal palmitoylation, is dependent on its first two PDZ domains and on its terminal 12 amino acid residues [62]. It may well be the case that in Densin-180, N-terminal palmitoylation and PDZ domain interactions, involving terminal amino acids, may constitute a mechanism protein clustering at the PSD.

The data presented in this thesis show that N-terminally eGFP-tagged Densin-180 constructs form cytosolic punctate formations when expressed in HEK cells, and that C-terminally eGFP-tagged Densin-180 constructs show strongly inhibited punctate formation. Further, preliminary data presented in this thesis show that tampering with Densin-180's PDZ domain and/or terminal amino acids also inhibit the formation of puncta. It is quite possible that Densin-180 dimerises or multimerises through interactions between its PDZ domain and its own terminal amino acid residues.

Densin-180 membrane association

Concerning membrane association of Densin-180, from observation of expressed constructs in HEK cells by eye, it is only possible to speculate that C-terminally eGFP-tagged constructs have a tendency towards membrane association over the N-terminally eGFP-tagged variants; this could be substantiated by membrane staining experiments, for example using a stain such as Cell Mask Orange [Invitrogen, Carlsbad, CA, USA], and by Western blot analysis of membrane associated proteins of cells expressing the various Densin-180 constructs presented here, to measure the colocalisation and membrane association of expressed Densin-180 proteins with cell membrane.

Possible involvement of N-terminal Cys14/16 and LRR region in membrane association

Although the possible role of Densin-180's Cys14/15 residues and of its LRR region was highlighted in the introduction section, the data presented here does not clarify this.

Membrane staining experiments and Western blot analysis of membrane associated proteins would help ascertain the role of Densin-180's N-terminal region: since palmitoylation is an enzyme dependent process, it could be expected that the process is inhibited in the N-terminally eGFP-tagged Densin-180 constructs, and C-terminally eGFP-tagged constructs, in which palmitoylation may not be inhibited in the same fashion, could be found to exhibit more membrane association.

The generation of new constructs, featuring mutations of Cys14/16 residues to Serine residues and/or featuring LRR region truncations, combined with expression studies using membrane staining and Western blot analysis of membrane bound protein fraction would offer some definitive gauge of the individual involvement of these Densin-180 features, if any, in its membrane association property.

Protein expression levels

The potentially varying expression levels of different constructs present a large source of variation in the results presented in this thesis. Expression levels may vary due to:

- The point in the cell cycle at which the imaged cell is in, which may affect protein expression levels and subcellular localisation.
- Variation in transfection efficiency depending on construct.
- Variation in expression of transfected construct, as well as post-translational modifications.

Variation in protein expression levels could cause variation in the size of punctate formations within a cell, such that a reduction in expression levels of transfected construct may cause a downward shift in the size and number of punctate formations and vice versa. This could mean that the type 1 and type 2 behaviours outlined above may not be due to variation in structure, affecting the function, of Densin-180, but simply to variations in protein expression levels. Variation in protein expression levels could also cause a shift in subcellular localisation of visible eGFP signal and could underlie the possible retargeting effect of C-terminally eGFP-tagged wild type Densin-180 by mRFP-tagged CaMKII-α observed.

Western blot analysis of transfected cells would offer a means of quantifying protein expression levels as well as to check that expressed proteins are of the correct size, and therefore that the correct protein is being expressed. Such an approach would offer a means of testing whether or not the effects observed are due to structure-function relationship of Densin-180, or to variation in protein expression levels, or to unexpected post-translational modification of expressed protein.

eGFP-tag may have altered subcellular behaviour of Densin-180

Since human Densin-180 was used as a starting point for engineering the constructs presented here, and since there were no anti-human Densin-180 antibody available at the time of experimentation, it was effectively impossible to check whether the introduction of the eGFP-tag caused any alteration to the normal localisation of Densin-180 in HEK cells. However, since anti-mouse Densin-180 antibody was available, Dr Agnes Thalhammer was able to show that, in mouse primary hippocampal neuron cultures, the subcellular localisation of native Densin-180 matches that of N-terminally eGFP-tagged Densin-180, pRK7a-N-eGFP-hLrrc7-WT, expressed in the same type of culture.

TTT865/868/869AAA phosphomutants and phosphorich region truncation constructs

The introduction of TTT865/868/869AAA phospho-null mutations caused an inhibition of puncta formation in both N-terminally and C-terminally eGFP-tagged Densin-180 (*figure 2-3*). As mentioned earlier, this triple phospho-null mutation is located right in the middle of Densin-180's phosphorylation rich region. No experiments were carried out to elucidate the subcellular behaviour of the phospho-rich region truncation constructs presented in this thesis. A bioinformatic motif scan, searching for phosphosites, matched a number of kinases to known phosphorylation sites in the truncated portion of the phospho-rich region truncation constructs (*table 3-1*).

Site	Score	Percentile	Sequence	SA	Kinase
T865	0.5319	0.00525	FPSKLET**T**PTTSPLP	2.662	GSK3 Kinase
S869	0.5323	0.0053	LETTPTT**S**PLPERKE	1.261	GSK3 Kinase
S869	0.4888	0.00369	LETTPTT**S**PLPERKE	1.261	Erk1 Kinase
S949	0.326	0.00023	NKFKKSQ**S**IDEIDIG	1.445	PKC epsilon
S949	0.4359	0.00163	NKFKKSQ**S**IDEIDIG	1.445	Calmodulin dependent Kinase 2
S1118	0.5708	0.00696	GFLRRAD**S**LVSATEM	0.425	Akt Kinase
S1118	0.6282	0.00874	GFLRRAD**S**LVSATEM	0.425	AMP_Kinase
S1209	0.5558	0.0025	ARSYSTE**S**YGASQTR	1.202	PDK1 Binding
S1213	0.5082	0.00602	STESYGA**S**QTRPVSA	1.503	DNA PK

Table 3-1. Motif scan results: Q96NW7 (human Densin-180). Showing predicted kinase interactions at known phosphorylation sites within truncation of phospho-rich region truncation constructs. Motifs scanned: All. Stringency: Medium. http://scansite.mit.edu/motifscan_id.phtml

The predicted involvement of the kinases, listed in *table 3-1*, which have roles in a wide array of cell functions which include cell survival, metabolism, Wnt signalling and LTP mediation, suggests that Densin-180 may have a role in the regulation of synaptic signalling in the central nervous system, with many parallels to the role played by Erbin in the regulation of NRG1 signalling and myelination in the peripheral nervous system [56]. Although the predicted involvement of GSK3 Kinase should be

taken note of, it should, however, be observed that since GSK3 kinase is not natively expressed in HEK cells, that effects seen in HEK cells expressing TTT865/868/869AAA variants may be due to changes in protein structure.

The phosphorich region truncation constructs offer tools of great value for the future exploration of such a hypothesis. This sort of study may involve experiments similar to those presented here, as well as electrophysiological measurements. The study of Densin-180's function in the regulation of neuronal cytoarchitecture in synaptic plasticity, in glomerular podocytes [52][53] and in Sertoli cells [54] could establish this protein as a pharmaceutical target for the synthetic regulation of learning and memory, kidney function [52][53] and for the development of a male contraception pill [54]. Such research will deserve careful and stringent review; their applications appropriate restriction.

References

1. NITIN NOHRIA, BORIS GROYSBERG, LINDA-ELING LEE, 2008. EMPLOYEE MOTIVATION: A POWERFUL NEW MODEL, HARVARD BUSINESS REVIEW, JULY-AUGUST, 78-84.

2. OLLE LINDVALL & ZAAL KOKAIA, 2006. STEM CELLS FOR THE TREATMENT OF NEUROLOGICAL DISORDERS. NATURE, VOL 441, 1094-1096.

3. OSAHIKO TSUJI, KYOKO MIURA, YOHEI OKADA, KANEHIRO FUJIYOSHI, MASAHIKO MUKAINO, NARIHITO NAGOSHI, KAZUYA KITAMURA, GENTARO KUMAGAI, MAKOTO NISHINO, SHUTA TOMISATO, HISANOBU HIGASHI, TOSHIHIRO NAGAI, HIROYUKI KATOH, KAZUHISA KOHDA, YUMI MATSUZAKI, MICHISUKE YUZAKI, EIJI IKEDA, YOSHIAKI TOYAMA, MASAYA NAKAMURA, SHINYA YAMANAKA, AND HIDEYUKI OKANO, 2010. THERAPEUTIC POTENTIAL OF APPROPRIATELY EVALUATED SAFE-INDUCED PLURIPOTENT STEM CELLS FOR SPINAL CORD INJURY. PNAS , VOL. 107, NO. 28, 12704-12709.

4. HTTP://WWW.BRAINGATE2.ORG/

5. SUNG-PHIL KIM, JOHN D. SIMERAL, LEIGH R. HOCHBERG, JOHN P. DONOGHUE, GERHARD M. FRIEHS, AND MICHEAL J. BLACK, 2010. POINT-AND-CLICK CURSOR CONTROL WITH AN INTRACORTICAL NEURAL INTERFACE SYSTEM IN HUMANS WITH TETRAPLEGIA. IEEE TRANS NEURAL SYST REHABIL ENG. 2011 JAN 28. [EPUB AHEAD OF PRINT]

6. DALE PURVES, GEORGE J. AUGUSTINE, DAVID FITZPATRICK, WILLIAM C. HALL, ANTHONY-SAMUEL LAMANTIA, JAMES O. MCNAMARA, S. MARK WILLIAMS, 2004. NEUROSCIENCE: THIRD EDITION.

7. HUMPHREY P. RANG, MAUREEN M. DALE, JAMES M. RITTER AND PHILIP MOORE, 2003. PHARMACOLOGY, 5TH EDITION.

8. STUART CULL-CANDY, STEPHEN BRICKLEY, MARK FARRANT, 2001. NMDA RECEPTOR SUBUNITS: DIVERSITY, DEVELOPMENT AND DISEASE. CURR OPIN NEUROBIOL 11(3):327-35.

9. STUART G. CULL-CANDY, DANIEL N. LESZKIEWICZ, 2004. ROLE OF DISTINCT NMDA RECEPTOR SUBTYPES AT CENTRAL SYNAPSES. SCI STKE 255:RE16.

10. HOLLY J. CARLISLE, MARY B. KENNEDY, 2005. SPINE ARCHITECTURE AND SYNAPTIC PLASTICITY. TRENDS NEUROSCI. 28(4): 182-7.

11. DAVID ATTWELL AND ALASDAIR GIBB, 2005.NEUROENERGETICS AND THE KINETIC DESIGN OF EXCITATORY SYNAPSES. NATURE REVIEWS, NEUROSCIENCE, 6: 841-849.

12. ANTHONY LAU, MICHAEL TYMIANSKI, 2010. GLUTAMATE RECEPTORS, NEUROTOXICITY AND NEURODEGENERATION. EUR J PHYSIOL 460:525-542.

13. P. JONAS, C. RACCA, B. SAKMANN, P.H. SEEBURG, AND H. MONYER, 1994. DIFFERENCES IN CA^{2+} PERMEABILITY OF AMPA-TYPE GLUTAMATE RECEPTOR CHANNELS IN NEOCORTICAL NEURONS CAUSED BY DIFFERENTIAL GLUR-B SUBUNIT EXPRESSION. NEURON, VOL. 12, 1281-1289.

14. J. BORMANN, O.P. HAMILL AND B, SAKMANN, 1987. MECHANISM OF ANION PERMEATION THROUGH CHANNELS GATED BY GLYCINE AND Γ-AMINOBUTYRIC ACID IN MOUSE CULTURED SPINAL NEURONES. J. PHYSIOL. VOL. 385 PP 243-286.

15. MARK FARRANT AND KAI KAILA, 2007. THE CELLULAR, MOLECULAR AND IONIC BASIS OF GABAA RECEPTOR SIGNALLING. PROGRESS IN BRAIN RESEARCH, VOLUME 160, PAGES 59-87.

16. YEHEZKEL BEN-ARI, ENRICO CHERUBINI, RENATO CORRADETTI AND JEAN-LUC GAIARSA, 1989. GIANT SYNAPTIC POTENTIALS IN IMMATURE RAT CA3 HIPPOCAMPAL NEURONES. JOURNAL OF PHYSIOLOGY, 416, PP. 303-325.

17. VALENTIN STEIN AND ROGER A. NICOLL, 2003. GABA GENERATES EXCITEMENT. NEURON, VOL. 37, 375-378.

18. YEHEZKEL BEN-ARI, 2002. EXCITATORY ACTIONS OF GABA DURING DEVELOPMENT: THE NATURE OF THE NURTURE. NAT REV NEUROSCI. 3(9):728-739.

19. JONATHAN C. TRINIDAD, AGNES THALHAMMER, CHRISTIAN G.SPECHT, AENOCH J. LYNN, PETER R. BAKER, RALF SCHOEPFER AND ALMA L. BURLINGAME, 2007. QUANTITATIVE ANALYSIS OF SYNAPTIC PHOSPHORYLATION AND PROTEIN EXPRESSION. MOLECULAR & CELL PROTEOMICS, 7, 684-696.

20. THOMAS M. NEWPHER AND MICHAEL D. EHLERS, 2008. GLUTAMATE RECEPTOR DYNAMICS IN DENDRITIC MICRODOMAINS. NEURON 58(4):472-497.

21. ALAA EL-DIN EL-HUSSEINI, ERIC SCHNELL, DANE M. CHETKOVICH, ROGER A. NICOLL, DAVID S. BREDT, 2000. PSD-95 INVOLVEMENT IN MATURATION OF EXCITATORY SYNAPSES. SCIENCE 290, 1364.

22. MARY B. KENNEDY, 1998. SIGNAL TRANSDUCTION MOLECULES AT THE GLUTAMATERGIC POSTSYNAPTIC MEMBRANE. BRAIN RESEARCH REVIEWS 26, 243-257.

23. SANG HYOUNG LEE AND MORGAN SHENG, 2000. DEVELOPMENT OF NEURON-NEURON SYNAPSES. CURRENT OPINION IN NEUROBIOLOGY 10:125-131.

24. MARY B. KENNEDY, 1997. THE POSTSYNAPTIC DENSITY AT GLUTAMATERGIC SYNAPSES. TRENDS NEUROSCI. 20, 264-268.

25. JOHN LISMAN, HOWARD SCHULMAN AND HOLLIS CLINE, 2002. THE MOLECULAR BASIS OF CAMKII FUNCTION IN SYNAPTIC AND BEHAVIOURAL MEMORY. NATURE REVIEWS NEUROSCIENCE 3, 175-190

26. ANDRES BARRIA, VICTOR DERKACH, AND THOMAS SODERLING, 1997. IDENTIFICATION OF THE CA^{2+}/CALMODULIN-DEPENDENT PROTEIN KINASE II REGULATORY PHOSPHORYLATION SITE IN THE A-AMINO-3-HYDROXYL-5-METHYL-4-ISOXAZOLE-PROPIONATE-TYPE GLUTAMATE RECEPTOR. JOURNAL OF BIOLOGICAL CHEMISTRY, 272, 32727-32730.

27. RAMAKRISHNAPILLAI V. OMKUMAR, MELINDA J. KIELY, ALAN J. ROSENSTEIN, KYUNG-TAI MIN AND MARY B. KENNEDY, 1996. IDENTIFICATION OF A PHOSPHORYLATION SITE FOR CALCIUM/CALMODULIN-DEPENDENT PROTEIN KINASE II IN THE NR2B SUBUNIT OF THE N-METHYL-D-ASPARTATE RECEPTOR. THE JOURNAL OF BIOLOGICAL CHEMISTRY, 271, 31670-31678.

28. J. MICHAEL BRADSHAW, ANDY HUDMON AND HOWARD SCHULMAN, 2002. CHEMICAL QUENCHED FLOW KINETIC STUDIES INDICATE AN INTRAHOLOENZYME AUTOPHOSPHORYLATION MECHANISM FOR CA^{2+}/CALMODULIN DEPENDENT PROTEIN KINASE II. J. BIOL. CHEM. 277:20991-20998.

29. ANDY HUDMON AND HOWARD SCHULMAN, 2002. NEURONAL CA^{2+}/CALMODULIN-DEPENDENT PROTEIN KINASE II: THE ROLE OF STRUCTURE AND AUTOREGULATION IN CELLULAR FUNCTION. ANNUAL REV. BIOCHEM. VOL. 71:473-510

30. AGNES THALHAMMER, YORK RUDHARD, CEZAR M. TIGARET, KIRILL E. VOLYNSKI, DMITRI A. RUSAKOV AND RALF SCHOEPFER, 2006. CAMKII TRANSLOCATION REQUIRES LOCAL NMDA RECEPTOR-MEDIATED CA^{2+} SIGNALLING. THE EMBO JOURNAL 25, 5873-5883.

31. B. KATZ AND R. MILEDI, 1968. THE ROLE OF CALCIUM IN NEUROMUSCULAR FACILITATION. J. PHYSIOL. 195, PP. 481-192.

32. LYNN E. DOBRUNZ AND CHARLES F. STEVENS, 1997. HETEROGENEITY OF RELEASE PROBABILITY, FACILITATION, AND DEPLETION AT CENTRAL SYNAPSES. NEURON, VOL. 18, 995-1008.

33. KARL PETER GIESE, NIKOLAI B. FEDOROV, ROBERT K. FILIPKOWSKI, ALCINO J. SILVA, 1998. AUTOPHOSPHORYLATION AT THR286 OF THE CALCIUM-CALMODULIN KINASE II IN LTP AND LEARNING. SCIENCE 179, 870.

34. AMI CITRI AND ROBERT C. MALENKA, 2008. SYNAPTIC PLASTICITY: MULTIPLE FORMS, FUNCTIONS, AND MECHANISMS. NEUROPSYCHOPHARMACOLOGY REVIEWS 33, 18-41.

35. RAFAEL YUSTE AND TOBIAS BONHOEFFER, 2001. MORPHOLOGICAL CHANGES IN DENDRITIC SPINES ASSOCIATED WITH LONG-TERM SYNAPTIC PLASTICITY. ANNU. REV. NEUROSCI. 24:1071-89.

36. JONATHAN C. TRINIDAD, AGNES THALHAMMER, CHRISTIAN G. SPECHT, AENOCH J. LYNN, PETER R. BAKER, RALF SCHOEPFER AND ALMA L. BURLINGAME, 2007. QUANTITATIVE ANALYSIS OF SYNAPTIC PHOSPHORYLATION AND PROTEIN EXPRESSION, MOLECULAR & CELL PROTEOMICS, 7, 684-696.

37. MICHELLE L. APPERSON, IL SOO MOON, MARY B. KENNEDY, 1996. CHARACTERISATION OF DENSIN-180, A NEW BRAIN-SPECIFIC SYNAPTIC PROTEIN OF THE O-SIALOGLYCOPROTEIN FAMILY, THE JOURNAL OF NEUROSCIENCE, 16(21), 6839-6852.

38. AGNES THALHAMMER, JONATHAN C. TRINIDAD, ALMA L. BURLINGAME, RALF SCHOEPFER, 2009. DENSIN-180: REVISED MEMBRANE TOPOLOGY, DOMAIN STRUCTURE AND PHOSPHORYLATION STATUS, JOURNAL OF NEUROCHEMISTRY, 109, 297-302.

39. MARIE-JOSÉE SANTONI, PIERRE PONTAROTTI, DANIEL BIRNBAUM, JEAN-PAUL BORG, 2002. THE LAP FAMILY: A PHYLOGENETIC POINT OF VIEW, TRENDS IN GENETICS, 18(10), 494-497.

40. HTTP://WWW.UNIPROT.ORG/UNIPROT/Q96NW7

41. KEITH VOSSELLER, LANCE WELLS, GERALD W. HART, 2001. NUCLEOCYTOPLASMIC O-GLYCOSYLATION: O-GLCNAC AND FUNCTIONAL PROTEOMICS, BIOCHIMIE, 83(7), 575-581.

42. ICHIRO IZAWA, MIWAKO NISHIZAWA, KAZUHIRO OHTAKARA, MASAKI INAGAKI, 2002. DENSIN-180 INTERACTS WITH δ-CATENIN/NEURAL PLAKOPHILIN-RELATED REPEAT PROTEIN AT SYNAPSES, THE JOURNAL OF BIOLOGICAL CHEMISTRY, 277(7), 5345-5350.

43. ICHIRO IZAWA, MIWAKO NISHIZAWA, YUKO HAYASHI, MASAKI INAGAKI, 2008. PALMYTOYLATION OF ERBIN IS REQUIRED FOR ITS PLASMA MEMBRANE LOCALISATION, GENES TO CELLS, 13, 691-701.

44. J. BELLA, K. L. HINDLE, P. A. MCEWAN, S. C. LOVELL, 2008. THE LEUCINE-RICH REPEAT STRUCTURE, CELL. MOL. LIFE SCI. 65, 2307-2333.

45. STEPHAN STRACK, A. J. ROBISON, MARTHA A. BASS, ROGER J. COLBRAN, 2000. ASSOCIATION OF CALCIUM/CALMODULIN-DEPENDENT KINASE II WITH DEVELOPMENTALLY REGULATED SPLICE VARIANTS OF THE POSTSYNAPTIC DENSITY PROTEIN DENSIN-180. THE JOURNAL OF BIOLOGICAL CHEMISTRY, 275(33), 25061-25064.

46. RANDALL S. WALIKONIS, ASAKO OGUNI, EUGENIA M. KHOROSHEVA, CHUNG-JIUAN JENG, FRANKLIN J. ASUNCION, MARY B. KENNEDY, 2001. DENSIN-180 FORMS A TERNARY COMPLEX WITH THE A-SUBUNIT OF

CA^{2+}/CALMODULIN DEPENDENT PROTEIN KINASE II AND α-ACTININ, THE JOURNAL OF NEUROSCIENCE, 21(2), 423-433.

47. A. J. ROBISON, MARTHA A. BASS, YUXIA JIAO, LEIGH B. MACMILLAN, LEIGH C. CARMODY, RYAN K. BARTLETT, ROGER J. COLBRAN, 2005. MULTIVALENT INTERACTIONS IF CALCIUM/CALMODULIN-DEPENDENT PROTEIN KINASE II WITH THE POSTSYNAPTIC DENSITY PROTEINS NR2B, DENSIN-180, AND α-ACTININ-2, THE JOURNAL OF BIOLOGICAL CHEMISTRY, 280(42), 35329-35336.

48. MEAGAN A. JENKINS, CARL J. CHRISTEL, YUXIA JIAO, SUNDAY ABIRIA, KRISTIN Y. KIM, YURIY M. USACHEV, GERALD J. OBERMAIR, ROGER J. COLBRAN, AMY LEE, 2010. CA^{2+}-DEPENDENT FACILITATION OF $CA_V1.3$ CA^{2+} CHANNELS BY DENSIN AND CA^{2+}/CALMODULIN-DEPENDENT PROTEIN KINASE II, THE JOURNAL OF NEUROSCIENCE, 30(15), 5124-5135.

49. KAZUHIRO OHTAKARA, MIWAKO NISHIZAWA, ICHIRO IZAWA, YUTAKA HATA, SATOSHI MATSUSHIMA, WARO TAKI, HIROYASU INADA, YOSHIMI TAKAI, MASAKI INAGAKI, 2002. DENSIN-180, A SYNAPTIC PROTEIN, LINKS TO PSD-95 THROUGH ITS DIRECT INTERACTION WITH MAGUIN-1, GENES TO CELLS, 7, 1149-1160.

50. SONJA BAREISS, KWONSEOP KIM, QUN LU, 2010. δ-CATENIN/NPRAP: A NEW MEMBER OF THE GLYCOGEN SYNTHASE KINASE-3β SIGNALLING COMPLEX THAT PROMOTES β-CATENIN TURNOVER IN NEURONS, JOURNAL OF NEUROSCIENCE RESEARCH, 88, 2350-2363.

51. ARNE QUITSCH, KERSTIN BERHÖRSTER, CHONG WEE LIEW, DIETMAR RICHTER, HANS-JÜRGEN KREIENKAMP, 2005. POSTSYNAPTIC SHANK ANTAGONISES DENDRITE BRANCHING INDUCED BY THE LEUCINE-RICH REPEAT PROTEIN DENSIN-180. THE JOURNAL OF NEUROSCIENCE, 25(2), 479-487.

52. HEIKKI AHOLA, EIJA HEIKKILÄ, EVA ÅSTRÖM, MASAKI INAGAKI, ICHIRO IZAWA, HERMANN PAVENSTÄDT, DONTSCHO KERJASCHKI, HARRY HOLTHÖFER, 2003. A NOVEL PROTEIN, DENSIN, EXPRESSED BY GLOMERULAR PODOCYTES, J AM SOC NEPHROL 14, 1731-1737.

53. EIJA HEIKKILÄ, MERVI RISTOLA, KARLHANS ENDLICH, SANNA LEHTONEN, MARKUS LASSILA, MARIKA HAVANA, NICOLE ENDLICH, HARRY HOLTHÖFER, 2007. DENSIN AND BETA-CATENIN FORM A COMPLEX AND CO-LOCALIZE IN CULTURED PODOCYTE CELL JUNCTIONS, MOL CELL BIOCHEM, 305, 9-18.

54. MARKUS LASSILA, JUUSO JUHILA, EIJA HEIKKILÄ AND HARRY HOLTHÖFER, 2007. DENSIN IS A NOVEL CELL MEMBRANE PROTEIN OF SERTOLI CELLS IN THE TESTIS. MOLECULAR REPRODUCTION AND DEVELOPMENT 74:641-645.

55. JEAN-PAUL BORG, SYLVIE MARCHETTO, ANDRÉ LE BIVIC, VINCENT OLLENDORFF, FANNY JAULIN-BASTARD, HIROKO SAITO, EMMANUEL FOURNIER, JOSÉ ADÉLAÏDE, BEN MARGOLIS, DANIEL BIRNBAUM, 2000. ERBIN: A BASOLATERAL PDZ PROTEIN THAT INTERACTS WITH THE MAMMALIAN ERBB2/HER2 RECEPTOR, NATURE CELL BIOLOGY, 2, 407-414.

56. YANMEI TAO, PENGGAO DIA, YU LIU, SYLVIE MARCHETTO, WEN-CHENG XIONG, JEAN-PAUL, LEI MEI, 2009. ERBIN REGULATES NRG1 SIGNALING AND MYELINATION. PNAS, 106(23), 9477-9482.

57. YANG Z. HUANG, MENGWEI ZANG, WEN C. XIONG, ZHIJUN LUO, LIN MEI, 2003. ERBIN SUPPRESSES THE MAP KINASE PATHWAY, THE JOURNAL OF BIOLOGICAL CHEMISTRY, 278(2), 1108-1114.

58. INOUE H., NOJIMA H., OKAYAMA H, 1990. HIGH EFFICIENCY TRANSFORMATION OF ESCHERICHIA COLI WITH PLASMIDS, GENE, 96(1), 23-8.

59. HTTP://PLAZA.UFL.EDU/GSHAW/293.XLS

60. GERRY SHAW, SILAS MORSE, MIGUEL ARARAT, AND FRANK L. GRAHAM, 2002. PREFERENTIAL TRANSFORMATION OF HUMAN NEURONAL CELLS BY HUMAN ADENOVIRUSES AND THE ORIGIN OF HEK 293 CELLS. THE FASEB JOURNAL Jun;16(8):869-71.

61. JÖRG STREISSNIG, HANNO JÖRN BOLZ, ALEXANDRA KOSCHAK, 2010. CHANNELOPATHIES IN CAV1.1, CAV1.3, AND CAV1.4 VOLTAGE-GATED L-TYPE CA2+ CHANNELS. EUR J PHYSIOL 460:361-374.

62. SARAH E. CRAVEN, ALAA E. EL-HUSSEINI, AND DAVID S. BREDT, 1999. SYNAPTIC TARGETING OF THE POSTSYNAPTIC DENSITY PROTEIN PSD-95 MEDIATED BY LIPID AND PROTEIN MOTIFS. NEURON, VOL. 22, 497-509, MARCH.

63. TERRENCE M WILLIAMS, MICHAEL P. LISANTI, 2004. THE CAVEOLIN PROTEINS

64. CAROL A. OTEY AND OLLI CARPEN, 2004. ALPHA-ACTININ REVISITED: A FRESH LOOK AT AN OLD PLAYER. CELL MOTILITY AND THE CYTOSKELETON 58:104-111.

65. IKUKO YAO, YUTAKA HATA, NOBUYUKI IDE, KAZUYO HIRAO, MAKI DEGUCHI, HIDEO NISHIOKA, AKIRA MIZOGUCHI, AND YOSHIMI TAKAI, 1999. MAGUIN, A NOVEL NEURONAL MEMBRANE-ASSOCIATED GUANYLATE KINASE-INTERACTING PROTEIN. THE JOURNAL OF BIOLOGICAL CHEMISTRY, VOL. 274, NO, 17, ISSUE OF APRIL 23, PP. 11889-11896.

66. MARIKO KATO HAYASHI, CHUNYAN TANG, CHIARA VERPELLI, RADHAKRISHNAN NARAYANAN, MARISSA H. STEARNS, RUI-MING XU, HUILIN LI, CARLO SALA, AND YASUNORI HAYASHI, 2009. THE POSTSYNAPTIC

DENSITY PROTEINS HOMER AND SHANK FORM A POLYMERIC NETWORK STRUCTURE. CELL. APRIL 3; 137(2): 159-171.

67. INBAL ISRAELY, RUI M. COSTA, CUI WEI XIE, ALCINO J. SILVA, KENNETH S. KOSIK, AND XIN LIU, 2004. DELETION OF THE NEURON-SPECIFIC PROTEIN DELTA-CATENIN LEADS TO SEVERE COGNITIVE AND SYNAPTIC DYSFUNCTION. CURRENT BIOLOGY, VOL. 14, 1657-1663, SEPTEMBER 21.

68. http://www.uniprot.org/uniprot/P35222

69. http://www.uniprot.org/uniprot/P19022

70. VARKI A, CUMMINGS RD, ESKO JD, ET AL., EDITORS, 2009. ESSENTIALS OF GLYCOBIOLOGY. 2ND EDITION

71. LEE S. GRIFFITH AND BRIGGITTE SCHMITZ, 1999. O-LINKED N-ACETYLGLUCOSAMINE LEVELS IN CEREBELLAR NEURONS RESPOND RECIPROCALLY TO PERTUBATIONS OF PHOSPHORYLATION. EUR. J. BIOCHEM. 262. 824-831.

Appendix

Digests

1. N-tag

1.1 PCR 3 shuffle into intermediate cloning vector

Preparative: PCR3 product / SacI / BglII

Component		µl
DNA		15
NEBuffer	***2***	2.5
BSA		2
Enzyme A	***BglII***	0.75
Enzyme B	***SacI***	1
H2O		3.75
Total		25

Preparative: pRSET6a-Ca-His / SacI / BglII

Component		µl
DNA		2
NEBuffer	***2***	2
BSA		2
Enzyme A	***BglII***	0.75
Enzyme B	***SacI***	1
H2O		17.25
Total		25

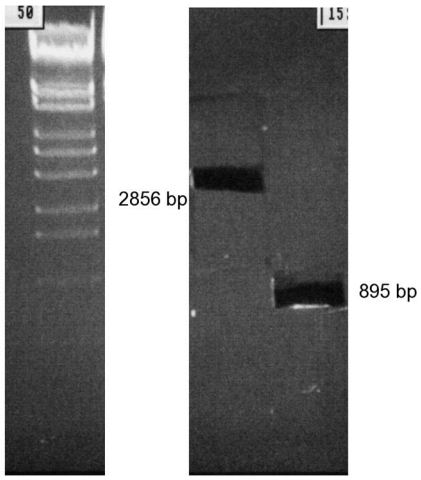

0.8% GTG Agarose, 1x TAE, 7V/cm, 60 mins, entire digest mixture was loaded onto lanes

Analytical: hLrrc7-pRSET6a-eGFP-PCR3 / BsrGI / SacII

Component		*µl*
DNA		1.5
NEBuffer	***3***	1.5
BSA		1.5
Enzyme A	***BsrGI***	0.5
Enzyme B	***SacII***	0.5
H2O		9.5
Total		15

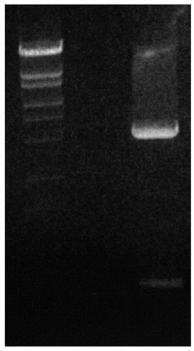

λ/StyI hLrrc7-pRSET6a-eGFP-PCR3 / BsrGI / SacII

0.8% LE Agarose Gel, 1x TAE, 7V/cm, 60 min

1.2 PCR4 shuffle into intermediate cloning construct

Preparative: hLrrc7-pRSET6a-eGFP-PCR3 / BglII / NcoI

Component		µl
DNA		1.3
NEBuffer	***3***	1
BSA		0
Enzyme A	***BglII***	0.5
Enzyme B	***NcoI***	0.5
H2O		6.7
Total		10

Preparative: PCR4 product / BamHI / NcoI

Component		µl
DNA		1.3
NEBuffer	***3***	1
BSA		0
Enzyme A	***BglII***	0.5
Enzyme B	***NcoI***	0.5
H2O		6.7
Total		10

Analytical: hLrrc7-pRSET6a-eGFP-PCR3-PCR4 / AccI

Component		µl
DNA		1.5
NEBuffer	***4***	1.5
BSA		0
Enzyme A	***AccI***	0.5
Enzyme B		0
H2O		11.5
Total		15

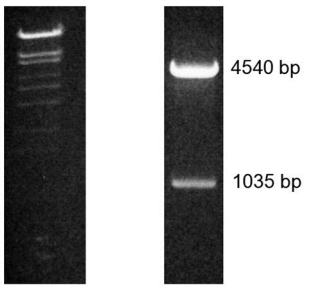

0.8% LE Agarose, 1x TAE, 7V/cm, 60 min

1.3 Shuffling eGFP-tagged Densin-180 N-terminus coding sequence into Densin-180 construct

Preparative: hLrrc7-pRSET6a-eGFP-PCR3-PCR4 / NotI / XhoI

Component		µl
DNA		0.7
NEBuffer	***3***	1
BSA		1
Enzyme A	***NotI***	0.5
Enzyme B	***XhoI***	0.5
H2O		6.3
Total		10

Preparative: KS+-hLrrc7-unrepaired / NotI / XhoI

Component		µl
DNA		0.7
NEBuffer	***3***	1
BSA		1
Enzyme A	***NotI***	0.5
Enzyme B	***XhoI***	0.5
H2O		6.3
Total		10

Analytical: KS+-N-eGFP-hLrrc7-unrepaired / AvrII / AflII

Component		µl
DNA		1.5
NEBuffer	***4***	1
BSA		1
Enzyme A	***AflII***	0.5
Enzyme B	***AvrII***	0.5
H2O		5.5
Total		10

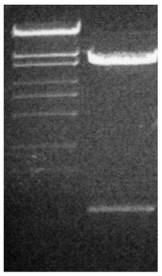

λ/StyI KS+-N-eGFP-hLrrc7-WT-unrepaired / AflII / AvrIII

0.8% LE Agarose, 1x TAE, 7V/cm, 60 min

2. C-tag

2.1 Shuffling tagged C-terminus into Densin-180 construct

Preparative: KS+-hLrrc7-unrepaired / KpnI / SmaI

Component		*µl*
DNA		6.66
NEBuffer	***3***	1
BSA		1
Enzyme A	***NotI***	0.5
Enzyme B	***XhoI***	0.5
H2O		0.34
Total		10

Preparative: PCR3' product / KpnI / SmaI

Component		*µl*
DNA		6.66
NEBuffer	***3***	1
BSA		1
Enzyme A	***NotI***	0.5
Enzyme B	***XhoI***	0.5
H2O		0.34
Total		10

Analytical: KS+-hLrrc7-eGFP-C-WT-unrepaired / EcoRI

Component		*µl*
DNA		6.66
NEBuffer	***3***	1
BSA		1
Enzyme A	***NotI***	0.5
Enzyme B	***XhoI***	0.5
H2O		0.34
Total		10

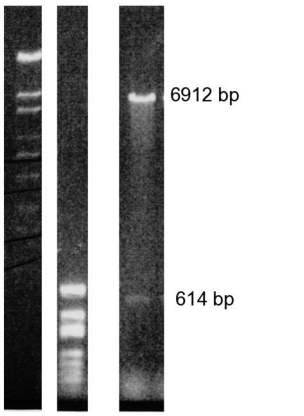

0.8% LE Agarose gel, 1x TAE, 60 min, 7V/cm, full digest product loaded

3. Repair of construct and insertion of mutations

3.1 Insertion repair fragment - PCR2 (Nested) product by AGT

Preparative: PCR2 (nested) product / BlnI (AvrII) / AflII

Component		*µl*
DNA		15
NEBuffer	***4***	2
BSA		2
Enzyme A	***BlnI***	0.5
Enzyme B	***AflII***	0.5
H2O		0
Total		20

Preparative: [KS+-N-eGFP-hLrrc7-WT-unrepaired / KS+-hLrrc7-eGFP-C-WT-unrepaired / BlnI (AvrII) / AflII

Component		*µl*
DNA		15
NEBuffer	***4***	2
BSA		2
Enzyme A	***BlnI***	0.5
Enzyme B	***AflII***	0.5
H2O		0
Total		20

Analytical: KS+-N-eGFP-hLrrc7-WT-FULL / EcoRV

Component		*µl*
DNA		1
NEBuffer	***3***	1
BSA		1
Enzyme A	***EcoRV***	0.5
Enzyme B		0
H2O		6.5
Total		10

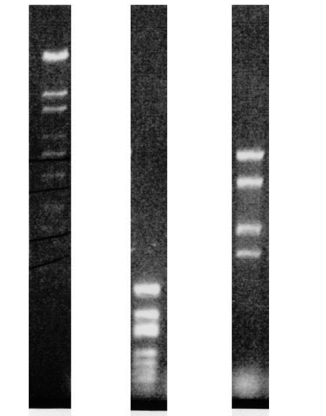

0.8% LE Agarose gel, 1x TAE, 7V/cm, 60 min

3.2 Inserting TTT865/868/869AAA mutation containing fragment

Preparative: KS+-hLrrc7-eGFP-C-WT-FULL / AflII / ClaI

Component		*µl*
DNA		2
NEBuffer	***4***	1.5
BSA		1.5
Enzyme A	***ClaI***	0.5
Enzyme B	***AflII***	0.5
H2O		9
Total		15

Preparative: KS+-N-eGFP-hLrrc7-TTT-unrepaired / AflII / ClaI

Component		*µl*
DNA		5
NEBuffer	***4***	1.5
BSA		1.5
Enzyme A	***ClaI***	0.5
Enzyme B	***AflII***	0.5
H2O		6
Total		15

Preparative: KS+-N-eGFP-hLrrc7-TTT-FULL or KS+-hLrrc7-eGFP-C-TTT-FULL / EcoRV

Component		*µl*
DNA		1
NEBuffer	***3***	1.5
BSA		1.5
Enzyme A	***EcoRV***	0.5
Enzyme B		0
H2O		10.5
Total		15

4. pRK7 vector modification and construct shuffle

4.1 Vector modification

Preparative: pRK7 / HindIII / SalI

Component		*µl*
DNA		2.5
SalI Buffer		1.5
BSA		1.5
Enzyme A	***HindIII***	0.5
Enzyme B	***SalI***	0.5
H2O		8.5
Total		15

2009-07-27

Analytical: pRK7a / ScaI / XhoI

Component		*µl*
DNA		1
NEBuffer 3		1.5
BSA		1.5
Enzyme A	***HindIII***	0.5
Enzyme B	***SalI***	0.5
H2O		10
Total		15

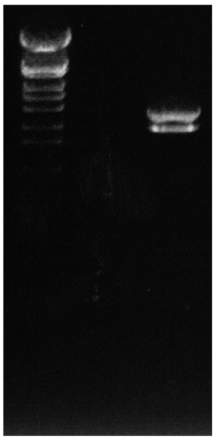

λ/StyI pRK7a / ScaI / XhoI

0.8% LE Agarose, 7V/ cm, 45 mins

4.2 Shuffling the Densin-180 constructs from KS+, cloning vector, and into pRK7a, expression vector

Preparative: pRK7a / NotI / KpnI

Component		µl
DNA		8
NEBuffer 2		5
BSA		5
Enzyme A	***NotI***	2
Enzyme B	***KpnI***	2
H2O		28
Total		50

Preparative: KS+-N-eGFP-hLrrc7-TTTorWT-FULL / NotI / KpnI

Component		µl
DNA		8
NEBuffer 2		5
BSA		5
Enzyme A	***NotI***	2
Enzyme B	***KpnI***	2
H2O		28
Total		50

Analytical : pRK7a-N-eGFP-hLrrc7-TTTorWT-FULL / ScaI / ClaI

Component		µl
DNA		1
NEBuffer 2		1.5
BSA		1.5
Enzyme A	***ScaI***	0.5
Enzyme B	***ClaI***	0.5
H2O		10
Total		15

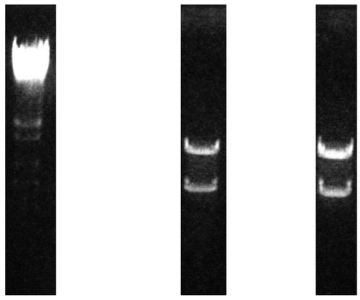

0.8% LE Agarose, 1x TAE, 7V/cm, 60 min

Preparative: KS+-hLrrc7-eGFP-C-TTTorWT-FULL / NotI / KpnI

Component		µl
DNA		2
NEBuffer 2		1.5
BSA		1.5
Enzyme A	***NotI***	0.5
Enzyme B	***KpnI***	0.66
H2O		8.34
Total		14.5

Analytical: pRK7a-hLrrc7-eGFP-C-TTTorWT-FULL / ScaI / ClaI

Component		µl
DNA		1
NEBuffer 3		1.5
BSA		1.5
Enzyme A	***ScaI***	0.25
Enzyme B	***ClaI***	0.25
H2O		10.5
Total		15

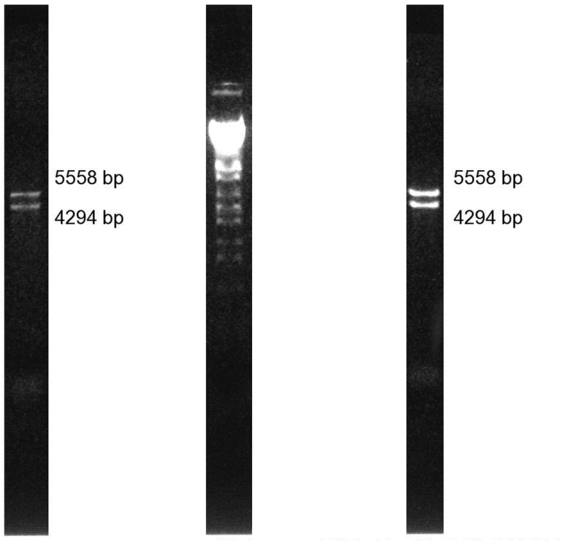

pRK7a-hLrrc7-eGFP-C-WT / ScaI / ClaI | λ/StyI | pRK7a-hLrrc7-eGFP-C-TTT / ScaI / ClaI

0.8% LE Agarose Gel, 1x TAE, 7V/cm, 60 min

Analytical: pRK7a-hLrrc7-eGFP-C-TTT-FULL / PstI

Component		µl
DNA		1
NEBuffer 3		1.5
BSA		1.5
Enzyme A	***PstI***	0.5
Enzyme B		
H2O		10.5
Total		15

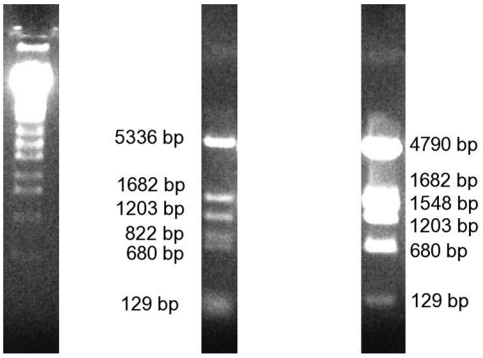

λ/StyI | pRK7a-hLrrc7-eGFP-C-TTT-FULL / PstI | pRK7a-N-eGFP-hLrrc7-TTT / PstI

0.8% LE Agarose, 1x TAE, 7V/cm, 60 min,
100% digestion product loaded per lane

5. PDZ truncation constructs

Preparative: pRK7a-N-eGFP-hLrrc7-WT-FULL vs BamHI / BspEI

Component		*µl*
DNA		1
NEBuffer	***3***	2
BSA		2
Enzyme A	***BamHI***	0.5
Enzyme B	***BspEI***	0.5
H2O		14
Total		20

Preparative: PCR fragments A, B and C / BamHI / BspEI

Component		*µl*
DNA		10
NEBuffer	***3***	2
BSA		2
Enzyme A	***BamHI***	0.5
Enzyme B	***BspEI***	0.5
H2O		5
Total		20

Analytical: PDZ deletion construct A, B and C / HpaI

Component		*µl*
DNA		1
NEBuffer	***4***	2
BSA		2
Enzyme A	***HpaI***	0.5
Enzyme B		0
H2O		14.5
Total		20

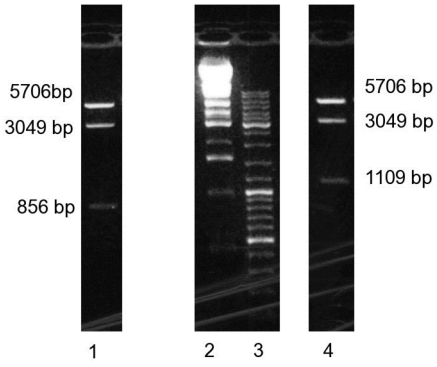

0.8% LE Agarose gel, 1x TAE, 7V/cm, 60 min. Lane 1: PDZ deletion construct A / HpaI. Lane 2: λ/StyI marker. Lane 3: GeneRuler DNA Ladder (Fermentas). Lane 4: PDZ deletion construct C / HpaI

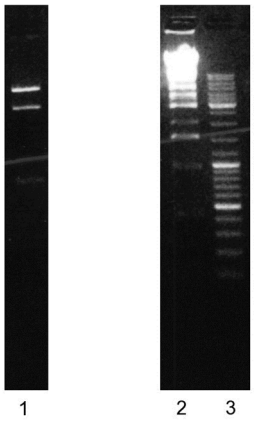

0.8 % LE Agarose gel, 1x TAE, 7V/cm, 60 min. Lane 1: PDZ deletion construct B. Lane 2: λ/StyI. Lane 3: GeneRuler DNA Ladder (Fermentas)

6. Phospho-rich region deletion constructs

Preparative: pRK7a-N-eGFP-hLrrc7-WT / XmaI and pRK7a-hLrrc7-eGFP-C-WT / XmaI

Component		*µl*
DNA		1
NEBuffer	***4***	2
BSA		2
Enzyme A	***XmaI***	0.5
Enzyme B	**-**	0
H2O		14.5
Total		20

Analytical digest: pRK7a-hLrrc7-eGFP-C-WT-no phosphorich / XhoI
pRK7a-N-eGFP-hLrrc7-WT-FULL-no phosphorich / XhoI

Component		*µl*
DNA		1
NEBuffe	***4***	2
BSA		2
Enzyme	***XmaI***	0.5
Enzyme	**-**	0
H2O		14.5
Total		20

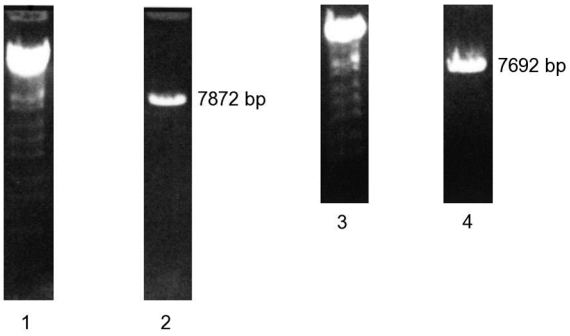

0.8% LE Agarose gel, 1x TAE, 7V/cm, 60 min. Lane 1: λ/StyI. Lane 2: pRK7a-N-eGFP-hLrrc7-WT-nophosphorich. Lane 3: λ/StyI. Lane 4: pRK7a-hLrrc7-eGFP-C-WT-nophosphorich

Polymerase Chain Reactions

1. KS+-N-eGFP-hLrrc7-WT

PCR1

Reaction Mixture

Component		µl	Final concentration
Template DNA	KS+-hLrrc7-unrepaired, 1:100 miniprep DNA in H_2O	1	
Sense Primer	KSpIMCS-Seq1-s, 10µM	2	0.4 µM
Anti-sense primer	EGFP-hLrrc7-PCR1-a, 10µM	2	0.4 µM
10x KOD Polymerase buffer		5	1 X
25 mM $MgCl_2$		2	1 mM
2.5 U/µl KOD Polymerase		0.2	0.010 U/µl
5 mM dNTP		2	0.2 mM
DMSO		0	0 %
H_2O		35.8	
Total volume		50	

PCR Cycle

Step			
1	95°C	5 min	
2	95°C	30 sec	
3	60°C	30 sec	
4	72°C	10 sec	*Repeat steps 2 - 4 for 29 cycles*
5	10°C	pause	

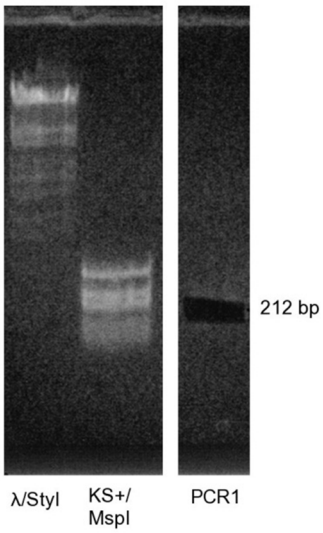

100% PCR product per lane, 16cm length gel, 0.8% GTG Agarose, 1X TAE, 7V/cm, 60 min
2009-03-22

PCR2

Reaction Mixture

Component		µl	Final concentration
Template DNA	pBS.EGFP.MT.CK2a, 1:100 miniprep DNA	1	
Sense Primer	EGFP-hLrrc7-PCR2-s, 10µM	2	0.4 µM
Anti-sense primer	EGFP-PCR2-a, 10µM	2	0.4 µM
10x KOD Polymerase buffer		5	1 X
25 mM $MgCl_2$		2	1 mM
2.5 U/µl KOD Polymerase		0.2	0.010 U/µl
5 mM dNTP		2	0.2 mM
DMSO		0	0 %
H_2O		35.8	
Total volume		50	

PCR Cycle

Step			
1	95°C	5 min	
2	95°C	30 sec	
3	70°C	30 sec	
4	72°C	10 sec	*Repeat steps 2 - 4 for 29 cycles*
5	10°C	pause	

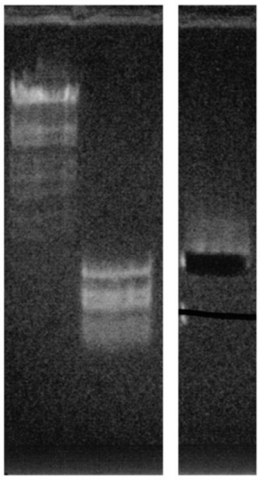

100% PCR product per lane, 16cm length gel, 0.8% GTG Agarose, 1X TAE, 7V/cm, 60 min
2009-03-22

PCR3

Reaction Mixture

Component		µl	Final concentration
Template DNA 1	Product of PCR1	1	
Template DNA 2	Product of PCR2	1	
Sense Primer	KSpIMCS-Seq1-s, 10µM	1	0.5 µM
Anti-sense primer	EGFP-PCR2-a, 10µM	1	0.5 µM
10x KOD Polymerase buffer		2.5	1.25 X
25 mM $MgCl_2$		1	1.25 mM
2.5 U/µl KOD Polymerase		0.1	0.013 U/µl
5 mM dNTP		1	0.25 mM
DMSO		0	0 %
H_2O		11.4	
Total volume		20	

PCR Cycle

Step			
1	95°C	5 min	
2	95°C	30 sec	
3	60°C	30 sec	
4	72°C	10 sec	*Repeat steps 2 - 4 for 29 cycles*
5	10°C	pause	

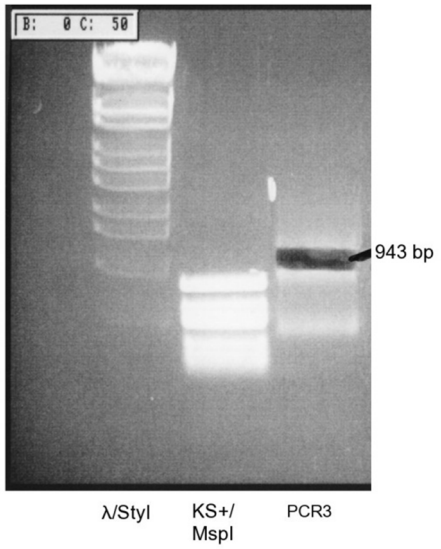

100% PCR product per lane, 16 cm length gel, 0.8% GTG Agarose, 1X TAE, 7V/cm, 60 min 2009-03-24

PCR4

Reaction Mixture

Component		µl	Final concentration
Template DNA 1	KS+-hLrrc7-unrepaired, 1:100 miniprep DNA	1	
Sense Primer	hLrrc7-PCR1-s, 10µM	1	0.2 µM
Anti-sense primer	hLrrc7-Seq11-a, 10µM	1	0.2 µM
10x KOD Polymerase buffer		5	1 X
25 mM $MgCl_2$		2	1 mM
2.5 U/µl KOD Polymerase		0.25	0.013 U/µl
5 mM dNTP		4	0.4 mM
DMSO		0	0 %
H_2O		35.75	
Total volume		50	

PCR Cycle

Step			
1	95°C	5 min	
2	95°C	30 sec	
3	50°C	30 sec	
4	72°C	15 sec	*Repeat steps 2 - 4 for 29 cycles*
5	10°C	pause	

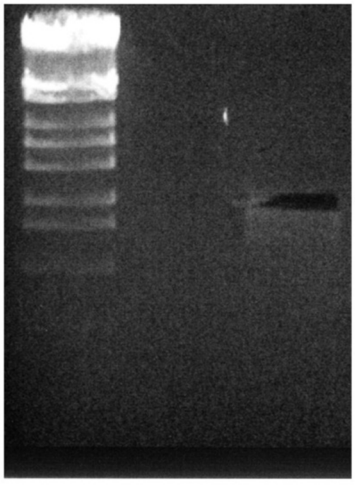

100% PCR product per lane, 16cm length gel, 0.8% GTG Agarose, 1X TAE, 7V/cm, 60 min
2009-04-20

2. KS+-hLrrc7-eGFP-C-WT

PCR1'

Reaction Mixture

Component		µl	Final concentration
Template DNA 1	KS+-hLrrc7-unrepaired, 1:100 miniprep DNA	1	
Sense Primer	hLrrc7-Seq6-s, 10µM	2	0.4 µM
Anti-sense primer	EGFP-hLrrc7-PCR4-a, 10µM	2	0.4 µM
10x KOD Polymerase buffer		5	1 X
25 mM $MgCl_2$		2	1 mM
2.5 U/µl KOD Polymerase		0.25	0.013 U/µl
5 mM dNTP		2	0.2 mM
DMSO		0	0 %
H_2O		35.75	
Total volume		50	

PCR Cycle

Step			
1	95°C	5 min	
2	95°C	30 sec	
3	50°C	30 sec	
4	72°C	30 sec	*Repeat steps 2 - 4 for 29 cycles*
5	10°C	pause	

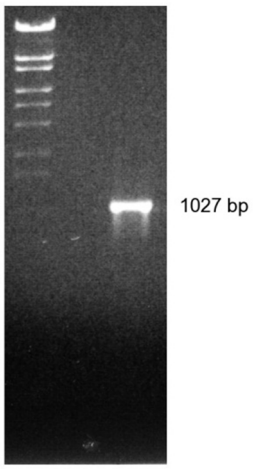

10% PCR product per lane, 10cm length gel, 0.8% GTG Agarose, 1X TAE, 7V/cm, 45 min
2009-04-27

PCR2'

Reaction Mixture

Component		µl	Final concentration
Template DNA 1	pBS.EGFP.MT.CK2a, 1:100 miniprep DNA	1	
Sense Primer	EGFP-hLrrc7-PCR3-s, 10µM	2	0.4 µM
Anti-sense primer	EGFP-PCR8-a, 10µM	2	0.4 µM
10x KOD Polymerase buffer		5	1 X
25 mM $MgCl_2$		2	1 mM
2.5 U/µl KOD Polymerase		0.25	0.013 U/µl
5 mM dNTP		2	0.2 mM
DMSO		0	0 %
H_2O		35.75	
Total volume		50	

PCR Cycle

Step			
1	95°C	5 min	
2	95°C	30 sec	
3	70°C	30 sec	
4	72°C	10 sec	*Repeat steps 2 - 4 for 29 cycles*
5	10°C	pause	

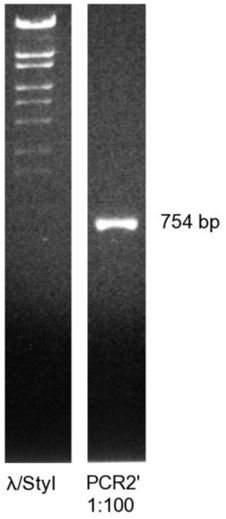

10% PCR product per lane, 10cm length gel, 0.8% GTG Agarose, 1X TAE, 7V/cm, 45 min
2009-04-27

PCR3’

Reaction Mixture

Component		µl	Final concentration
Template DNA 1	Product of PCR1'	1	
Template DNA 2	Product of PCR2'	2	
Sense Primer	hLrrc7-Seq6-s, 10µM	1	0.2 µM
Anti-sense primer	EGFP-PCR8-a, 10µM	1	0.2 µM
10x KOD Polymerase buffer		5	1 X
25 mM $MgCl_2$		1	0.5 mM
2.5 U/µl KOD Polymerase		0.5	0.025 U/µl
2 mM dNTP		5	0.2 mM
DMSO		0	0 %
H_2O		33.5	
Total volume		50	

PCR Cycle

Step			
1	95°C	5 min	
2	95°C	30 sec	
3	56°C	30 sec	
4	72°C	15 sec	*Repeat steps 2 - 4 for 29 cycles*
5	10°C	pause	

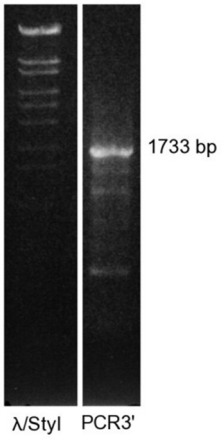

20% PCR product, 10cm length gel,
0.6% LE Agarose, 1X TAE, 7V/cm,
60 min
2009-06-25

3. PDZ truncations

PCR A

Reaction Mixture

Component		µl	Final concentration
Template	pRK7a-N-eGFP-hLrrc7-WT / SacII l	1	
Sense Primer (10µM)	hLrrc7-Seq6-s	2	0.4 µM
Anti-sense primer (10µM)	hLrrc7-PCR11-a	2	0.4 µM
10x KOD Polymerase buffer		5	1 X
25 mM $MgCl_2$		3	1.5 mM
2.5 U/µl KOD Polymerase		0.5	0.025 U/µl
2 mM dNTP		5	0.2 mM
DMSO		0	0 %
H_2O		31.5	
Total volume excluding DNA			
Final total volume		50	

PCR Cycle

Step			
1	95°C	5 min	
2	95°C	30 sec	
3	55°C	30 sec	
4	72°C	10 sec	*Repeat steps 2 - 4 for 29 cycles*
5	10°C	pause	

PCR B

Reaction Mixture

Component		µl	Final concentration
Template	pRK7a-N-eGFP-hLrrc7-WT / SacII l	1	
Sense Primer (10µM)	hLrrc7-Seq6-s	2	0.4 µM
Anti-sense primer (10µM)	hLrrc7-PCR12-a	2	0.4 µM
10x KOD Polymerase buffer		5	1 X
25 mM $MgCl_2$		3	1.5 mM
2.5 U/µl KOD Polymerase		0.5	0.025 U/µl
2 mM dNTP		5	0.2 mM
DMSO		0	0 %
H_2O		31.5	
Total volume excluding DNA			
Final total volume		50	

PCR Cycle

Step			
1	95°C	5 min	
2	95°C	30 sec	
3	55°C	30 sec	
4	72°C	10 sec	*Repeat steps 2 - 4 for 29 cycles*
5	10°C	pause	

PCR C

Reaction Mixture

Component		µl	Final concentration
Template	pRK7a-N-eGFP-hLrrc7-WT / SacII l	1	
Sense Primer (10µM)	hLrrc7-Seq6-s	2	0.4 µM
Anti-sense primer (10µM)	hLrrc7-PCR13-a	2	0.4 µM
10x KOD Polymerase buffer		5	1 X
25 mM $MgCl_2$		3	1.5 mM
2.5 U/µl KOD Polymerase		0.5	0.025 U/µl
2 mM dNTP		5	0.2 mM
DMSO		0	0 %
H_2O		31.5	
Total volume excluding DNA			
Final total volume		50	

PCR Cycle

Step			
1	95°C	5 min	
2	95°C	30 sec	
3	55°C	30 sec	
4	72°C	10 sec	*Repeat steps 2 - 4 for 29 cycles*
5	10°C	pause	

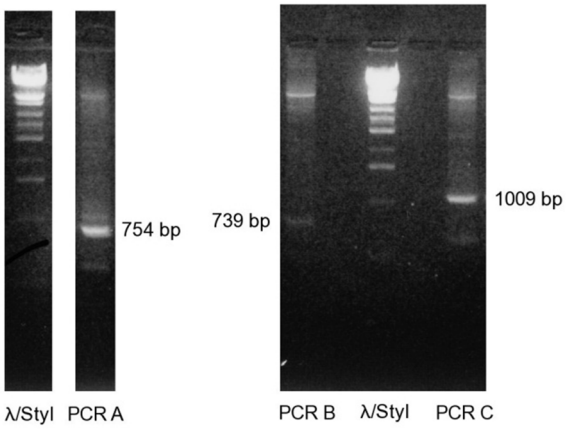

16.66•% PCR product per lane, 16cm length gel, 1.5% GTG Agarose, 1X TAE, 7V/cm, 60 min
2010-06-04

DNA sequences

Primers

KSpIMCS-Seq1-s
ACTCACTATAGGGCGAATTGGAGCTCCAC

EGFP-hLrrc7-PCR1-a
tcgcccttgctcaccatACTGCAGTGGGAGTAATCT

EGFP-hLrrc7-PCR2-s
AGATTACTCCCACTGCAGTatggtgagcaagggcgaggagctg

EGFP-PCR2-a (by CET)
cgccggtaccgctagcgatatcagatctgagCTTGTACAGCTCGTCCATG
CCGAG

hLrrc7-PCR1-s
cgggatccCTTCAGCAGGTGCCAAAGGAGGTC

hLrrc7-Seq11-a
TACCAATGTCAATCTCATCG

hLrrc7-Seq6-s
AAGCTACAGTACAGAGAG

EGFP-hLrrc7-PCR4-a
cagctcctcgcccttgctcaccatGACAGTAAGCTCACGTTGAATAAC

EGFP-hLrrc7-PCR3-s
GTTATTCAACGTGAGCTTACTGTCatggtgagcaagggcgaggagctg

EGFP-PCR8-a
cgccggtaccTTACTTGTACAGCTCGTCCATGCCGAG

hLrrc7-PCR11-a
ATGggatccTTAGACAGTAAGCTCACGTTGTGGATATCCATCCATACTCC

hLrrc7-PCR12-a
ATGATGggatccTTATGGATATCCATCCATACTCCT

hLrrc7-PCR13-a
ATGATGggatccTTACTCACGTTGAATAACTAGGTC

Amino acid sequence alignments

Whole sequence alignment

```
Q80TE7  LRRC7_MOUSE
P70587  LRRC7_RAT
Q96NW7  LRRC7_HUMAN

CLUSTAL 2.0.12 multiple sequence alignment


Q80TE7          -----MTTKRKLIGRLVPCRCFRGEEEIISVLDYSHCSLQQVPKEVFNFERTLEELYLDA 55
P70587          MQCLEMTTKRKLIGRLVPCRCFRGEEEIISVLDYSHCSLQQVPKEVFNFERTLEELYLDA 60
Q96NW7          -----MTTKRKIIGRLVPCRCFRGEEEIISVLDYSHCSLQQVPKEVFNFERTLEELYLDA 55
                     ******:**************************************************

Q80TE7          NQIEELPKQLFNCQALRKLSIPDNDLSSLPTSIASLVNLKELDISKNGVQEFPENIKCCK 115
P70587          NQIEELPKQLFNCQALRKLSIPDNDLSSLPTSIASLVNLKELDISKNGVQEFPENIKCCK 120
Q96NW7          NQIEELPKQLFNCQALRKLSIPDNDLSNLPTTIASLVNLKELDISKNGVQEFPENIKCCK 115
                ***************************.***:**************************

Q80TE7          CLTIIEASVNPISKLPDGFTQLLNLTQLYLNDAFLEFLPANFGRLVKLRILELRENHLKT 175
P70587          CLTIIEASVNPISKLPDGFTQLLNLTQLYLNDAFLEFLPANFGRLVKLRILELRENHLKT 180
Q96NW7          CLTIIEASVNPISKLPDGFTQLLNLTQLYLNDAFLEFLPANFGRLVKLRILELRENHLKT 175
                ************************************************************

Q80TE7          LPKSMHKLAQLERLDLGNNEFSELPEVLDQIQNLRELWMDNNALQVLPGSIGKLKMLVYL 235
P70587          LPKSMHKLAQLERLDLGNNEFSELPEVLDQIQNLRELWMDNNALQVLPGSIGKLKMLVYL 240
Q96NW7          LPKSMHKLAQLERLDLGNNEFGELPEVLDQIQNLRELWMDNNALQVLPGSIGKLKMLVYL 235
                *********************.**************************************

Q80TE7          DMSKNRIETVDMDISGCEALEDLLLSSNMLQQLPDSIGLLKKLTTLKVDDNQLTMLPNTI 295
P70587          DMSKNRIETVDMDISGCEALEDLLLSSNMLQQLPDSIGLLKKLTTLKVDDNQLTMLPNTI 300
Q96NW7          DMSKNRIETVDMDISGCEALEDLLLSSNMLQQLPDSIGLLKKLTTLKVDDNQLTMLPNTI 295
                ************************************************************

Q80TE7          GNLSLLEEFDCSCNELESLPPTIGYLHSLRTLAVDENFLPELPREIGSCKNVTVMSLRSN 355
P70587          GNLSLLEEFDCSCNELESLPPTIGYLHSLRTLAVDENFLPELPREIGSCKNVTVMSLRSN 360
Q96NW7          GNLSLLEEFDCSCNELESLPSTIGYLHSLRTLAVDENFLPELPREIGSCKNVTVMSLRSN 355
                *******************.**************************************

Q80TE7          KLEFLPEEIGQMQRLRVLNLSDNRLKNLPFSFTKLKELAALWLSDNQSKALIPLQTEAHP 415
P70587          KLEFLPEEIGQMQRLRVLNLSDNRLKNLPFSFTKLKELAALWLSDNQSKALIPLQTEAHP 420
Q96NW7          KLEFLPEEIGQMQKLRVLNLSDNRLKNLPFSFTKLKELAALWLSDNQSKALIPLQTEAHP 415
                *************:**********************************************

Q80TE7          ETKQRVLTNYMFPQQPRGDEDFQSDSDSFNPTLWEEQRQQRMTVAFEFEDKKEDDESAGK 475
P70587          ETKQRVLTNYMFPQQPRGDEDFQSDSDSFNPTLWEEQRQQRMTVAFEFEDKKEDDESAGK 480
Q96NW7          ETKQRVLTNYMFPQQPRGDEDFQSDSDSFNPTLWEEQRQQRMTVAFEFEDKKEDDENAGK 475
                ************************************************************.***

Q80TE7          VKALSCQAPWDRGQRGITLQPARLSGDCCTPWARCDQQIQDMPVPQSDPQLAWGCISGLQ 535
P70587          VKALSCQAPWDRGQRGITLQPARLSGDCCTPWARCDQQIQDMPVPQSDPQLAWGCISGLQ 540
Q96NW7          VKDLSCQAPWERGQRGITLQPARLSGDCCTPWARCDQQIQDMPVPQNDPQLAWGCISGLQ 535
                ** *******:**********************************.*************

Q80TE7          QERSMCAPLPVAAQSTTLPSLSGRQVEINLKRYPTPYPEDLKNMVKSVQNLVGKPSHGVR 595
P70587          QERSMCAPLPVAAQSTTLPSLSGRQVEINLKRYPTPYPEDLKNMVKSVQNLVGKPSHGVR 600
Q96NW7          QERSMCTPLPVAAQSTTLPSLSGRQVEINLKRYPTPYPEDLKNMVKSVQNLVGKPSHGVR 595
                ******:*****************************************************

Q80TE7          VENSNPTANTEQTVKEKFEHKWPVAPKEITVEDSFVHPANEMRIGELHPSLAETPLYPPK 655
P70587          VENANPTANTEQTVKEKFEHKWPVAPKEITVEDSFVHPANEMRIGELHPSLAETPLYPPK 660
Q96NW7          VENSNPTANTEQTVKEKYEHKWPVAPKEITVEDSFVHPANEMRIGELHPSLAETPLYPPK 655
                ***:*************:*****************************************

Q80TE7          LVLLGKDKKESTDESEVDKTHCLNNSVSSGTYSDYSPSQASSASSNTRMKVGSLQATAKD 715
P70587          LVLLGKDKKESTDESEVDKTHCLNNSVSSGTYSDYSPSQASSASSNTRVKVGSLQPTTKD 720
Q96NW7          LVLLGKDKKESTDESEVDKTHCLNNSVSSGTYSDYSPSQASSGSSNTRVKVGSLQTTAKD 715
                ****************************************.*****:******.*:**

Q80TE7          AVHNSLWGNRIAPPFPQPLDAKPLLSQREAVPPGNIPQRPDRLPMSDAFPDNWTDGSHYD 775
P70587          AVHNSLWGNRIAPPFPQPLDAKPLLTQREAVPPGNLPQRPDRLPMSDAFPDNWTDGSHYD 780
Q96NW7          AVHNSLWGNRIAPSFPQPLDSKPLLSQREAVPPGNIPQRPDRLPMSDTFTDNWTDGSHYD 775
                *************.******:****:*********:***********:*.**********
```

```
Q80TE7          NTGFVSEEAAGENANNNPLLSSKARSVPAHGRRPLIRQERIVGVPLELEQSTHRHTPETE 835
P70587          NTGFVSEEATGENANNNPLLSSKARSVPAHGRRPLIRQERIVGVPLELEQSTHRHTPETE 840
Q96NW7          NTGFVAEETTAENANSNPLLSSKSRSTSSHGRRPLIRQDRIVGVPLELEQSTHRHTPETE 835
                *****:**::.****.*******:**..:*********:**********************

Q80TE7          VPPSNPWQNWTRTPSPFEDRTAFPSKLETTPTTSPLPERKDHMKEPTETPGPFSPGVPWE 895
P70587          VPPSNPWQNWTRTPSPFEDRTAFPSKLETTPTTSPLPERKDHMKEPTETPGPFSPGVPWE 900
Q96NW7          VPPSNPWQNWTRTPSPFEDRTAFPSKLETTPTTSPLPERKEHIKESTEIPSPFSPGVPWE 895
                ****************************************:*:**.** *.*********

Q80TE7          YHDPTPNRSLGNVFSQIHCRPDSSKGVIAISKSTERLSPLMKDIKSNKFKKSQSIDEIDV 955
P70587          YHDPTPNRSLGNVFSQIHCRPDSSKGVIAISKSTERLSPLMKDIKSNKFKKSQSIDEIDV 960
Q96NW7          YHDSNPNRSLSNVFSQIHCRPESSKGVISISKSTERLSPLMKDIKSNKFKKSQSIDEIDI 955
                ***..*****.*********:******:*****************************:

Q80TE7          GTYKVYNIPLENYASGSDHLGSHERPDKFLGPEHGMSSMSRSQSVPMLDDEMLMYGSSKG 1015
P70587          GTYKVYNIPLENYASGSDHLGSHERPDKFLGPEHGMSSMSRSQSVPMLDDEMLMYGSSKG 1020
Q96NW7          GTYKVYNIPLENYASGSDHLGSHERPDKMLGPEHGMSSMSRSQSVPMLDDEMLTYGSSKG 1015
                ***************************:********************** ******

Q80TE7          PPQQKASMTKKVYQFDQSFNPQGAVEVKAEKRIPPPFAHNSEYVQQPSKNIAKDLVSPRA 1075
P70587          PPQQKASMTKKVYQFDQSFNPQGAVEVKAEKRIPPPFAHNSEYVQQPGKNIAKDLVSPRA 1080
Q96NW7          PQQQKASMTKKVYQFDQSFNPQGSVEVKAEKRIPPPFQHNPEYVQQASKNIAKDLISPRA 1075
                * **********************:************* **.*****..*******:****

Q80TE7          YRGYPPMEQMFSFSQPSVNEDAMVNAQFASQGPRAGFLRRADSLASSTEMAMFRRVSEPH 1135
P70587          YRGYPPMEQMFSFSQPSVNEDAMVNAQFASQGPRAGFLRRADSLASSTEMAMFRRVSEPH 1140
Q96NW7          YRGYPPMEQMFSFSQPSVNEDAVVNAQFASQGARAGFLRRADSLVSATEMAMFRRVNEPH 1135
                **********************:*********.***********.*:*********.***

Q80TE7          ELPPGDRYGRATYRGGLEGQSSISMTDPQFLKRNGRYEDEHPSYQEVKAQAGSFPAKNLT 1195
P70587          ELPPGDRYGRAAYRGGLEGQSSVSMTDPQFLKRNGRYEDEHPSYQEVKAQAGSFPAKNLT 1200
Q96NW7          ELPPTDRYGRPPYRGGLDRQSSVTVTESQFLKRNGRYEDEHPSYQEVKAQAGSFPVKNLT 1195
                **** *****..*****: ***:::*:.**************************.****

Q80TE7          QRRPLSARSYSTESYGASQTRPVSARPTMAALLEKIPSDYNLGNYGDKTSDNSDIKTRPT 1255
P70587          QRRPLSARSYSTESYGASQTRPVSARPTMAALLEKIPSDYNLGNYGDKTSDNSDIKTRPT 1260
Q96NW7          QRRPLSARSYSTESYGASQTRPVSARPTMAALLEKIPSDYNLGNYGDKPSDNSDLKTRPT 1255
                ***********************************************.*****:*****

Q80TE7          PVKGEESCGKMPADWRQQLLRHIEARRLDR------------------------------ 1285
P70587          PVKGEESCGKMPADWRQQLLRHIEARRLDR------------------------------ 1290
Q96NW7          PVKGEESCGKMPADWRQQLLRHIEARRLDRNAAYKHNTVNLGMLPYGGISAMHAGRSMTL 1315
                ******************************

Q80TE7          -----------------TPSQQSNILDNGQEDVSPSGQWNPYPLGRRDVPPDTITKKAGS 1328
P70587          -----------------TPSQQSNILDNGQEDVSPSGQWNPYPLGRRDVPPDTITKKAGS 1333
Q96NW7          NLQTKSKFDHQELPLQKTPSQQSNILDNGQEDVSPSGQWNPYPLGRRDVPPDTITKKAGS 1375
                                  ****************************************

Q80TE7          HIQTLMGSQSLQHRSREQQPYEGNINKVTIQQFQSPLPIQIPSSQATRGPQPGRCLIQTK 1388
P70587          HIQTLMGSQSLQHRSREQQPYEGNINKVTIQQFQSPLPIQIPSSQATRGPQPGRCLIQTK 1393
Q96NW7          HIQTLMGSQSLQHRSREQQPYEGNINKVTIQQFQSPLPIQIPSSQATRGPQPGRCLIQTK 1435
                ************************************************************

Q80TE7          GQRSMDGYPEQFCVRIEKNPGLGFSISGGISGQGNPFKPSDKGIFVTRVQPDGPASNLLQ 1448
P70587          GQRSMDGYPEQFCVRIEKNPGLGFSISGGISGQGNPFKPSDKGIFVTRVQPDGPASNLLQ 1453
Q96NW7          GQRSMDGYPEQFCVRIEKNPGLGFSISGGISGQGNPFKPSDKGIFVTRVQPDGPASNLLQ 1495
                ************************************************************

Q80TE7          PGDKILQANGHSFVHMEHEKAVLLLKSFQNTVDLVIQRELTV 1490
P70587          PGDKILQANGHSFVHMEHEKAVLLLKSFQNTVDLVIQRELTV 1495
Q96NW7          PGDKILQANGHSFVHMEHEKAVLLLKSFQNTVDLVIQRELTV 1537
                *****************************************


Mouse (Q80TE7) vs Rat (P70587): 99%
Mouse (Q80TE7) vs Human (Q96NW7): 92%


----------------------
```

Phosphorich region (aa 826 to aa 1213)

```
CLUSTAL 2.0.12 multiple sequence alignment


mouse           -----STHRHTPETEVPPSNPWQNWTRTPSPFEDRTAFPSKLETTPTTSPLPERKDHMKE 55
rat             LELEQSTHRHTPETEVPPSNPWQNWTRTPSPFEDRTAFPSKLETTPTTSPLPERKDHMKE 60
human           -----STHRHTPETEVPPSNPWQNWTRTPSPFEDRTAFPSKLETTPTTSPLPERKEHIKE 55
                     **************************************************:*:**

mouse           PTETPGPFSPGVPWEYHDPTPNRSLGNVFSQIHCRPDSSKGVIAISKSTERLSPLMKDIK 115
rat             PTETPGPFSPGVPWEYHDPTPNRSLGNVFSQIHCRPDSSKGVIAISKSTERLSPLMKDIK 120
human           STEIPSPFSPGVPWEYHDSNPNRSLSNVFSQIHCRPESSKGVISISKSTERLSPLMKDIK 115
                .** *.************..*****.**********:******:***************

mouse           SNKFKKSQSIDEIDVGTYKVYNIPLENYASGSDHLGSHERPDKFLGPEHGMSSMSRSQSV 175
rat             SNKFKKSQSIDEIDVGTYKVYNIPLENYASGSDHLGSHERPDKFLGPEHGMSSMSRSQSV 180
human           SNKFKKSQSIDEIDIGTYKVYNIPLENYASGSDHLGSHERPDKMLGPEHGMSSMSRSQSV 175
                **************:****************************.****************

mouse           PMLDDEMLMYGSSKGPPQQKASMTKKVYQFDQSFNPQGAVEVKAEKRIPPPFAHNSEYVQ 235
rat             PMLDDEMLMYGSSKGPPQQKASMTKKVYQFDQSFNPQGAVEVKAEKRIPPPFAHNSEYVQ 240
human           PMLDDEMLTYGSSKGPQQQKASMTKKVYQFDQSFNPQGSVEVKAEKRIPPPFQHNPEYVQ 235
                ******** ******* ********************:************* **.****

mouse           QPSKNIAKDLVSPRAYRGYPPMEQMFSFSQPSVNEDAMVNAQFASQGPRAGFLRRADSLA 295
rat             QPGKNIAKDLVSPRAYRGYPPMEQMFSFSQPSVNEDAMVNAQFASQGPRAGFLRRADSLA 300
human           QASKNIAKDLISPRAYRGYPPMEQMFSFSQPSVNEDAVVNAQFASQGARAGFLRRADSLV 295
                *..*******:*************************:*********.***********.

mouse           SSTEMAMFRRVSEPHELPPGDRYGRATYRGGLEGQSSISMTDPQFLKRNGRYEDEHPSYQ 355
rat             SSTEMAMFRRVSEPHELPPGDRYGRAAYRGGLEGQSSVSMTDPQFLKRNGRYEDEHPSYQ 360
human           SATEMAMFRRVNEPHELPPTDRYGRPPYRGGLDRQSSVTVTESQFLKRNGRYEDEHPSYQ 355
                *:*********.******* *****..*****: ***:::*:.*****************

mouse           EVKAQAGSFPAKNLTQRRPLSARSYSTESYGAS 388
rat             EVKAQAGSFPAKNLTQRRPLSARSYSTE----- 388
human           EVKAQAGSFPVKNLTQRRPLSARSYSTESYGAS 388
                **********.*****************

Sequence identity
Rat vs mouse – 99%
Rat vs human – 90%


----------------------
```

Rat Repair region

```
CLUSTAL 2.0.12 multiple sequence alignment


Rat             DLGNNEFSELPEVLDQIQNLRELWMDNNALQVLPGSIGKLKMLVYLDMSKNRIETVDMDI 60
Human           DLGNNEFGELPEVLDQIQNLRELWMDNNALQVLPGSIGKLKMLVYLDMSKNRIETVDMDI 60
                *******.**************************************************

Rat             SGCEALEDLLLSSNMLQQLPDSIGLLKKLTTLKVDDNQLTMLPNTIGNLSLLEEFDCSCN 120
Human           SGCEALEDLLLSSNMLQQLPDSIGLLKKLTTLKVDDNQLTMLPNTIGNLSLLEEFDCSCN 120
                ************************************************************

Rat             ELESLPPTIGYLHSLRTLAVDENFLPELPREIGSCKNVTVMSLRSNKLEFLPEEIGQMQR 180
Human           ELESLPSTIGYLHSLRTLAVDENFLPELPREIGSCKNVTVMSLRSNKLEFLPEEIGQMQK 180
                ******.*****************************************************:

Rat             LRVLNLSDNRLKNLPFSFTKLKELAALWLSDNQSKALIPLQTEAHPETKQRVLTNYMFPQ 240
Human           LRVLNLSDNRLKNLPFSFTKLKELAALWLSDNQSKALIPLQTEAHPETKQRVLTNYMFPQ 240
                ************************************************************

Rat             QPRGDEDFQSDSDSFNPTLWEEQRQQRMTVAFEFEDKKEDDESAGKVKALSCQAPWDRGQ 300
Human           QPRGDEDFQSDSDSFNPTLWEEQRQQRMTVAFEFEDKKEDDENAGKVKDLSCQAPWERGQ 300
                ****************************************.***** *******:***

Rat             RGITLQPARLSGDCCTPWARCDQQIQDMPVPQSDPQLAWGCISGLQQERSMCAPLPVAAQ 360
Human           RGITLQPARLSGDCCTPWARCDQQIQDMPVPQNDPQLAWGCISGLQQERSMCTPLPVAAQ 360
                *******************************.******************:*******

Rat             STTLPSLSGRQVEINLKRYPTPYPEDLKNMVKSVQNLVGKPSHGVRVENANPTANTEQTV 420
Human           STTLPSLSGRQVEINLKRYPTPYPEDLKNMVKSVQNLVGKPSHGVRVENSNPTANTEQTV 420
                ************************************************:***********

Rat             KEKFEHKWP 429
Human           KEKYEHKWP 429
                ***:*****

rat vs human: 97%
```